NERO

NUUK ECOLOGICAL RESEARCH OPERATIONS

9th Annual Report 2015

GEM

Greenland Ecosystem Monitoring

Aarhus University
DCE – Danish Centre for Environment and Energy

NUUK ECOLOGICAL RESEARCH OPERATIONS

9th Annual Report 2015

AARHUS
UNIVERSITY
DCE – DANISH CENTRE FOR ENVIRONMENT AND ENERGY

Data sheet

Title:	Nuuk Ecological Research Operations
Subtitle:	9th Annual Report 2015
Editors:	Elmer Topp-Jørgensen, Jannik Hansen and Torben R. Christensen Department of Bioscience, Aarhus University
Publisher:	Aarhus University, DCE – Danish Centre for Environment and Energy
URL:	http://dce.au.dk
Year of publication:	2017
Please cite as:	Topp-Jørgensen, E., Hansen, J. and Christensen, T.R. (Eds.). 2017. Nuuk Ecological Research Operations 9th Annual Report, 2015, Aarhus University, DCE – Danish Centre for Environment and Energy. 80 pp.

Layout and drawings:	Tinna Christensen, Department of Bioscience, Aarhus University
Front cover photo:	Katrine Raundrup
Back cover photo:	Top to bottom: Jakob Abermann, Laura H. Rasmussen, Bula Larsen, Thomas Juul-Pedersen and Michele Citterio
ISSN:	1904-0407
ISBN:	978-87-93129-46-7
Number of pages:	80
Internet version:	The report is available in electronic format (pdf) on www.nuuk-basic.dk/Publications and on www.dce.au.dk
Supplementary notes:	Nuuk Basic Secretariat Department of Bioscience, Aarhus University P. O. Box 358, Frederiksborgvej 399 DK-4000 Roskilde E-mail: nuuk-basic@au.dk Phone: +45 87158657

Together with Zackenberg Ecological Research Operations (ZERO), Nuuk Ecological Research Operations (NERO) is operated as a centre without walls with a number of Danish and Greenlandic institutions involved. The two programmes are gathered under the umbrella organization Greenland Ecosystem Monitoring (GEM). The following institutions are involved in NERO:
Department of Bioscience, Aarhus University: GeoBasis, BioBasis and MarineBasis programmes
Greenland Institute of Natural Resources: BioBasis and MarineBasis programmes
Asiaq – Greenland Survey: ClimateBasis programme
University of Copenhagen: GeoBasis programme

The programmes are coordinated by a secretariat at the Department of Bioscience at AarhusUniversity and are financed with contributions from:
The Danish Energy Agency
The Environmental Protection Agency
The Government of Greenland
Private foundations
The participating institutions

Contents

Executive summary

Torben R. Christensen, Elmer Topp-Jørgensen, Jannik Hansen, Jakob Abermann, Birger Ulf Hansen, Maia Olsen and Thomas Juul-Pedersen

ClimateBasis

The ClimateBasis programme is dedicated to describing the climatological and hydrological conditions in Kobbefjord. Two automatic climate stations, C1 and C2 (Station 652 and Station 653), two automatic hydrometric stations, H1 and H2 (Station 650 and Station 651), and four diver stations, H3, H4 and H5 (Stations 654, 655, 656 and 658) are located in the Kobbefjord basin.

The two climate stations are placed next to each other to ensure data continuity and fill data gaps.

2015 was an unusually cold year with a mean annual air temperature of -2.5°C, which is 2.3°C below average since the programme started in 2008. All months showed below average temperatures, with 5 months being more than 3°C colder than average. There was no freezing between 14 June and 14 September.

Hydrological measurements in the Kobbefjord basin started in 2006 at H1, in 2007 at H2, H3 and H4, and in 2008 at H5. In 2014, a new site was chosen at Langesø, which drains into H1. Manual measurements of discharge were performed at H1, H4, H5 and Langesø. Since 2014, a year-round measurement setup has been in operation at all stations, also allowing for assessing very early and late runoff.

For H1, which is placed at the main river in Kobbefjord, the total discharge during the hydrological year 2014/2015 was $41.48*10^6$ m^3, which is less than half a standard deviation above average. The peak discharge in 2015 was recorded on 16 October along with a heavy precipitation event.

GeoBasis

The 2015 season was the eighth full season for the GeoBasis programme, with a field season between May and late September. However, due to cooperation with other research projects, the programme continued until late October. Data collected by the Danish Meteorological Institute (figure 3.3) shows that in 2015, the annual mean air temperature in Nuuk reached -2.9 °C, which is 1.5 °C colder than normal (Cappelen 2015). The two summer months, July-August, were both warmer than normal. The warmest month was July, with an average temperature of 8.6 °C, which was 1.9 °C warmer than normal, but 1.8 °C colder than July 2012, which was the warmest July recorded in the period 1866-2016. Eight months in 2015 (January-May and October-December) were colder than normal. The coldest month in 2015 was March with -11.9 °C, which was 4.5 °C colder than normal, but 2.5 °C warmer than the record low from March 1993.

Sea ice cover in Kobbefjord in the winter 2014/15 developed as late as 20 January, which is rather late compared to the previous eight years of monitoring in Kobbefjord. The fjord became ice free on 15 June, which is nearly 15 days later than the average for the seven previous years. The snow cover survey in 2015 was carried out on 21-22 April, and the average snow depth for the three sites was 119 cm, which is the highest snow depth measured in the period 2010-2015 – almost twice as high as the average of 66 cm. An average of 355 kg m^{-3} in density is also well above the average of 323 kg m^{-3} for the six year period.

At the micrometeorological station – SoilFen - in Kobbefjord, March 2015 was the coldest month, with -12.9 °C, while July was the warmest month with 9.3 °C. In general, 2015 was a cold year, and March, June and December set new minimums records for the station with respectively -12.5, 5.2 and -10.9 °C, while the rest of the months in 2015 were only 0.5-1.0 degrees above the previous minimum records. These measurements are in line with the air temperature measured in Nuuk located 30 km away. The M500 is located south of Badesø, approxi-

mately 500 m a.s.l. In 2008-2015, the mean air temperature in July at the M500 station was between 6.6 °C and 10.4 °C, in 2015 it was only 8.8 °C, only +0.3 °C above the average for the period. The relative humidity measured at the M500 station in the period 2008-2014 shows an annual average of 77%, with maximum values of 90-91% during the snow melt in April and in the cold rainy autumn from September to November. The incoming shortwave irradiance in the period 2008-2015 was between 211-295 W m^{-2} in June, and in 2015 it was 218W m^{-2}, or 24 W m^{-2} below average. The annual average shortwave irradiance was 102 W m^{-2} for the period 2008-2014.

In 2015, forty-two water samples were collected from mid-June to start October, which was a field season one month shorter than the previous year due to a very late snow/ice melt. In situ measurements of river water temperature, conductivity and pH were carried out along with the water sampling. The minimum river water temperature was 1-2 °C from mid-June, which was 1.0 °C lower than the previous years, and the water temperature peaked with a maximum temperature of 12.5 °C in the beginning of August, which was 1.9 °C higher and 2 weeks later than in 2014. The conductivity measurements showed a normal decrease in conductivity within the snow melting period from 19 µSc m^{-1} to a level of 15.5 +/- 1.5 µSc m^{-1}. From the beginning of July and through the rest of the field season, the conductivity showed no significant trend, which is normal for the period. pH showed a normal trend from 7.2 at the beginning of the field season – dropping fast to a more stable value around 6.7 with minor fluctuations over the summer season due to rain events.

Mean CH_4 fluxes across chambers were initially relatively high, peaking around 7 July with maximum values above 6 mg CH_4 m^{-2} h^{-1}. This mid-season peak was of similar magnitude as the previous year; however, it occurred approximately three weeks earlier in 2015 (figure 3.14). The variation between years is likely related to variations in timing of snow melt, meteorological conditions, and primary production in the fen. After the peak, CH_4 fluxes decreased steadily and reached approximately 1 mg CH_4 m^{-2} h^{-1} in late September.

Eddy covariance measurements of the CO_2 and H_2O exchange in the fen were initiated 24 June and continued until 21 October. A snow patch covered parts of the fen when measurements began. During this pre-growing season period, daily CO_2 emissions were just below 1 g C m^{-2} d^{-1}. As the vegetation developed, photosynthetic uptake of CO_2 started, and on 7 July the fen ecosystem switched from being a net source to a net sink of atmospheric CO_2 on a daily basis. The fen acted as a consistent sink for atmospheric CO_2 until 2 September, except during three days (10, 28-29 August) with overcast conditions and low incoming solar radiation limiting photosynthesis. During the net uptake period, the fen accumulated 56.3 g C m^{-2}. Post-growing season measurements indicate consistent daily net CO_2 emissions ranging between 0.2-0.8 g C m^{-2} d^{-1} related to variations in temperature. During the entire measurement period, the fen constituted a sink for atmospheric CO_2 amounting to -31.0 g C m^{-2}.

The 2015 season was the eighth full year and it provided valuable learning lessons and ensured improvements of the monitoring that will improve the programme in the following years. All methods and sampling procedures are described in detail in a new manual 'GeoBasis Manual - Guidelines and sampling procedures for the geographical monitoring programme of Nuuk Basic in Kobbefjord', which can be downloaded from www.nuuk-basic.dk. In 2015, all data from the GeoBasis Nuuk programme were uploaded to the new GEM (Greenland Ecosystem Monitoring) database, which can be found at http://data.g-e-m.dk/. In the coming years, the data will be regularly updated after each field season.

BioBasis

Reproductive plant phenology

Due to late snow melt, a later budding, flower production, and senescence was observed in 2015 than in most other years, with recording of phenology starting on 17 June and ending on 29 September.

L. procumbens had the latest budding and timing of 50% flowering observed so far; furthermore, we observed more flowers in this species than ever before.

This season, *S. acaulis* had a high level of predation on the flower petals between 7 July and 21 July, resulting in very low total counts. All vegetative phenology of *S. aucalis* occurred later than previous seasons.

Even though both male and female catkins of *S. glauca* had a later appearance in 2015 than in other years, appearance of hair seems to occur at roughly the same time every year. The number of catkins produced in 2015 was average compared to all other years, except for the two years with the larvae outbreak (2010 and 2011).

Vegetation greening, NDVI

2015 had a very short season with a late peak in production and generally low NDVI values, in some cases the lowest measured, with the exception of 2011. NDVi was measured from 17 June to 23 September, making it the shortest season (98 days total) since the beginning of the programme in 2008. Season lengths from 2009–2014 ranged between 104 and 142 days. Since 2014, NDVI has been measured in the CO_2 flux plots, and there was little to no difference in values between manipulations (control, temperature and shade) between 2014 and 2015.

Carbon dioxide exchange

CO_2 flux was measured on 12 occasions from 17 June (DOY 168) until 25 September. Generally, all plots functioned as sinks for atmospheric CO_2 at the time of the measurement (midday). Similarly to previous years, NEE was generally more negative (i.e. higher CO_2 uptake) in Control (C) plots compared with Temperature (T) and Shade (S) plots. As photosynthesis is driven by solar radiation, shading decreases GPP and build-up of biomass. In 2014 and 2015, R_{eco} rates from T plots were not higher than those from C plots.

Since the extensive outbreak of the larvae *Eurois occulta* in 2011, which defoliated large parts of the heath vegetation in the area, CO_2 flux magnitudes have been high in following years. This trend continued in 2015.

UV-B exclosure plots

The plots were set up between 24 June and 1 July and taken down 1 October. The ambient UV-B radiation on fluorescence parameters was monitored on *V. uliginosum* and *B. nana*. The measurements varied considerably at each measurement and through the season, i.e. we found no response of reducing the UV-B radiation. We have no explanation for this. However, previous years have reported a positive effect for the studied species when excluding UV-B radiation.

Arthropods

In Kobbefjord, all four pitfall trap stations (each with eight traps) established in 2007 and the two window trap stations (each with two traps) established in 2010 were opened between 17 June and 7 July, and they all worked continuously until 29 September, when the liquid began to freeze. This resulted in 3420 trap days (including 3040 pitfall trap days and 380 window trap days). Former seasons ranged from 3496-5818 trap days (with a mean of 4524 trap days), making 2015 the shortest season since 2010.

Microarthropods

Three sampling sessions for microarthropods in Kobbefjord took place in July, August and September. The collembolan communities of the four plant communities have retained their characteristic structure during the sampling period covering 2007, 2009, 2010, 2014 and 2015.

The individual plots have unique ecological properties, particularly true for the *Loiseleuria* and *Empetrum* plots, and most species were rather stable in their abundance and consistently affiliated with a certain plant community. The structure of the population abundances has been stable during the period spanning eight years, and samples from 2015 conformed to the same pattern.

Birds

Four passerine bird species, Lapland bunting (LB, *Calcarius lapponicus*), snow bunting (SB, *Plectrophenax nivalis*), northern wheatear (NW, *Oenanthe oenanthe*) and common redpoll (RP, *Carduelis flammea*), were counted at 13 census points within the 32 km^2 Kobbefjord catchment area. A total of 11 censuses were carried out from 23 June to 23 September 2015. Although shorter than previous seasons, which have ranged from 118-142 days, the frequency of censuses was stable with one census roughly every eight days.

There were fewer observations of SB in 2015 than in 2014, but LB, NW and RP showed little change from the previous season. Observations of SB peaked in July, while the remaining passerines peaked in numbers in September. All species but RP had low counts per census in 2015, with SB and NW displaying the lowest counts ever observed during the monitoring in Kobbefjord. Hence, counts of birds per census of SB and NW were 3.1 and 3.2 birds, respec-

tively, while there were 5.4 LB per census. RP counts were 2.4 birds per census, but this species has fluctuated a great deal over the years, and so a trend is not readily obvious.

Mammals

The Kobbefjord catchment area is only sparsely populated with mammals. During the field season, no mammals were observed. Faeces of fox and hare was found from time to time.

Lakes

Due to a very late ice breakup compared to previous years, the ice free period was short in 2015, thus, the summer was slightly cooler than average. Overall, 2015 was a year with high precipitation; however, the summer was drier than the average summer. Water chemistry showed higher concentrations of nitrogen and phosphorus than average levels compared to the previous monitored years. In both lakes, chlorophyll levels were close to or a little lower than the average for the monitoring period. The best explanation for the lower chlorophyll a levels despite increasing nutrients is lower temperature and, consequently, reduced primary production. Zooplankton communities are generally different in Qassi-sø compared to Badesø, which is consistent with the lack of fish in Qassi-sø; e.g. more dominance of calanoid copepods in Qassi-sø in combination with less importance of the tolerant rotifers. Overall, the vegetation coverage has its maximum at intermediate depths due to less physical disturbance and preferable light conditions. Coverage in 2015 increased at the shallow and intermediate depth compared to the previous years, but decreased at the deeper sites, probably responding to the cooler and shorter summer of 2015.

MarineBasis

The MarineBasis programme in Nuuk represents the marine component of the comprehensive ecosystem monitoring programme NuukBasic. The programme was initiated in late 2005, and this report presents the data and results from the tenth full year of sampling. The programme samples key hydrographical parameters, including sea ice conditions, physical and chemical hydrography, biological components of the water column and sediment as well as observations of whales and sea birds. The collected data provide essential information for understanding and describing the ecosystem. The long time series also makes it possible to study, identify and quantify seasonal and inter-annual patterns and variability as well as aiming to identify possible effects of climate related changes. A parallel marine programme is operating at the high Arctic Zackenberg area (MarineBasis-Zackenberg); both programmes collaborate closely and supplement each other.

Satellite images (AMSR) of Baffin Bay were collected daily until 2015, but these images are no longer available. The collected image series represents a valuable baseline on the seasonality and inter-annual variability in sea ice conditions in the Baffin Bay region if it, or a similar product, becomes available again. Satellite images (MODIS) of the Godthåbsfjord system covering part of the Fyllas Banke shelf region revealed unusually high sea ice concentrations outside the Godthåbsfjord system lasting until late April. In most years, the sea ice edge is found further north as early as February/March. Nevertheless, sea ice inside the Godthåbsfjord system was limited to the innermost part and smaller fjord branches, as observed in previous years. Most of the sea ice and glacial ice is melting within the fjord, but a part of the ice is exported from the fjord in seasonal burst events. This seasonal pattern is monitored by a camera cross section of the fjord.

Key abiotic and biotic hydrographical parameters were measured during the monthly sampling programme in the outer sill region along with a length and cross sections of the fjord. An event of deep inflow of warm saline coastal water is often recorded in winter, but in 2015 this was recorded in both January, March and again towards the end of the year in November and December. Tidal forces create vertical mixing at the outer sill region (Main Station, GF3) during winter and spring. As a result, the water column depicts largely homogenous temperatures, salinities and phytoplankton biomass (i.e. chlorophyll a) with depth. Similarly to previous years, an early stratification with high surface phytoplankton biomasses was observed inside the fjord during the annual length section in May. The phytoplankton biomass increases in spring due to the improving light conditions. In 2015, an intense spring

bloom with high phytoplankton biomass values was recorded in April and May, which lead to low nutrient levels and low biomass values in June. Increased freshwater runoff from land, along with ice melt, solar heating of the surface layer and air-sea heat exchange, strengthen the pycnocline, thus withstanding vertical mixing in the outer sill region. A second bloom phytoplankton bloom was observed during summer, which resulted in elevated phytoplankton biomass values until October in 2015. Decreasing freshwater runoff during autumn weakens the stratification within the fjord and vertical mixing of the water column re-established in the outer sill region.

The phytoplankton community in the outer sill region was mainly comprised of haptophytes *Phaeocystis* sp. and diatoms throughout the year, as observed in previous years. *Phaeocystis* sp. dominated the phytoplankton community from March-June. In April, large colonies of the typically ice-associated genus *Fragilariopsis* were observed in Godthåbsfjord, which could be linked to the extensive and long-lasting sea ice cover observed in Baffin Bay in winter 2015. Chrysophytes showed and unusually high abundance during the summer bloom. Diatoms, such as *Thalassiosira* spp. and *Chaetoceros* spp., were the dominant groups during winter, autumn and summer. Other phytoplankton groups, such as dinoflagellates and silicoflagellates, also contributed significantly to the seasonal species assemblages identified during 2015. Zooplankton data were not processed in time for this report, but they will be made available subsequently. The fish larvae showed interannual variation in abundances. In general, sandeel *Ammodytes* sp. larvae dominate the fish larvae assemblage in late winter/early spring, while arctic shanny *Stichaeus punctatus* larvae dominate in spring and capelin *Mallotus villosus* larvae in summer/autumn. American Plaice usually peak in June, while Atlantic cod *Gadus morhua* larvae appear to peak in different months during spring and summer. In 2015, the total abundance of fish larvae was among the lowest recorded in the time series caused by the numbers of capelin larvae being lower than previous years. The length section generally showed higher fish larvae abundances on Fyllas Banke compared to inside Godthåbsfjord, dominated by a high number of sandeel larvae. For the first time, Atlantic cod larvae showed higher values deep in the fjord and were present at all fjord stations, while not all stations outside the fjord showed Atlantic Cod larvae. Nevertheless, arctic shanny still dominated the fish larvae composition inside the fjord.

At the Main Station (GF3), the shellfish larvae community showed the characteristic peak of *Pandalus* sp. in April, which is one month earlier than normally recorded (i.e. May). *Chionoecetes opilio* and *Hyas* spp. peaked two months later in June. The community in the outer sill region was dominated by *Ctenophora* and *Sagitta* spp., except in the spring period (April-June), where *Pandalus* spp., *Chionoecetes opilio* and *Hyas* spp. became more abundant. Along the length section, larvae of the commercial species *Chionoecetes opilio* showed significantly higher values than in previous years. *Pandalus* sp. are found at almost all stations along the length section, and in May 2015 record high values were observed on the outside of Fyllas Banke, while record low densities were observed on the inside of the bank. For the past two years, larvae of *Chionoecetes opilio* have been less abundant at all stations, compared to previous years.

Unfortunately, the vertical sinking flux samples were not analysed in time for this report, but the data will be made available subsequently.

The benthic community generally increases the oxygen uptake into the sediment during spring and summer, when primary production in the photic zone and sinking flux are highest. The established time series of water-sediment exchange of solutes represents a baseline for future sampling, but for the time being this sampling has been put on hold.

Previous monitoring of benthic fauna and flora has established a solid baseline for future comparisons. Since 2012, the monitoring of benthic flora and fauna has focused on population dynamics of key species of the intertidal zone - the brown macroalgae knotted wrack *Ascophyllum nodosum* and blue mussel *Mytilus edulis*, in relation to temperature, ice cover/light availability and tidal level. Temperature loggers also showed less variability during the 2013-14 winter compared to the ice free winter in 2012-13 because an insulating layer of ice covered the shore. Over the period 2012-2015, this tip growth rate was largest in 2012-2013, likely reflecting the mild winter of this year with very limited sea ice-cover likely exposing the algae to full incident irradiance. Popula-

tion density, biomass and age structure of *Ascophyllum nodosum* individuals are being estimated as part of the monitoring. The growth of established shoots ensured a biomass increase of the population during the assessment period 2012-15, which by far outweighed the biomass of lost individuals. The blue mussel data from 2015 was not processed in time for the report, but will be made available subsequently.

Two major seabird colonies in the vicinity of Nuuk are being monitored by the MarineBasis programme, but additional colonies are also included in this report. The Qeqertannguit bird colony holds the largest diversity of breeding seabirds in the Nuuk area and is influenced by legal and illegal egg harvesting. The Arctic tern *Sterna paradisaea* was not observed at the island in 2015, 2014, 2013 and 2008. Small and mid-sized colonies of Arctic tern in Greenland are known to fluctuate considerably in population size, but the reason is poorly understood. On the southeast side, kittiwakes *Rissa tridactyla* were present in larger numbers than in recent years. In addition, the Iceland gull *Larus glaucoides* showed an increase in nesting individuals.

In order to address the proportion of the boreal distributed common guillemot versus the arctic Brünnich's guillemot *Uria lomvia* in the Nunngarussuit colony, an analysis of digital photographs is usually performed. This is interesting in the context of climate change, where the proportion of common guillemot is expected to increase in a warmer climate. However, distinguishing the two species requires a high photo quality, thus this analysis is not always possible. In 2015, nervous behaviour made the birds take flight early, thus reducing the quality of the photos, as they were taken from a greater distance.

West Greenland is a summer feeding ground for an estimated 3200 humpback whales, *Megaptera novaeangliae*. A photo-identification programme is used to estimate the number of humpback whales present and returning to the Godthåbsfjord system. In 2015, 18 ID pictures were collected in Godthåbsfjord identifying 13 different individuals. In the period 2007-2015, a total of 637 ID photos were collected, and with these a total of 109 individual whales have been identified in Godthåbsfjord so far. Due to an influx of whales on their northward migration, most whales are seen in the fjord in the months of May and early June. The individuals with the highest degree of site fidelity are also the individuals that stay within the fjord for the longest periods of time during the feeding period and therefore are encountered more often.

Research projects

Five research projects were carried out in the Kobbefjord and Godthåbsfjord in 2015. See chapter 6 for details.

1 Introduction

Josephine Nymand

The year 2015 was the ninth year of operation of the fully implemented Nuuk Basic programme with both a marine and a terrestrial component, and it was the seventh year with a complete annual time series for all sub-programmes. For the marine programme, the season began on 28 January and continued until 18 December, while the field season in the Kobbefjord area began 12 June and continued until 13 October, thus having a season of 324 and 123 days, respectively.

VIP visits

We had one VIP visit during the summer season at the field station. It was by the Greenland Minister for Nature, Environment and Energy, Mala Høy Kúko, and the Danish Minister for Energy, Utilities and Climate, Lars Christian Lilleholt.

Furthermore, the Nordic Council of Ministers, Climate and Air Pollution Group (KoL) visited the field station as did the Nordic Committee of Senior Officials for Education & Research.

Funding

Nuuk Basic is funded by the Danish Energy Agency and the Environmental Protection Agency with contributions from Greenland Institute of Natural Resources, Asiaq - Greenland Survey, Aarhus University and the University of Copenhagen. Aage V. Jensen Charity Foundation has generously provided most of the necessary research infrastructure, including boats, research house, boathouse, warehouse, office house, and accommodation facilities at Greenland Institute of Natural Resources in Nuuk.

New initiatives

The work on acquiring data for a high-resolution map of Kobbefjord area started in 2015 and will continue in 2016.

For the first time, the annual marine survey in May, covering the whole transect from the banks off shore to the most inner parts of Godthåbsfjord, was an integrated part of the university course "Arctic Marine Ecosystems".

MarineBasis also participated in the "CALVE" project with the University of Glasgow. CALVE looks at paleoclimate and glaciers.

Outreach

Results from the Nuuk Basic monitoring programme are continuously published in scientific papers, popular science articles and at scientific meetings and conferences. Furthermore, data from Nuuk Basic programme is freely available and was used for reporting purposes in a number of international fora and by a number of externally funded research projects in 2015. In Nuuk, the GEM researchers contribute to education of high school students as well as undergraduate and graduate students by giving lectures and supervising small research projects in relation to fieldwork. Researchers from GEM programmes also participate in the Arctic Science Partnership working groups and research teams.

In 2015, more than 11 scientific papers were published by the researchers from the Nuuk Basic programme and from externally funded research projects.

Further information

Further information about the Nuuk Ecological Research Operations (NERO) programme and Kobbefjord Field Station have been presented in previous annual reports, which can be found on the NERO web site (www.nuuk-basic.dk). On the web site, one can find much more information, including manuals for the different monitoring programmes, a database holding freely available data from the monitoring, up-to-date weather information, a NERO bibliography and a collection of public outreach papers in PDF format.

The NERO programme's address is:

Nuuk Basic Secretariat
Department of Bioscience.
Aarhus University
P. O. Box 358
Frederiksborgvej 399
DK-4000 Roskilde
Denmark
Phone: +45 5715 8657
E-mail: nuuk-basic@au.dk
Website: www.nuuk-basic.dk

Greenland Institute of Natural Resources provides the logistics in the Nuuk area:

Logistics Coordinator
Greenland Institute of Natural Resources
P.O. Box 570
Kivioq 2
3900 Nuuk
Greenland
Phone: +299 55 05 62
E-mail: heph@natur.gl
Website: www.natur.gl

2 Nuuk Basic

The ClimateBasis Programme

Jakob Abermann, Louise Holm Christensen, Stefan Jansen, Frederik Mathiassen, Malik Naamansen, Dorthe Petersen, Majbritt Westring Sørensen and Stefan Wacker

The ClimateBasis programme is dedicated to describing the climatological and hydrological conditions in Kobbefjord. Two automatic climate stations, C1 and C2 (Station 652 and Station 653), two automatic hydrometric stations, H1 and H2 (Station 650 and Station 651), and four diver stations, H3, H4, H5 and Langesø (Stations 654, 655, 656 and 658), monitor the physical parameters related to climate and hydrology. The Langesø measuring site was established in 2014 through a recent collaboration with BioBasis. In 2012, a small mountain glacier on the northern side of the basin was included in the programme in the framework of a strategic initiative in order to better understand the cryospheric component of the water-cycle, glacier mass balance and since 2013 also energy balance.

The location of the different stations can be seen in figure 2.1. ClimateBasis is operated by Asiaq – Greenland Survey.

2.1 Meteorological data

In 2015, the climate stations in Kobbefjord were visited nine times by Asiaq personnel. A full description of the climate stations has been given in Iversen et al. (2008). This annual report describes the eighth full year of data for all climate parameters and refers to data collected in the period from 1 January to 31 December 2015. Figure 2.2 gives an overview of selected meteorological parameters in 2015. Unfortunately, there was a period with major data gaps due to a series of technical breakdowns, which

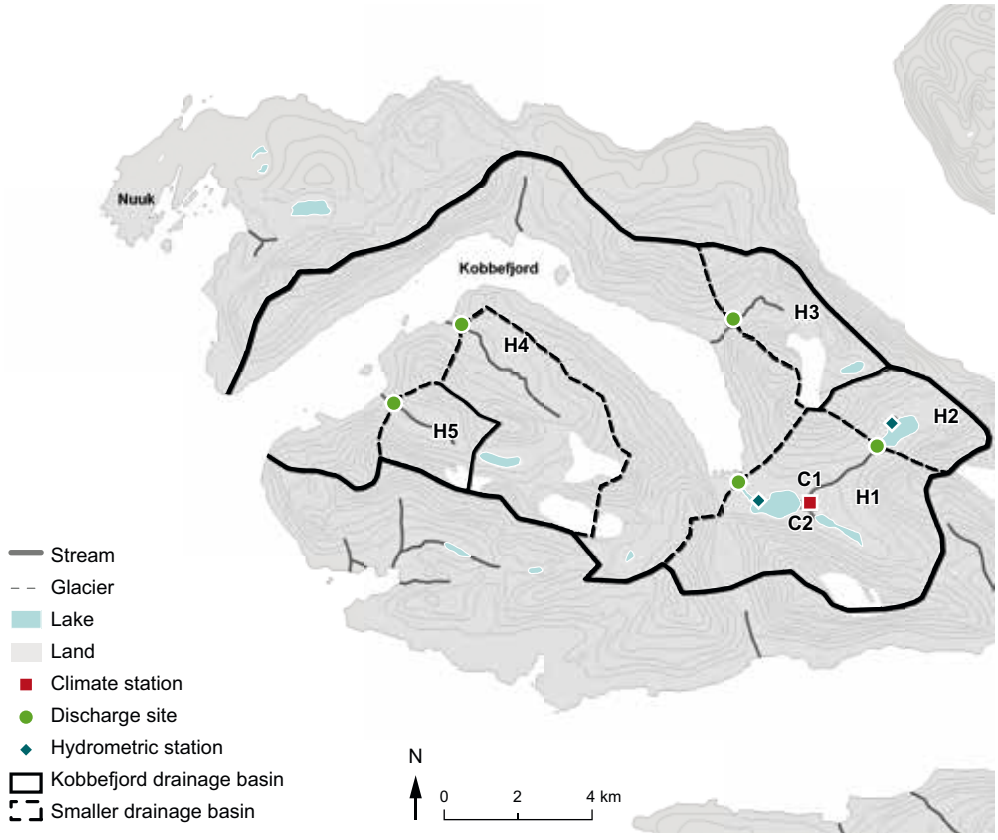

Figure 2.1 Location of the climate station (square), the hydrometric (H1, H2) and diver stations (H3, H4, H5) in Kobbefjord together with the respective drainage basins.

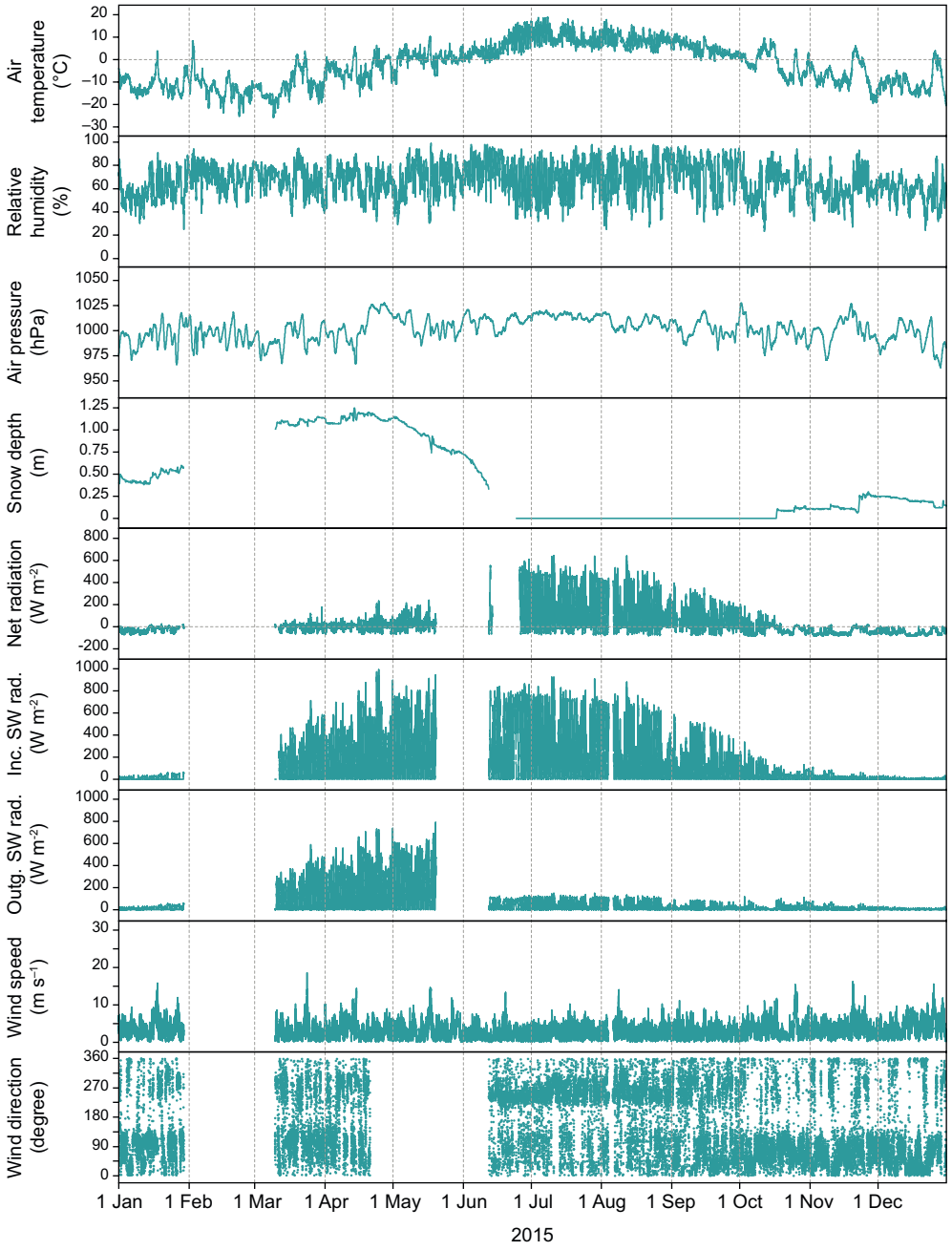

Figure 2.2 Variation of selected climate parameters in 2015. From above: Air temperature (°C), relative humidity (%), air pressure (hPa), snow depth (m), net radiation (Wm^{-2}), incoming short wave radiation (Wm^{-2}), outgoing short wave radiation (Wm^{-2}), wind speed (ms^{-1}) and wind direction (°). Wind speed and direction are measured 10 m above terrain; the remaining parameters are measured 2 m above terrain.

we filled with neighboring stations, where homogeneity allowed. Details can be found in Westring Sørensen et al. (in prep).

The mean annual temperature in 2015 was -2.5 °C, which is 2.3 degrees colder than the average between 2008 and 2015 (tables 2.1 and 2.2). All monthly temperature means were colder than average, and five months (all winter months) were more than 3 °C colder than average. March and December set the new negative temperature record. Absolute maximum temperature was 18.9 °C on 8 July, which is the second lowest maximum temperature ever recorded and the lowest on 10 March (-25.9 °C). During all months of the year, positive temperature occurred at least once, and during 3 months (14 June to 14 September) no negative temperatures were recorded. Comparing Nuuk with Kobbe-fjord, the generally stronger continentality in Kobbefjord is a clear climatological feature with higher temperatures in summer and lower temperatures in winter (figure 2.3.). In 2015, this was even more pronounced than usual during winter and less during summer.

2015 was the second most snow-rich year (2014 now being the third most snow-rich year on record); only in 2011 more snow was recorded. Maximum snow depth in 2015 was 1.25 m on 14 April, which was only 14 cm less than the all-time maximum in 2011. The annual snow survey took place only a week after the maximum

Table 2.1 Monthly mean values of selected climate parameters from January to December 2015 and the annual average.

Month-year	Rel. hum. (%)	Snow depth (m)	Air temp. (°C)	Air pressure (hPa)	Precip. (mm)	Wind (m/s)	Wind dir. most frequent
Jan-15	59	0.47	-11.2	995	44.1	3.9	ESE
Feb-15	71	---	-12.7	996	---	---	
Mar-15	70	---	-12.1	992	29.0	---	ESE
Apr-15	67	1.12	-4.5	1004	77.9	3.3	WNW
May-15	68	0.91	0.3	1004	45.0	3.2	
Jun-15	74	---	5.5	1009	24.5	2.1	WSW
Jul-15	69	0.00	10.2	1015	27.9	2.9	WSW
Aug-15	72	0.00	8.7	1008	139.8	2.8	WSW
Sep-15	75	0.00	4.7	1001	85.2	2.6	NE
Oct-15	64	0.05	-1.6	999	135.9	3.5	ENE
Nov-15	60	0.13	-7.5	1001	31.3	3.6	NE
Dec-15	58	0.18	-10.5	992	3.8	4.2	NNE
2015	67	---	-2.5	1001	644.4	---	---

Table 2.2 Comparison of monthly mean air temperatures 2007 to 2015 (italic text represents months with incomplete coverage).

	Air temperature °C								
Month	**2007**	**2008**	**2009**	**2010**	**2011**	**2012**	**2013**	**2014**	**2015**
Jan	——	–12.0	–5.4	–3.8	–5.4	–8.7	–5.9	–6.1	–11.2
Feb	——	–13.3	–6.1	–1.6	–8.7	–7.7	–7.2	–8.4	–12.7
March	——	–8.3	–11.7	–4.5	–9.2	–11.0	–3.1	–8.9	–12.1
April	——	–0.9	–3.2	–0.1	–9.5	–1.7	–0.8	–6.0	–4.5
May	0.6	3.9	0.3	7.1	0.3	3.2	–0.4	2.5	0.3
June	5.3	7.9	6.4	8.8	6.2	9.4	6.6	8.4	5.5
July	10.8	10.9	10.6	10.7	10.0	12.1	9.7	11.8	10.2
Aug	10.6	8.7	9.3	11.7	8.7	10.0	8.8	10.7	8.7
Sept	4.0	4.4	3.8	7.8	3.9	6.6	4.7	4.9	4.7
Oct	–0.5	0.0	–0.6	2.9	–2.4	3.0	0.9	0.1	–1.6
Nov	–3.5	–1.7	–7.9	1.2	–6.2	–3.0	–3.5	–3.9	–7.5
Dec	–8.7	–7.8	–2.8	0.5	–7.5	–6.1	–8.2	–6.6	–10.5
Year	——	–0.7	–0.6	3.4	–1.6	0.5	0.2	–0.1	–2.5

snow depth in 2015. The winter snow cover started to form on 17 October 2015.

On a monthly average, relative humidity was at a record low twice (January and December 2015), which went along with low precipitation values (only 3.8 mm during December). Total precipitation was more than 644 mm, but the data gap during February and March was not included. Both August and October were particularly rainy, exceeding these months' average by 29 and 38 mm, respectively. September, November and December, in turn, were much drier than usual, which resulted in a very snow-poor end of 2015.

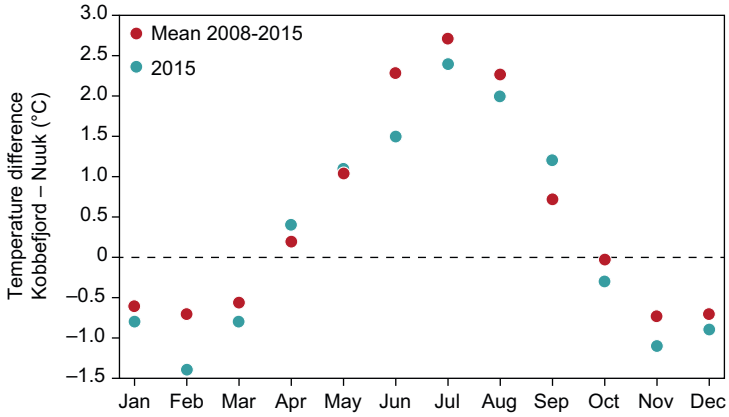

Figure 2.3 Difference in monthly average temperature in Kobbefjord – Nuuk (°C): red: mean for the period 2008-2015, blue: 2015.

Table 2.3 Monthly mean values of selected radiation parameters in 2015.

Month-year	Short wave rad		Long wave rad.		Net rad.	PAR
	(W/m²)	(W/m²)	(W/m²)	(W/m²)	(W/m²)	(µmol/s/m²)
	in	out	in	out		
Jan-15	4.5	4.5	222.3	249.8	-29.2	11.6
Feb-15	---	---	---	---	---	---
Mar-15	---	---	---	---	---	---
Apr-15	163.7	163.7	259.5	286.3	-0.6	392.0
May-15	---	---	---	---	---	---
Jun-15	---	---	---	---	---	---
Jul-15	252.4	252.4	308.2	382.6	138.3	519.2
Aug-15	161.2	161.2	309.1	362.7	80.8	331.1
Sep-15	71.2	71.2	300.2	335.4	26.1	150.0
Oct-15	21.2	21.2	261.3	294.0	-21.3	48.7
Nov-15	6.5	6.5	220.3	264.7	-44.1	16.4
Dec-15	2.2	2.2	205.5	253.7	-48.8	5.6

Air pressure was around average in total, but particularly high during July (average: 1014.8 hPa).

The predominant wind direction was from the eastern sector in winter, during spring it turned towards west and in the summer months an in-valley flow (from the western sector) indicated a valley wind system (table 2.1.). Wind speed followed the general cycle of higher wind speed in winter than in summer and individual storms are clearly seen in figure 2.2.

Table 2.3 summarizes the radiation components on a monthly basis measured in Kobbefjord. The short-wave balance clearly determines the net-radiation in summer, while the long-wave balance does so in winter. Most net radiation input happened in June with 138.3 Wm^{-2} on average being added to the surface while net radiation minimum happened in December, where radiative cooling is not compensated by significant incoming shortwave radiation. November and December showed all-time minima of the net-radiation, which were caused by little moisture in the air and, thus, less downward longwave radiation than usual.

2.2 River water discharge

Hydrometric stations

Hydrological measurements were carried out at six locations in the Kobbefjord catchment. Two hydrometric stations were established in 2007, and various divers are set up every year in three minor rivulets to Kobbefjord. The drainage basins of the six locations cover a total of 58 km^2, corresponding to 56% of the 115 km^2 catchment area of Kobbefjord.

In figure 2.1, the locations of the hydrometric stations (H1, H2) and the diver stations (H3, H4, H5) are marked. For further descriptions of the stations and their respective drainage area, see Jensen and Rasch (2009). For descriptions of the hydrometric stations, see Jensen and Rasch (2008).

In terms of hydrological fieldwork, obtaining manual discharge measurements at the new station at Langesø and at H2 has been in focus. Nine discharge measurements have been performed there and one at H1.

Q/h-relation

Manual discharge measurements were carried out at station H1 (3) and Langesø (7), H4 (1) and H5 (1). The purpose was to establish and validate a stage-discharge relation (Q/h-relation). It is generally recommended to base a Q/h-relation on a minimum of 12-15 discharge measurements covering the water levels normally observed at the station (ISO 1100-2, 1998). For H2, H3, H4, H5 and Langesø, not enough discharge measurements have been made yet to produce a reliable Q/h-relation. Particularly, measurements at high water levels are missing. Therefore, data from these stations are not presented yet.

A Q/h-relation was established for H1 in 2009 based upon a total of 17 discharge measurements. The Q/h-relation was updated in 2011 in order to account for winter conditions with the outlet being affected by ice/snow. Details can be found in (Pernosky et al. 2012).

River water discharge at H1

Figure 2.4 shows the discharge at H1 for 2015. There was only one major winter runoff event before the snow pack started to melt (start February, due to rain). From there onward, it took until the snow melt set in and a first maximum of discharge happened in the second half of June (9.2 $m^3 s^{-1}$) still associated with snow melt, which occurred particularly late in 2015. After Mid-July, it was only on four occasions that values higher than 4 $m^3 s^{-1}$ were recorded along with major precipitation events. The strongest of these was on October 16, where 11.0 $m^3 s^{-1}$ were measured at the station.

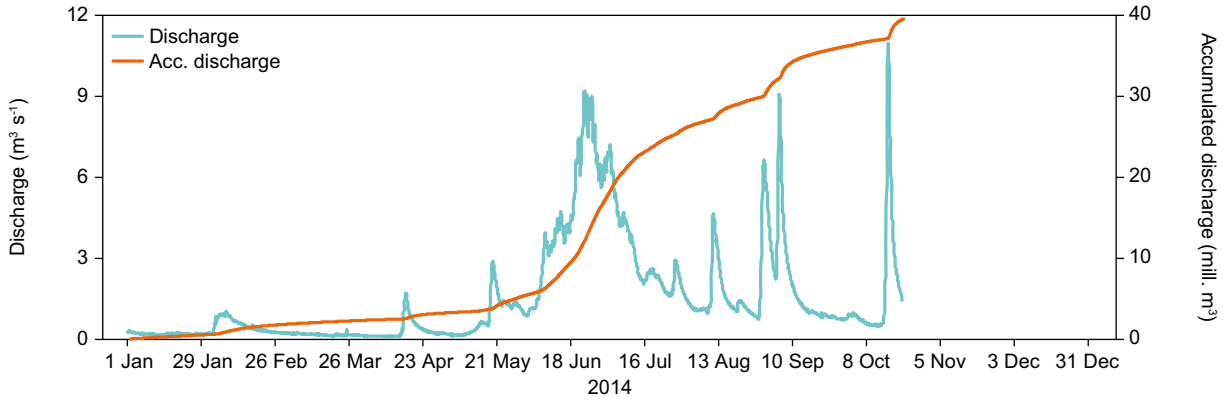

Figure 2.4 River water discharge at H1 during 2015. The blue line is the instantaneous discharge ($m^3 s^{-1}$) and refers to the left axis, the red line is the accumulated discharge over the calendar year (106 m^3) and refers to the right axis.

Data from after October 21 will be presented in the next annual report, as the divers were still in the lake and it will not be read out till summer 2016. Considering the precipitation data, it can be anticipated that the 11.0 m^3s^{-1} are the valid maximum discharge value for 2015

Table 2.4 summarizes the total discharge for the hydrological years from 2007/2008 until 2014/2015. The four latest seasons show above average discharge, and 2014-2015 is ranked fourth Interannual variations are high, the maximum year showing more than double the runoff than the minimum year. Taking the drainage basin of 31 km^2 into account, the overall water loss was 1338 mm in 2014/2015, thus slightly less than the year before.

Table 2.4 Total discharge (106 m^3) and mean water loss (mm) for hydrological years 2007-2008 to 2012-2015.

Hydrological year	Total discharge (million m^3)	Water loss (mm)
2007-2008	32,79	1058
2008-2009	40,83	1317
2009-2010	23,21	749
2010-2011	34,34	1108
2011-2012	49,06	1583
2012-2013	42,41	1368
2013-2014	42,85	1382
2014-2015	41,48	1338

3 Nuuk Basic

The GeoBasis programme

Birger Ulf Hansen, Louise Holm Christensen, Magnus Lund, Maria Libach Burup, Kerstin Krøier Rasmussen, Jakob Abermann, Mikhail Mastepanov, Andreas Westergaard and Torben Røjle Christensen

Figure 3.1 The power supply at the heath site was heavily damaged by a snow avalanche in early spring. The battery box with 3 100Ah batteries, each weighing 42 kg, was moved 100 meters into a nearby river bed and all electrical cables were torn.

The GeoBasis programme provides long term data of climatic, hydrological and physical landscape variables describing the environment in the Kobbefjord drainage basin close to Nuuk. In 2015, GeoBasis was operated by the Department of Geoscience and Natural Resource Management, Copenhagen University, in collaboration with the Department of Bioscience, Aarhus University. In 2015, GeoBasis was funded by the Danish Ministry for Climate and Energy as part of the environmental support programme DANCEA – Danish Cooperation for Environment in the Arctic. A part-time position is placed in Nuuk at Asiaq – Greenland Survey. The GeoBasis programme includes monitoring of the physical variables within snow and ice, soils, vegetation and carbon flux. The programme runs from May to the end of October with some year-round measurements from automated stations.

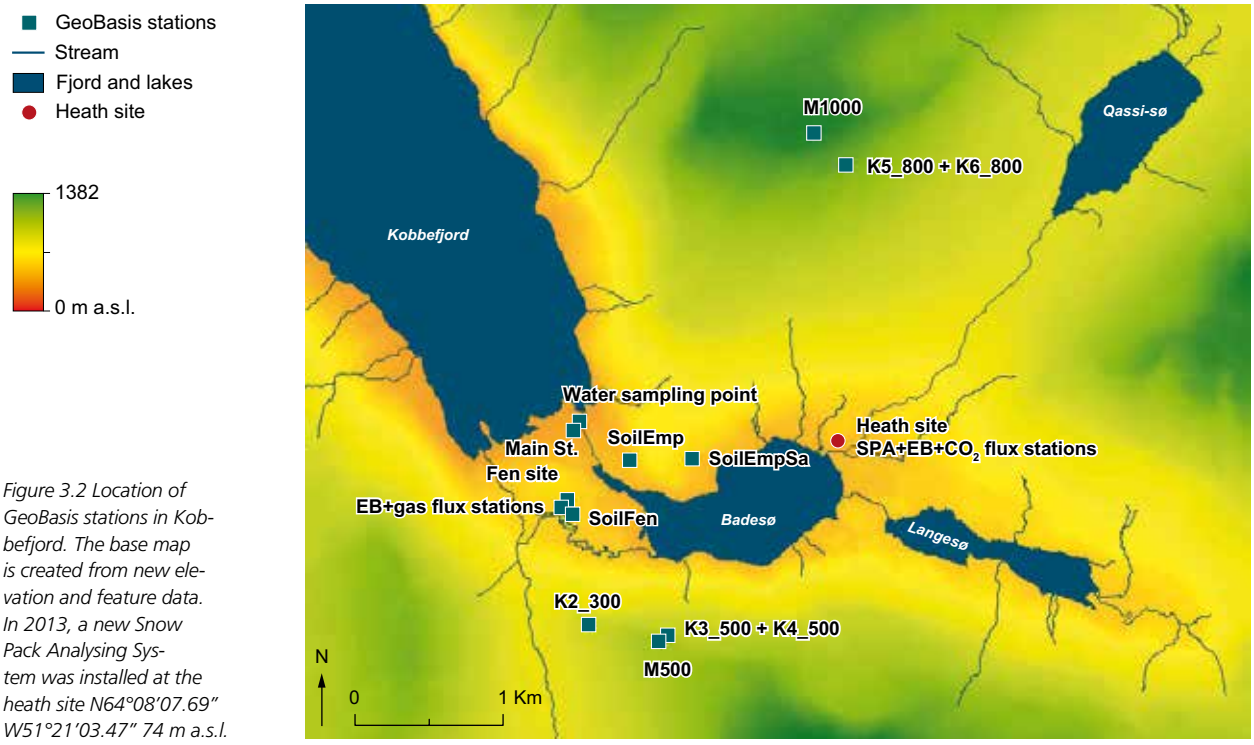

Figure 3.2 Location of GeoBasis stations in Kobbefjord. The base map is created from new elevation and feature data. In 2013, a new Snow Pack Analysing System was installed at the heath site N64°08'07.69" W51°21'03.47" 74 m a.s.l.

The 2015 season was the eighth full season for the GeoBasis programme. In 2007, the field programme was initiated during a three week intensive field campaign in August, where most of the equipment was installed, although some installations had to be postponed until 2008. Methods and sampling procedures are described in detail in a new manual 'GeoBasis Manual – Guidelines and sampling procedures for the geographical monitoring programme of Nuuk Basic in Kobbefjord', which can be downloaded from www.nuuk-basic.dk. In 2015, all data from the GeoBasis Nuuk programme were uploaded to the new GEM (Greenland Ecosystem Monitoring) database, which can be founded at http://data.g-e-m.dk/. In the coming years, the data will be regularly updated after each field season.

In 2011, Geobasis installed two new energy balance stations in cooperation with the INTERACT programme. One station was located at a new site over heath vegetation (figure 3.2.) and the second station was installed at the existing fen site (Hansen et al. 2014). The remote placing of the heath site and the use of fuel cells caused numerous breaks in the time series, although the station was visited frequently even outside the normal field season. In 2013, a more stable power supply was installed combining a wind generator with a nominal effect of 350 W and a 18 W solar panel. With that, the time-series recording at both the energy balance and the SPA stations have been more stable with only a few minor breaks.

In 2013, Geobasis installed a Snow Pack Analysing System (SPA) on the heath site close to the energy balance and CO_2 stations (figure 3.2.). The heath site was chosen as it is the dominating ecosystem within the drainage basin. The SPA constitutes an innovation in snow measurements, as it automatically and continuously measures all relevant snow parameters, such as snow depth and snow density at three levels (10, 35 and 55 cm), snow water equivalent and contents of liquid water and ice. In early spring 2015, both the SPA-station and the power supply were heavily damaged by a snow avalanche (figure 3.1 and 3.9). By mid-June, the power supply was reestablished and the SPA-station was repaired in early autumn.

Unfortunately, the micromet station, M1000, has been out of order since February 2012, although it has been repaired several times. Frequent strong winds and icing have damaged all sensors shortly after each repair, so it has now been decided to close down the station during the field season 2015. In order to minimize the number of gaps in the time series from the climate station and the two fluxstations at the fen location, two 350W wind generators and four new 100Ah batteries were added to the existing power supply of six 110W solar panels and 8 100Ah batteries

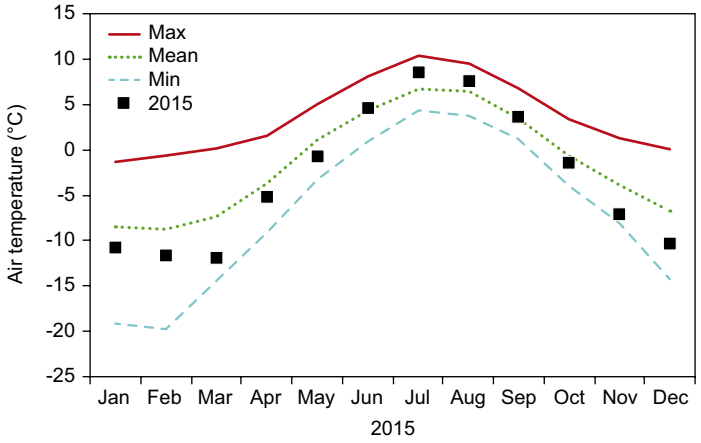

Figure 3.3 The monthly minimum, mean and maximum air temperature for the period 1866-2015 measured at Nuuk (lines solid and dashed) and monthly mean air temperature for 2015 (squares) (Cappelen, 2016).

Data collected by the Danish Meteorological Institute (figure 3.3) shows that in 2015, the annual mean air temperature in Nuuk reached -2.9 °C, which is 1.5 °C colder than normal (Cappelen, 2015). The two summer months, July-August, were both warmer than normal. The warmest month was July with 8.6 °C, which was 1.9 °C warmer than normal, but 1.8 °C colder than the July 2012, which was the warmest July in the period 1866-2016. Eight months in 2015 (January-May and October-December) were colder than normal. The coldest month in 2015 was March with -11.9 °C, which was 4.5 °C colder than normal, but 2.5 °C warmer than the record from March 1993.

3.1 Snow and ice

Snow cover extent

The first four automatic cameras were installed in 2007 at 300 and 500 m a.s.l. to monitor the snow cover extent in the central parts of the Kobbefjord drainage basin (Tamstorf et al. 2007). In September 2009, two snow-monitoring cameras K5 and K6 were installed. Both cameras were installed at position N64°9'06.25'' W51°20'46.47'' 770 m a.s.l. (figure 3.2). K5 monitors the central parts of the drainage basin with Badesø and Langsø, while K6 monitors Qassi-lake

Figure 3.4 Summer inspection of camera K3_500 (N64°7'21.46" W51°22'19.31") in mid-July 2015.The background shows the field of view for camera K3, which monitors Kobbefjord and the fen location.

in the northern valley of the drainage basin (figure 3.4). In 2011, a new camera was reinstalled at K1_300 (N64°7'26" W51°22'55") overlooking the fen area. This automatic camera takes photos three times daily March through November, and once daily during the winter months.

One of the main advantages of camera-based snow monitoring is that it is relatively insensitive to cloud cover (in contrast to satellite-based techniques). Only low clouds and foggy conditions can make the image data unsuitable for mapping purposes. A new updated and more user-friendly algorithm for snow cover monitoring has been developed in MatLab, so it is now possible to construct snow-cover depletion curves for user specified regions of interest (ROI) for each melting season on the basis of image data obtained at daily frequency. In the previous years, depletion curves for 3 regions of interest seen from K2_300 have been shown (Hansen et al. 2012), but due to technical problems it has not be possible to show any depletions curves from these ROI in 2012 and 2013.

Instead, three new ROI are shown in figure 3.5. They cover the vegetation types copse (willow with a maximum height of 1 meter), fen and dwarf shrub heath. Fen is very similar to the footprint for the CO_2-station in the fen. All ROI are covered by K1_300 and K3_500, so a future monitoring of the two ROI should be more stable. Figure 3.5 shows the snow's depletion curves for all three ROI. The DOY (day of year) for the 50% of the snow cover in the dwarf shrub heath shows a minimum (earliest) of 112, a median of 141 and a maximum (latest) of 170. For the copse ROI, the same figures were 122, 150 and 172, and for the ROI they were 122, 153 and 172. For all three ROIs, minimum depletion curves were equal to 2010 and the maximum curves were equal to 2015. The long lasting snow cover in 2015 moved the 50% snow depletion curve 10 days from the previous snow covers in the period 2010-2015. Although a measuring site in the dwarf shrub heath had the earliest DOY for 50% snow cover (ten days earlier than the two other ROI) due to a thinner layer of snow at this location, this habitat also had the widest range of days in the 50% snow cover between plots, namely 58 days (nine days more than the two other ROIs). This means that the latest 50% snow cover for a plot was more or less on the same DOY for all habitat types, namely 170-172. In 2015, the

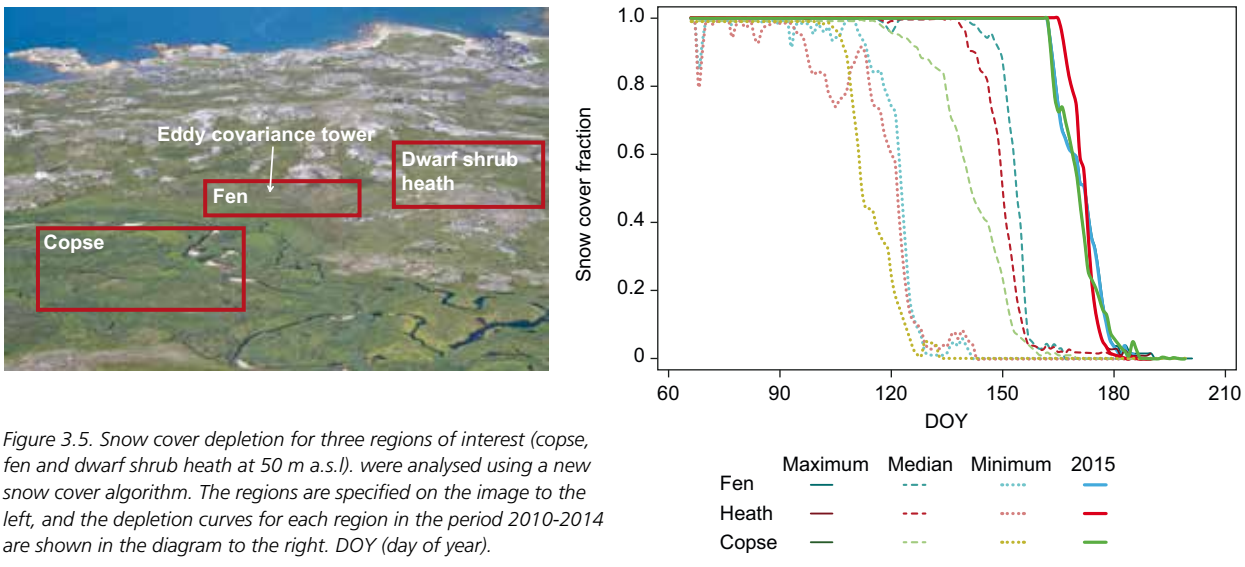

Figure 3.5. Snow cover depletion for three regions of interest (copse, fen and dwarf shrub heath at 50 m a.s.l). were analysed using a new snow cover algorithm. The regions are specified on the image to the left, and the depletion curves for each region in the period 2010-2014 are shown in the diagram to the right. DOY (day of year).

Table 3.1 Comparison of snow depth/densities (in brackets) at GeoBasis sites A-C, 2009-2015. No snow pit was dug at SoilEmpSa in 2010.

Snow survey dates	Soil Fen (A) Average depth (m) Density (kg/m³)	Soil Emp Salix (B) Average depth (m) Density (kg/m³)	Soil Emp (C) Average depth (m) Density (kg/m³)
April 15-16, 2009	0.91 (237)	0.90 (275)	1.02 (329)
April 15-16, 2010	0.20 (339)	0.19 (n.a.)	0.17 (366)
April 7-9, 2011	0.87 (364)	0.92 (297)	0.91 (383)
April 17-18, 2012	0.96 (373)	0.74 (353)	0.92 (320)
March 20-22, 2013	0.42 (316)	0.35 (311)	0.32 (282)
April 8-9, 2014	0.67 (283)	0.81 (329)	0.55 (302)
April 21-22, 2015	1.16 (324)	1.27 (353)	1.15 (387)

melting season for the copse and fen ROI started as late as DOY 162, and three days later it started at the dwarf shrub heath, which is placed a little higher in the terrain. Although all three ROI's were covered with more than 1 meter of snow, the late snow melt caused a very rapid snow melt that only lasted a fortnight, so all three ROIs ended the melting season within four days (DOY 178-182).

Snow cover

To support the studies under the Nuuk Basic monitoring programme, a snow cover survey using ground penetrating radar (GPR), combined with manual stake measurements, was carried out in the main parts of the Kobbefjord drainage basin on 21-22 April 2015. A comparison of average snow depth for the three GeoBasis sites can be seen in table 3.1. A snow depth of 119 cm as an average for the three sites is the highest snow depth measured in the period 2010-2015 – almost twice as high as the average of 66 cm. An average of 355 kg m^{-3} in density is also well above the average of 323 kg m^{-3} for the six-year period.

Even though the snow survey is carried out at nearly the same time every year, snow depth has large variations from year to year, and the maximum snow cover date also varies strongly from year to year, see figure 3.6. The snow cover in the winter 2014/2015 started on 18 October, and

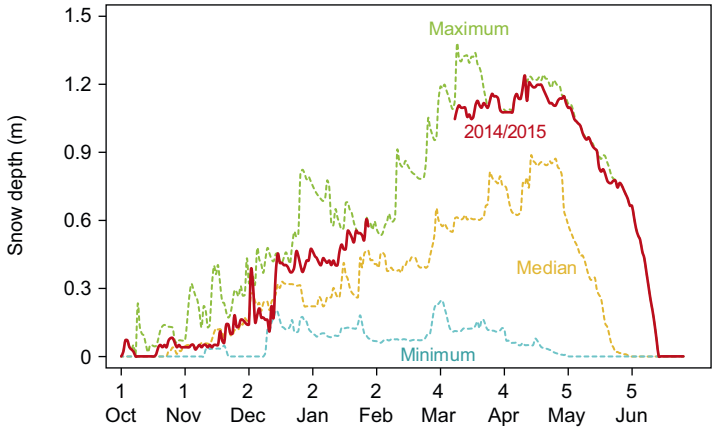

Figure 3.6 Snow depth measured at the ClimateBasis station 2009-2015.

over the following two months it reached 45 cm, where it remained for the next two months. Unfortunately, a gap in the time series occurred from 29 January to 11 March, where the snow depth might have increased from 60 cm to 105 cm. Around 14 April, the snow depth reached the maximum height of 120 cm. On 4 May, the snow melt slowly started, and over the next 45 days a steady snow melt took place, which ended on 18 June, approximately 3 weeks later than the previous year. Figure 3.6 shows the maximum (2014/2015), minimum (2009/2010) and the median for the period 2009-2015, and it is seen that the winter 2014/2015 was very close to the maximum for the period.

Table 3.2 Snow pit depth, average density, snow depth, standard deviation of the snow depth, average snow temperature and average water equivalents.

Site	Snow pit depth (cm)	Avg. density (kg m^{-3})	Snow depth (min-avg.-max) (cm)	Standard dev. of snow depth (cm)	Avg. snow temperature (°C)	Avg. water eq. (mm)
SoilFen (A1)	116	324	92-129-190	13.5	–4,7	418
SoilEmpSa (B1)	127	353	69-122-187	23.6	–1.3	431
SoilEmp (C1)	115	387	88-124-175	23.3	–1,6	480

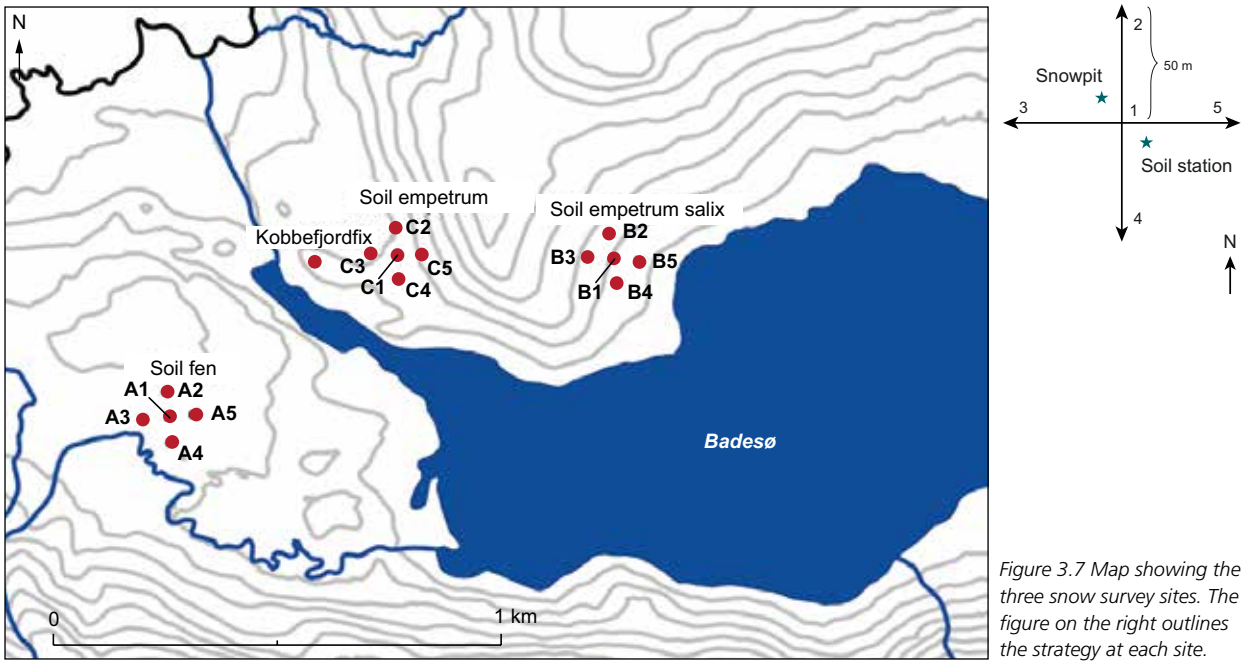

Figure 3.7 Map showing the three snow survey sites. The figure on the right outlines the strategy at each site.

Table 3.2 describes snow depths and densities at the three GeoBasis soil micro-climate stations SoilFen, SoilEmpSa and SoilEmp using ground penetrating radar (GPR) and manual stake measurements (figure 3.7). The snow survey strategy used in Kobbefjord is outlined in the 3rd Annual Report, page 18 (Hansen et al. 2010). In order to document the properties of the snowpack, snow pits were dug at SoilFen in point A1, at SoilEmpSa in point B1 and at SoilEmp in point C1 (figure 3.7). The examination of the snowpack included temperature profiling, density measurements and texture description. Table 3.2 summarizes the snow depth, density and temperature results from the three stations. The texture of the snow profile at all three sites is characterised as homogenous coarse grained snow, with densities between 324-387 kg m^{-3}. The densities are the highest measured in the period 2009-2015 (Hansen et al. 2014), and again, the normal huge variation in snow depths ranging from 69 cm to 190 cm causes a huge variation in snow water equivalents, ranging from 244 to 660 mm within few meters at SoilEmpSa.

Ice cover

Sea ice cover in Kobbefjord in the winter 2014/15 developed as late as 20 January, which is rather late compared to the previous eight years' of monitoring in Kobbefjord (table 3.3). The fjord was only ice

Table 3.3 Visually estimated dates for perennial formation (50%) of ice cover and date for break-up of ice cover on selected lakes within the Kobbefjord drainage basin and on Kobbefjord from 2007 to 2015. Dates are reported for perennial formation of ice cover in the fall and for the break-up of ice cover in the spring. Badesø is the main lake in the area and Qassi-sø is the lake at 250 m a.s.l. in the northern valley of the drainage basin.

Year	Badesø		Langsø		Qassi-sø		Kobbefjord	
	Break-up	Formation	Break-up	Formation	Break-up	Formation	Break-up	Formation
2007		23 Oct		22 Oct		22 Oct		27 Dec - 12 Feb*
2008	2 Jun	5 Nov	13 May	5 Nov.	9 Jun	4 Nov	17 May	no data
2009	13 Jun	1 Nov	11 June	6 Oct.	22 Jun	10 Oct	4 Jun	12 Feb
2010	14 May	22 Nov	18 May	31 Oct	24 May	6-11 Nov	2 Jun	23 Nov
2011	18 Jun	22 Oct	no data	no data	28 Jun	20 Oct	23 May	16 Nov
2012	9 Jun	15 Nov	no data	10 Nov	18 Jun	11 Nov	22 May	24 Feb
2013	14 Jun	24 Oct	13 Jun	23 Oct	22 Jun	26 Oct	26 Apr	15 Oct
2014	10 Jun	12 Nov	16 Jun	22 Oct	20 Jun	21 Oct	1 Jun	20 Jan
2015	2 Jul	24 Oct	1 Jul	22 Oct	13 Jul	19 Oct	15 Jun	17 Dec
2016	18 May						17 Apr	

*indicate no data in the period and the formation of ice cover took place within the period.

free on 15 June, which is nearly 15 days later than normal for the 7 previous years.

In 2014/15, the ice cover was already formed on 21 October on Qassi-sø (250 m a.s.l.) and it was formed 3 weeks later on Badesø (30 m a.s.l.). In the spring 2015, the ice cover broke up on Badesø and Langsø around 1 July, which is rather late compared to previous years, and as usual the ice cover on Qassi-sø broke up 14 days later than the ice cover on Badesø. The difference in the period of ice cover is due to the difference in elevation of the two lakes.

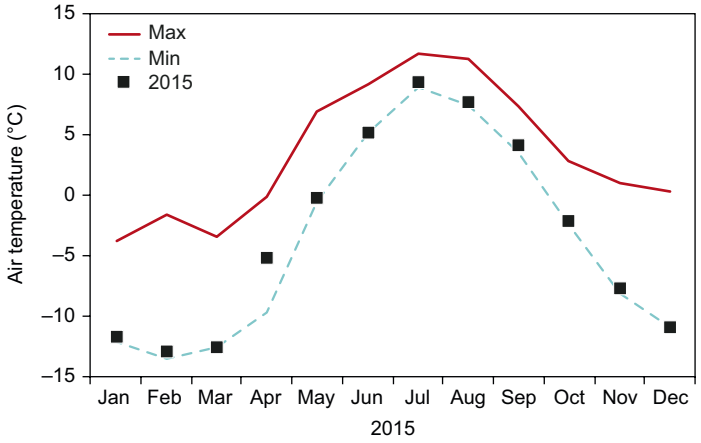

Figure 3.8 Monthly mean air temperatures in 2015 (square), maximum (red line), average (thin line) and minimum (dashed line) monthly mean air temperatures from 2012-2015. Measured at the SoilFen station 2.5 meter above ground.

Micrometeorology

Table 3.4 reports the monthly mean air temperature, relative humidity, surface temperature and soil temperature measured at SoilFen 2012-2015 (monthly data for the period 2007-2011 can be found in previous annual reports). February 2015 was the coldest month with -12.9 °C, while July with 9.3 °C was the warmest month. In general, 2015 was a cold year, and March, June and December set new minimum records for the station with respectively -12.5, 5.2 and -10.9 °C, while the rest of the months in 2015 were only 0.5-1.0 degrees above the previous minimum records. These measurements are in line with the air temperature measured in Nuuk located 30 km away (figure 3.1).

For the GeoBasis monitoring period 2007–2015, the minimum monthly mean air temperature was -13.5 °C measured at SoilFen in February 2008 and the maximum monthly mean air temperature was 11.7 °C measured in July 2012.

The micrometeorological station M500 measured air temperature, relative humidity, surface temperature and shortwave irradiance are presented in table 3.5 (monthly data for the period 2007-2011 can be found in Hansen el al. 2014). M500 is placed approximately 500 m a.s.l. south of Badesø. These measurements are in line with the air temperature measured in Nuuk located 30 km away (figure 3.1) and at SoilFen 1 km away (figure 3.8). In 2008-2015, the mean air temperature in July at the M500 station was between 6.6 °C and 10.4 °C, in 2015 it was only 8.8 °C, only +0.3 °C above the average for the period. The relative humidity measured at the M500 station in the period 2008-2015 shows an annual average of 77% with maximum values of 90-91% during the snow melt in April and in the cold rainy autumn from September to November. The incoming shortwave irradiance in the period 2008-2015 was between 211-295 W m^{-2} in June, and in 2015 it was 218 W m^{-2} or 24 W m^{-2} below the average. As an average, the annual shortwave irradiance was 102 W m^{-2} for the period 2008-2015. Unfortunately, the micromet station, M1000, has been out of order since February 2012. Although it has been repaired several times, frequent strong winds and icing have damaged all sensors shortly after each repair, so it has now been decided to close the station.

3.2 Soil

Physical soil properties

The results of selected parameters for the soil stations SoilFen, SoilEmp and SoilEmpSa are presented in tables 3.4, 3.6 and 3.7 (monthly data for the period 2008-2011 can be found in Hansen el al. 2014). The difference in soil properties that were detected in previous years between the three locations are also seen in the data collected in 2015, i.e. higher winter soil temperatures at SoilFen than at SoilEmp and SoilEmpSa, as the snow depth at SoilFen was significantly higher. During summer, the soil temperatures at SoilFen were significantly higher, as the site is more protected from cold winds from Kobbefjord and Badesø. At SoilFen, the temperature in 30 cm depth was less affected by fluctuations in surface temperature than at SoilEmp and SoilEmpSa, where the soil is well-drained. The results of the measured soil water content showed markedly lower values for the well-drained soil at SoilEmp than at SoilEmpSa. The summer season (June-September) mean soil moisture was 20-24% at SoilEmp and 34-36% at SoilEmpSa in the period 2008-2015. At all three soil stations,

Table 3.4 Air temperature, relative humidity, surface temperature and soil temperature at six depths (1 cm, 5 cm, 10 cm, 30 cm, 50 cm and 75 cm) from the SoilFen station in the fen area from January 2012 to October 2015.

Month - year	Air temp. 2.5 m (°C)	Rel. hum. 2.5 m (%)	Surface temp. 0 m (°C)	Soil temp. –1 cm (°C)	Soil temp. –5 cm (°C)	Soil temp. –10 cm (°C)	Soil temp. –30 cm (°C)	Soil temp. –50 cm (°C)	Soil temp. –75 cm (°C)
2012									
January	–8.8	70.6	–11.2	–0.7	–0.7	–0.6	0.1	0.4	0.8
February	–7.8	74.0	–9.8	–0.4	–0.4	–0.4	0.1	0.3	0.7
March	–11.1	73.2	–12.2	–1.2	–1.1	–0.9	0.0	0.2	0.6
April	–1.7	81.0	–2.7	–0.1	–0.1	–0.1	0.1	0.3	0.6
May	3.2	78.8	2.7	1.0	0.3	0.0	0.2	0.3	0.6
June	9.2	74.4	11.2	11.3	9.3	6.6	1.3	1.1	1.0
July	11.7	78.7	13.2	14.7	14.1	13.0	8.6	7.5	5.9
August	9.3	80.2	9.8	11.4	11.3	11.0	9.3	8.7	7.7
September	6.0	76.3	5.7	6.2	6.4	6.6	6.8	6.8	6.5
October	2.6	72.4	1.6	1.6	1.8	2.2	3.4	3.7	4.1
November	–3.3	71.2	–4.4	–0.4	–0.2	0.2	1.7	2.0	2.5
December	–6.2	68.8	–8.3	–0.4	–0.3	–0.1	0.9	1.2	1.6
2013									
January	–6.2	65.2	–7.7	–0.7	–0.6	–0.3	0.6	0.8	1.3
February	–7.4	69.7	–8.4	–0.9	–0.7	–0.5	0.4	0.6	1.0
March	–3.4	67.9	–4.3	–0.5	–0.4	–0.3	0.3	0.5	0.9
April	–1.3	63.8	–1.4	–0.2	–0.2	–0.1	0.4	0.5	0.8
May	–0.6	69.9	0.0	0.0	0.0	0.0	0.3	0.5	0.8
June	6.1	76.3	7.6	7.3	5.6	3.7	1.3	1.2	1.1
July	8.9	74.4	10.2	11.9	11.3	10.3	6.7	5.8	4.7
August	7.9	71.5	8.5	10.0	10.0	9.8	8.5	8.0	7.0
September	4.2	81.0	4.2	4.6	4.7	4.8	5.2	5.2	5.2
October	0.5	77.0	0.2	0.5	0.9	1.3	2.8	3.1	3.4
November	–4.1	72.8	–4.8	–0.6	–0.4	–0.1	1.1	1.4	1.9
December	–8.8	69.2	–9.7	–0.6	–0.5	–0.3	0.7	0.9	1.3
2014									
January	–6.6	64.7	–7.7	–0.6	–0.5	–0.4	0.5	0.7	1.0
February	–9.1	70.1	–9.7	–0.9	–0.8	–0.5	0.3	0.5	0.9
March	–9.4	70.2	–9.1	–0.7	–0.7	–0.5	0.2	0.4	0.7
April	–6.6	70.3	–6.0	–0.4	–0.3	–0.3	0.2	0.4	0.7
May	2.1	73.4	–	0.0	0.0	0.0	0.3	0.4	0.7
June	7.6	73.5	–	7.7	5.8	3.7	0.9	0.9	0.9
July	10.7	71.4	–	13.3	12.5	11.2	6.8	5.9	4.6
August	9.8	74.7	–	11.4	11.3	10.9	8.9	8.3	7.2
September	4.3	73.7	–	5.1	5.4	5.7	6.3	6.3	6.1
October	–0.4	70.9	–	1.0	1.2	1.5	2.8	3.1	3.5
November	–4.5	68.2	–	–0.3	–0.1	0.1	1.3	1.6	2.0
December	–7.2	72.6	–	–0.3	–0.2	–0.1	0.7	1.0	1.4
2015									
January	–11.7	66.9	–	–0.3	–0.3	–0.2	0.6	0.8	1.1
February	–12.9	74.7	–	–0.2	–0.2	–0.2	0.5	0.6	1.0
March	–12.5	75.4	–	–0.1	–0.2	–0.1	0.5	0.6	0.9
April	–5.2	73.6	–	–0.1	–0.1	0.0	0.5	0.6	0.9
May	–0.2	72.4	–	0.0	0.0	0.1	0.5	0.6	0.9
June	5.2	75.1	–	2.5	1.8	1.3	0.7	0.8	0.9
July	9.3	73.3	–	13.4	12.7	11.7	7.6	6.6	5.1
August	7.7	76.5	9.6	9.9	9.7	9.4	7.9	7.5	6.6
September	4.1	79.6	4.7	5.1	5.3	5.5	5.9	5.9	5.7
October	–2.1	71.1	–4.2	0.2	0.4	0.8	2.3	2.7	3.1
November	–7.7	67.0	–10.6	–0.6	–0.3	0.0	1.0	1.3	1.8
December	–10.9	66.5	–13.9	–1.2	–1	–0.6	0.5	0.8	1.2

Table 3.5 Air temperature, relative humidity, surface temperature and shortwave irradiance measured at the M500 station from January 2012 to December 2015.

Month-year	Air temp. 2.5 m (°C)	Rel. hum. 2.5 m (%)	Surface irradiance temp. 0 m (°C)	Shortwave irradiance 2.5 m (W m^{-2})
2012				
January	–11.3	74.8	–13.7	6.5
February	–10.2	81.7	–12.3	29.0
March	–13.1	78.3	–14.9	72.8
April	–4.0	90.0	–5.1	134.6
May	1.2	82.5	0.2	192.3
June	8.7	68.2	11.1	265.9
July	10.4	74.9	12.2	194.6
August	7.5	79.5	7.4	131.6
September	2.7	85.2	1.8	60.4
October	–0.4	78.5	–2.9	31.3
November	–6.1	77.2	–8.4	8.7
December	–7.3	68.7	–11.7	3.0
2013				
January	–8.4	66.9	–12.1	6.8
February	–10.3	77.8	–12.9	28.5
March	–4.7	64.5	–8.3	80.2
April	–4.0	68.5	–6.1	155.4
May	–4.3	82.3	–5.0	204.8
June	3.8	80.2	5.7	230.6
July	6.6	76.2	7.7	201.5
August	5.6	73.1	6.2	155.3
September	0.9	90.0	–0.6	58.6
October	–1.4	77.8	–4.4	34.5
November	–6.8	81.0	–9.4	9.7
December	–11.0	75.3	–13.9	2.8
2014				
January	–8.6	67.3	–12.6	5.7
February	–10.9	75.9	–13.4	24.6
March	–12.2	79.7	–14.1	79.8
April	–9.7	82.3	–11.6	157.7
May	–0.7	81.2	0.9	230.0
June	6.0	74.4	8.2	231.9
July	9.5	66.8	11.1	232.2
August	7.8	75.0	8.2	146.8
September	0.6	85.9	0.0	59.3
October	–3.0	75.0	–5.5	32.6
November	–6.2	69.2	–10.3	11.0
December	–10.0	82.8	–11.8	2.4
2015				
January	–14.9	77.6	–16.9	6.2
February	–15.4	84.1	–16.6	27.8
March	–14.9	83.9	–15.8	75.0
April	–8.0	83.4	–9.5	153.1
May	–3.6	83.0	–4.5	215.2
June	4.1	72.3	4.3	265.2
July	7.8	69.8	10.9	237.6
August	6.1	72.4	6.4	157.5
September	0.9	87.5	0.1	73.6
October	–4.9	80.0	–7.5	33.2
November	–10.0	70.1	–13.6	11.1
December	–13.5	76.1	–16.4	3.5

Table 3.6 Soil temperature and soil moisture at four depths measured at SoilEmp from January 2012 to December 2015.

Month-year	Soil temp. –1 cm (°C)	Soil temp. –5 cm (°C)	Soil temp. –10 cm (°C)	Soil temp. –30 cm (°C)	Soil moist. –5 cm (%)	Soil moist. –10 cm (%)	Soil moist. –30 cm (%)	Soil moist. –50 cm (%)
2012								
January	–2.5	–2.4	–2.3	–2.0	2.9	8.7	3.6	4.1
February	–1.7	–1.6	–1.6	–1.5	3.2	10.3	3.7	4.2
March	–3.8	–3.7	–3.5	–3.1	2.8	8.5	3.4	4.0
April	–0.1	–0.2	–0.2	–0.3	3.6	12.9	3.8	4.3
May	1.0	0.9	0.7	0.2	19.5	27.9	19.0	17.5
June	11.3	10.5	10.0	8.2	17.3	40.1	25.7	22.9
July	13.3	12.8	12.4	11.3	7.7	32.5	16.3	13.0
August	10.6	10.4	10.3	9.9	16.3	39.6	23.6	20.3
September	5.9	6.1	6.2	6.4	25.4	41.7	25.6	23.5
October	2.0	2.1	2.3	2.6	31.7	46.1	35.6	32.9
November	–1.2	–0.9	–0.7	0.0	11.9	20.5	21.4	19.0
December	–1.7	–1.5	–1.4	–0.8	4.6	10.8	7.5	5.8
2013								
January	–3.3	–3.2	–3.0	–2.5	4.1	9.1	6.5	4.4
February	–3.4	–3.3	–3.2	–2.8	4.0	9.0	6.4	4.2
March	–2.3	–2.3	–2.3	–2.2	4.1	9.6	6.3	4.1
April	–0.7	–0.6	–0.6	–0.5	4.4	11.5	7.7	6.0
May	0.5	0.3	0.1	0.0	22.9	30.5	10.4	13.7
June	8.9	8.0	7.5	5.8	18.5	39.8	28.7	24.8
July	10.8	10.2	9.9	8.9	7.1	31.7	9.5	6.9
August	9.3	9.2	9.2	8.8	8.9	22.1	12.0	10.0
September	4.3	4.3	4.4	4.4	38.8	48.1	40.9	37.2
October	0.0	0.4	0.6	1.2	20.4	33.3	28.5	22.8
November	–2.6	–2.3	–2.0	–1.0	6.6	13.2	12.6	9.2
December	–1.5	–1.3	–1.2	–0.8	5.0	12.6	9.7	6.5
2014								
January	–1.9	–1.8	–1.7	–1.4	4.3	10.7	6.7	4.7
February	–2.8	–2.6	–2.5	–2.1	4.1	10.2	6.4	4.5
March	–3.3	–3.2	–3.1	–2.9	4.0	9.7	6.2	4.2
April	–2.0	–2.0	–2.0	–1.9	4.1	10.3	6.2	4.2
May	0.6	0.3	0.2	0.0	9.9	19.2	11.4	10.7
June	8.5	7.6	6.9	5.1	20.9	40.8	31.5	25.1
July	12.1	11.3	10.8	9.5	8.4	27.7	18.1	14.6
August	10.6	10.4	10.2	9.7	5.3	18.4	9.3	6.8
September	4.6	4.8	5.0	5.3	16.5	36.0	26.5	21.8
October	0.8	1.1	1.3	1.7	13.9	35.0	20.5	15.9
November	–2.2	–1.8	–1.5	–0.5	3.2	8.1	7.4	6.2
December	–1.7	–1.5	–1.3	–0.8	3.9	9.8	5.9	5.1
2015								
January	–1.1	–1.0	–0.9	–0.6	5.3	12.8	6.2	5.6
February	–0.7	–0.7	–0.6	–0.6	9.5	18.8	10.6	8.6
March	–1.6	–1.5	–1.4	–1.1	6.5	12.7	8.6	5.9
April	–0.8	–0.8	–0.8	–0.7	6.7	13.9	8.4	5.5
May	0.0	0.0	0.0	–0.1	7.8	18.9	8.8	5.8
June	2.8	2.5	2.1	1.2	18.2	31.9	17.0	17.5
July	11.5	10.8	10.4	9.2	6.9	26.4	15.9	12.2
August	9.3	9.1	8.9	8.4	7.6	27.9	11.0	8.3
September	4.5	4.8	4.9	5.2	17.0	39.5	24.1	20.1
October	0.1	0.3	0.5	1.1	17.2	35.9	23.2	19.9
November	–3.4	–3.1	–2.5	–1.1	3.3	9.8	8.5	5.9
December	–4.1	–3.9	–3.6	–2.8	2.7	8	6.5	4.4

Table 3.7 Soil temperature and soil moisture at four depths measured at SoilEmpSa from January 2012 to December 2015.

Month-year	Soil temp. –1 cm (°C)	Soil temp. –5 cm (°C)	Soil temp. –10 cm (°C)	Soil temp. –30 cm (°C)	Soil moist. –5 cm (%)	Soil moist. –10 cm (%)	Soil moist. –30 cm (%)	Soil moist. –50 cm (%)
2012								
January	–0.9	–0.7	–0.9	–0.5	21.3	13.4	15.6	32.2
February	–0.6	–0.5	–0.6	–0.4	23.1	14.0	15.8	22.2
March	–1.6	–1.3	–1.5	–1.0	20.0	12.5	14.5	17.0
April	0.0	0.0	0.0	0.0	27.2	14.9	16.2	17.3
May	0.6	0.2	0.3	0.1	45.1	26.4	18.0	18.8
June	8.6	6.3	7.1	5.7	58.8	45.5	44.4	37.6
July	11.9	10.6	11.2	10.2	57.6	42.3	44.9	42.7
August	10.2	9.7	9.8	9.6	59.5	49.7	46.1	47.7
September	6.6	6.8	6.7	6.9	58.9	48.5	45.6	45.7
October	2.8	3.1	3.0	3.1	60.4	56.7	46.8	50.0
November	–0.1	0.4	0.3	0.5	52.8	50.9	46.4	49.2
December	–0.8	–0.2	–0.4	0.0	27.0	30.0	44.3	41.9
2013								
January	–1.4	–0.8	–1.2	–0.4	21.6	14.1	35.6	35.3
February	–2.2	–1.6	–2.0	–1.1	19.6	13.2	14.7	25.8
March	–1.3	–1.0	–1.1	–0.8	21.1	14.4	14.8	16.1
April	–0.1	–0.1	–0.1	–0.1	25.8	15.4	16.0	16.9
May	0.2	0.0	0.0	0.0	30.5	16.8	17.3	17.8
June	4.4	1.6	2.5	1.1	58.7	40.7	32.3	23.9
July	9.1	7.2	8.0	6.7	57.6	39.9	45.2	44.0
August	9.0	8.4	8.7	8.2	55.2	35.1	43.8	38.9
September	4.5	4.5	4.5	4.5	60.4	56.7	46.5	46.4
October	1.2	1.5	1.5	1.6	60.3	53.3	46.8	49.9
November	–1.1	–0.3	–0.5	–0.1	31.1	21.7	45.1	43.4
December	–1.2	–0.6	–0.8	–0.3	24.6	20.1	39.0	41.3
2014								
January	–1.7	–1.4	–1.6	–0.9	20.3	13.9	15.0	24.8
February	–2.5	–2.2	–2.5	–1.7	19.2	13.4	14.3	15.9
March	–2.3	–2.1	–2.3	–1.8	18.9	13.1	14.1	15.2
April	–1.1	–1.1	–1.1	–0.9	20.0	13.5	14.3	15.3
May	0.3	0.1	0.1	0.0	29.0	16.3	15.9	16.1
June	4.7	2.0	3.0	1.2	59.9	44.2	33.2	23.3
July	9.3	7.3	8.0	6.6	57.9	42.4	45.5	45.8
August	10.0	9.1	9.4	8.8	56.7	39.6	44.7	42.2
September	5.2	5.4	5.4	5.5	59.9	53.8	46.0	48.1
October	1.3	1.7	1.6	1.7	60.5	54.1	46.6	50.1
November	–0.7	–0.1	–0.3	0.1	30.3	26.2	44.7	44.4
December	–0.8	–0.4	–0.6	–0.1	22.9	15.1	43.6	37.7
2015								
January	–0.9	–0.6	–0.8	–0.3	22.3	14.5	31.8	35.0
February	–0.8	–0.6	–0.6	–0.6	25.9	17.6	23.4	34.7
March	–1.1	–0.8	–0.9	–0.7	22.8	14.3	16.7	32.9
April	–0.4	–0.3	–0.3	–0.3	25.3	15.4	16.7	31.7
May	0.2	0.2	0.2	0.2	31.3	18.2	19.6	37.6
June	1.3	0.9	1.0	0.7	45.8	30.8	24.0	43.0
July	9.8	8.2	8.8	7.7	57.0	38.7	45.9	42.7
August	8.7	7.9	8.1	7.7	57.7	42.1	45.6	42.8
September	5.1	5.3	5.2	5.3	60.4	53.7	47.2	49.1
October	0.7	1.3	1.2	1.4	59.9	51.2	46.9	49.1
November	–0.8	–0.1	–0.3	0.0	31.7	27.6	45.2	44.3
December	–2.2	–1.1	–1.5	–0.6	20.5	13.7	31.9	37.4

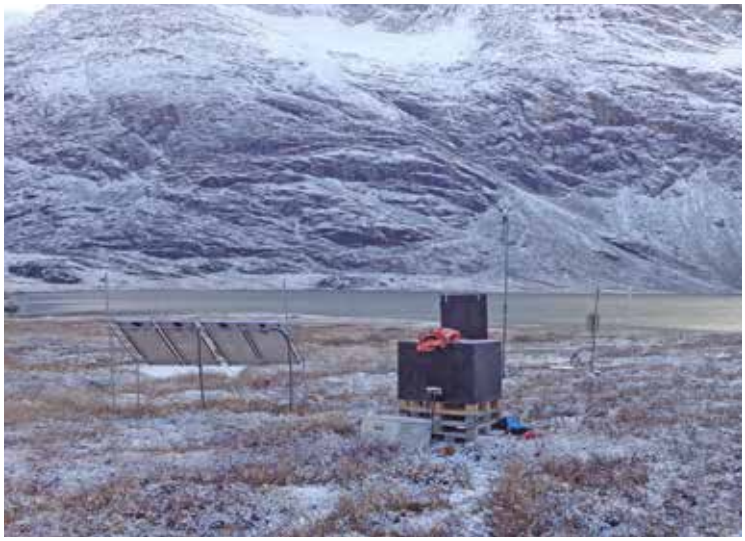

Figure 3.9 In early spring 2015, both the SPA-station and the power supply were heavily damaged by a snow avalanche (figure 3.1). By mid-June, the power supply was re-established and the SPA-station was repaired in early autumn. The picture shows the new power supply established inside the black wooden box, which has been raised above the ground.

the soil was 4 °C colder in June than most of the years in the period 2008-2015 due to a colder and more prolonged winter season in 2014/2015.

Throughout the season, soil water was collected from two depths at three characteristic soil profiles representing the dominating plant communities in the drainage basin. During the period 20 June to 1 October 2015, thirty soil water samples were collected from the soil water stations at SoilFen (10 and 80 cm).

At the research house in Kobbefjord, measurements of pH, temperature and conductivity were carried out on each sample. In August 2011, laboratory equipment was installed in the research house, which enabled analyses of soil water alkalinity. After the field season, the soil water samples were analysed for all major anions and cations as well as for dissolved organic carbon content, and all data can now be downloaded from the database.

River water

In 2015, forty-two water samples were collected from mid-June to start October, which is a field season one month shorter than the previous year due to a very late snow/ice melt. In situ measurements of river water temperature, conductivity and pH were conducted along with the water sampling. The measured values are presented in figure 3.10. The water temperature varied through the season 2015, as it did in the previous years (Hansen et al. 2014). The minimum river water temperature was 1-2 °C from mid-June, which was 1.0 °C lower than the previous years, and the water temperature peaked with a maximum temperature of 12.5 °C in the beginning of August, which was 1.9 °C lower and 2 weeks later than in 2014. The conductivity measurements showed a normal decrease in conductivity within the snow melting period from 19 µSc m^{-1} to a level of 15.5 +/- 1.5 µSc m^{-1}. From the beginning of July and through the rest of the field season, the conductivity showed no significant trend, which is normal for the period. pH showed a normal trend from 7.2 in the beginning of the field season – dropping fast to a more stable value around 6.7 with minor fluctuations over the summer season due to rain events.

3.3 Vegetation

Vegetation in the Kobbefjord area is monitored both by the BioBasis and GeoBasis programmes. While BioBasis monitors individual plants and plant phenology using plot scale sites and transects, the GeoBasis programme monitors the phenology of the vegetation communities from satellite.

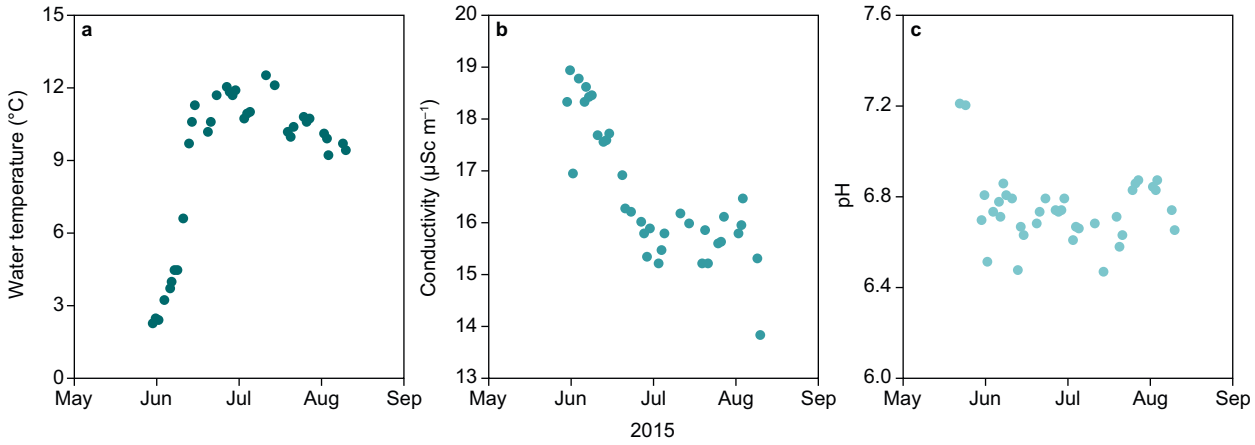

Figure 3.10 a) water temperatures, b) conductivity and c) pH measured in 2015 in Kobbefjord river at the water sampling point near the research station.

Satellite imagery

Unlike the previous years, it was not possible to acquire QuickBird, WorldView or Aster image data due to cloudy conditions in the requested period (optimum of growing season in end of July). Instead, a Landsat8-scene was acquired from 2 August at around 14:30 GMT. The scene was geometrically corrected with RPC and known ground control points from former campaigns in Kobbefjord (30 GCP also used to correct previous QuickBird scenes). Moreover, it was orthorectified using the 10 m digital elevation model. Furthermore, it was atmospherically corrected using a dark object subtraction approach and data was converted from digital numbers to top of atmosphere reflectance. Finally, NDVI was derived from the reflectance (see figure 3.11) and average NDVI was extracted from regions of interest covering a fell field, an open mixed heath, an *Empetrum nigrum* dominated heath, a fen, a copse and the heath monitored by the INTERACT station (see figure 3.12). Over the seven years, Fell field had significantly lower NDVI-values around 0.15±0.07, while copse had significant higher values around 0.57±0.13 all eight years. The four other vegetation classes had NDVI-values around 0.36-0.40 ± 0.09. As also noticed from ground truth measurements of NDVI (BioBasis, 2013), higher NDVI values were observed in 2013 than 2011 and 2012, probably as a result of the shrubs recovering from the Eurois occulta larvae attack in 2011 combined with a more dominating understory resulting from the decreased competition from shrubs during the attack. The higher NDVI values were most prominent in heaths as expected.

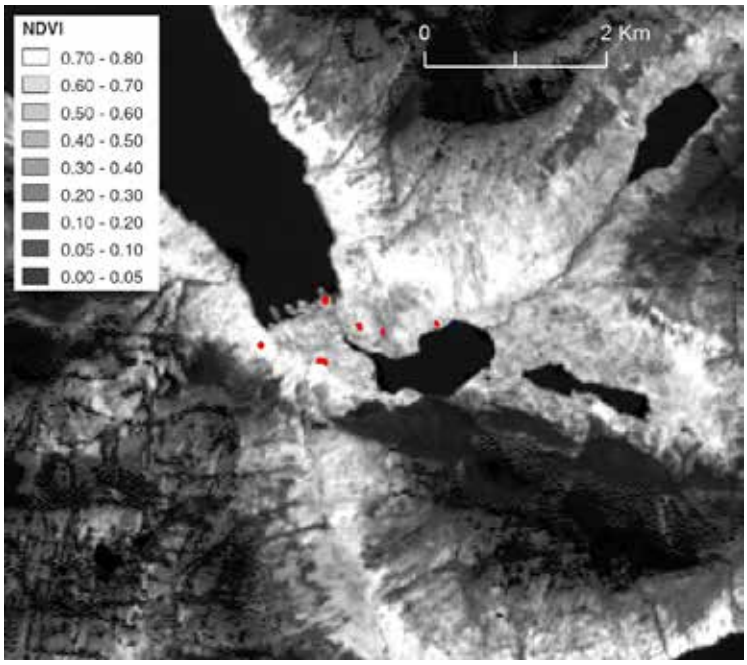

Figure 3.11 Normalised Difference Vegetation Index (NDVI) based on a Landsat8 scene from 2 August 2015. Data are dark subtracted as atmospheric correction and lack the topographic correction.

Digital camera imagery

Phenology studies of Arctic ecosystems are still dependent on spatial scale and quality (e.g. percent cloud cover) of the image data. Furthermore, the sparse vegetation and heterogeneous surface can be difficult to trace with coarse spatial resolution NDVI. Greatly improved spatial and temporal scale can be achieved by monitoring the ecosystems with automated digital cameras. Better still, image data can thus be acquired under cloudy conditions, which is advantageous in Arctic ecosystems with short intense growing seasons, where a high frequency of data is important. Major

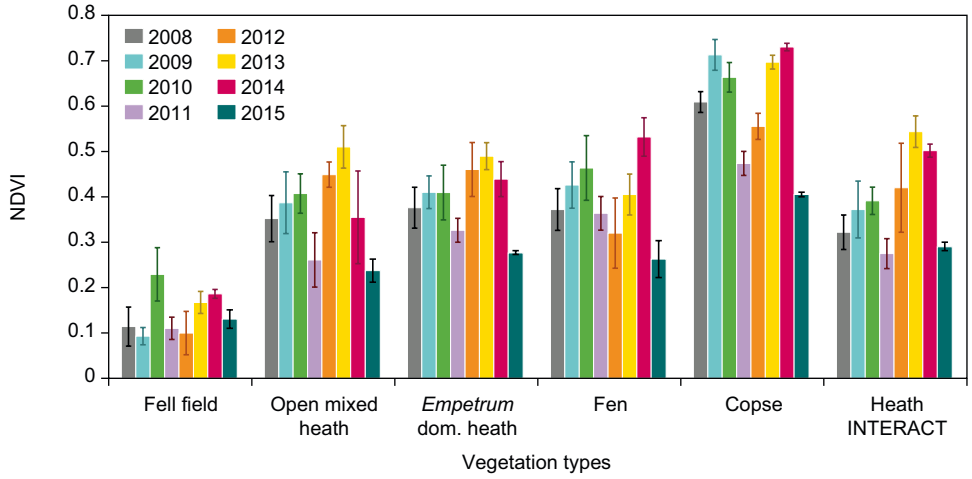

Figure 3.12 NDVI from 17 July 2008 and 2009, 10 July 2010, 14/30 July 2011, 25 July 2012, 28 July 2013, 14 July 2014, 2 August for the six different vegetation types. Note that changes between greenness are due not only to phenology differences between years, but also to seasonal phenology, as the images are acquired approx. 2 weeks around the maximum greenness dates.

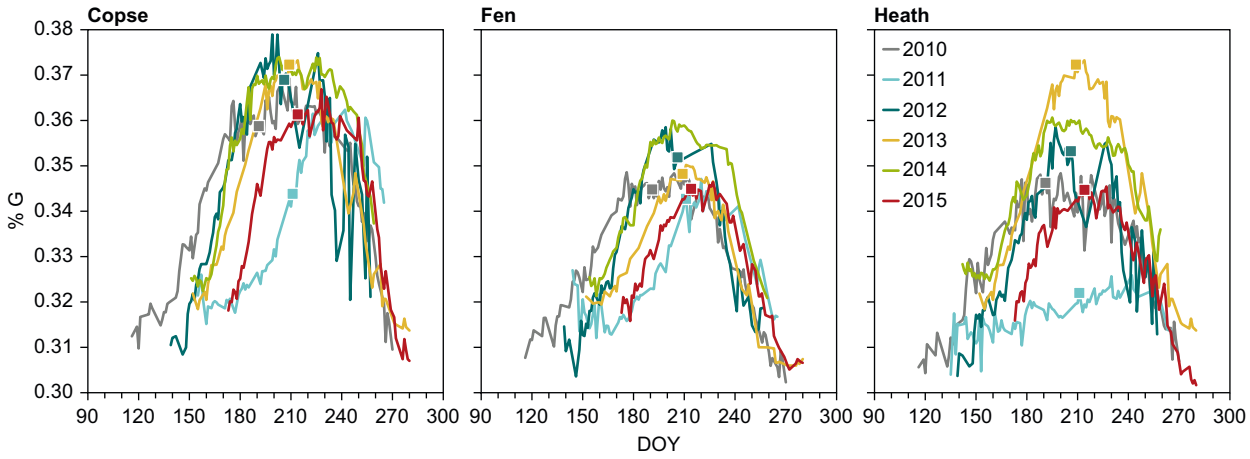

Figure 3.13 Greenness index for three ecosystems, copse, fen and heath, at 50 m a.s.l. have been analysed using a new greenness index, %G. The regions are specified in figure 3.5 left, and the fen area is very similar to the footprint for the CO_2- station in the fen. The %G for all three ecosystems in the period 2010-2015 is shown in the figure. The small squares represent the days for the satellite measurements. DOY (day of year).

challenges when using digital cameras are compensating for changes in incoming radiation as well as having the limitation of low spectral resolution. Even so, indices based on visual bands available from unmodified digital cameras have been found to correlate with NDVI over numerous types of ecosystems. However, of the few existing studies, none investigate the performance in Arctic environments with high variability in species composition. The use of conventional RGB cameras as a tool to monitor landscape wide phenology has gained a lot of attention over the past few years. Mostly, a measure of canopy greenness for a region of interest (ROI) has been used to produce yearly time series, reflecting canopy phenology. The use of RGB prevents the use of established vegetation indices, such as NDVI or RVI. However, since photosynthesis by vegetation is related to chlorophyll content and biomass in various vegetation types, we hypothesize that indices based on the excess of the green channel can describe seasonal growth patterns in vegetation. The most common is a greenness index, calculated as Percent Greenness,%G = DN(G) / (DN(R)+DN(G)+DN(B)), where DN is the digital value in each of the RGB channels. Figure 3.13 shows the significantly lower%G-values in 2011 due to the outbreaks of *Eurois occulta* larvae, but the figure also shows that all three ecosystems in 2013 seem to have recovered from the outbreak. Figure 3.13 also shows that copse had a fast and earlier greenness compared to fen and heath, but all three ecosystems reached the maximum within the same week in ultimo July. In 2015, the%G-values for all three sites started almost 3 weeks later than normal due to the late snow cover, and they reached rather low maximum values in late summer and autumn.

3.4 Carbon gas fluxes

Carbon gas fluxes are monitored on plot and landscape level in a fen area in Kobbefjord using two techniques:

- Automatic chamber measurements of CH_4 and CO_2 exchange on plot scale
- Eddy covariance measurements of CO_2 and H_2O exchange on landscape scale

Automatic chamber measurements

An automatic chamber system consisting of six flux chambers for monitoring the exchange of CH_4 and CO_2 was installed in the fen in August 2007 (Tamstorf et al. 2008). In 2015, measurements started 28 June and lasted until 17 October (figure 3.14), with ca. 2% data loss due to maintenance, calibration and preventive system close-downs (e.g. due to expected high winds that may break chamber lids).

The spatial and temporal variation in CH_4 emissions is primarily related to temperature, water table depth and primary production. The fen in Kobbefjord is a source of CH_4 due to the permanently wet conditions that promote anaerobic decomposition, by which CH_4 is an end product.

Mean CH_4 fluxes were initially relatively high, peaking around 7 July with maximum values above 6 mg CH_4 m^{-2} h^{-1}. This mid-season peak is of similar magnitude as last year; however, it occurred

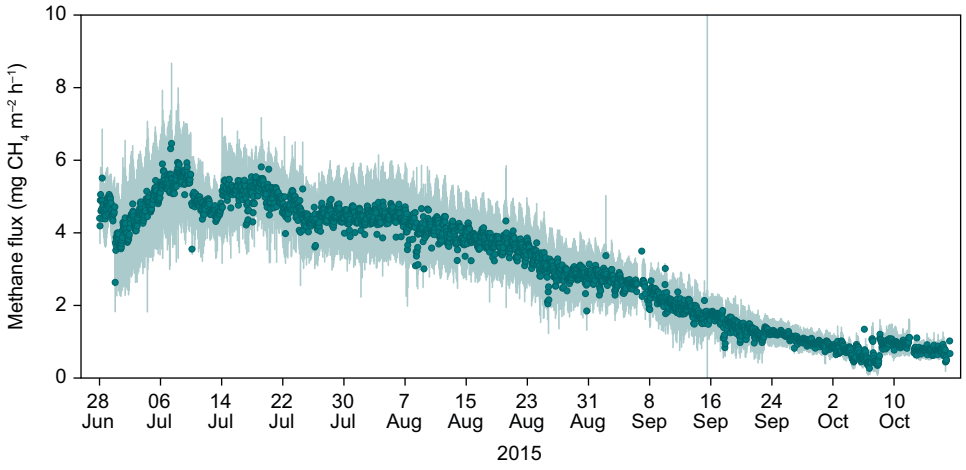

Figure 3.14 Methane (CH_4) emissions from the fen during 2015. Dots represent mean values and lines standard deviation across chambers.

approximately three weeks earlier in 2015 (figure 3.14). The variation between years is likely related to variations in timing of snow melt, meteorological conditions, and primary production in the fen. After the peak, CH_4 fluxes decreased steadily and reached approximately 1 mg CH_4 m^{-2} h^{-1} in late September.

Eddy covariance measurements

In order to describe the inter-annual variation of the seasonal CO_2 budget, the land-atmosphere exchange of CO_2, H_2O and energy in the fen has been monitored using the eddy covariance technique since 2008. The eddy covariance system consists of a 3D sonic anemometer and closed path infrared CO_2 and H_2O gas analyser (Tamstorf et al. 2009). Raw data from the eddy covariance system was calculated using the software package EdiRe (Robert Clement, University of Edinburgh). For more details on the flux calculation procedures, see Hansen et al. (2010).

The temporal variation in mean daily net ecosystem exchange of CO_2 (NEE) and air temperature during 2015 for the fen site is shown in figure 3.15, and various variables are summarized in table 3.8. NEE refers to the sum of all CO_2 exchange processes at the ecosystem scale; including photosynthetic CO_2 uptake by plants, plant respiration and microbial decomposition. The CO_2 exchange is controlled by climatic conditions, mainly temperature and photosynthetic active radiation (PAR), along with amount of biomass and soil moisture content. The sign convention used in figures and tables is the standard for micrometeorological measurements; fluxes directed from the surface to the atmosphere are positive, whereas fluxes directed from the atmosphere to the surface are negative.

Eddy covariance measurements of the CO_2 and H_2O exchange in the fen were initiated 24 June and continued until 21 October. A snow patch covered parts of the fen when measurements began. During this pre-growing season period, daily CO_2 emissions were just below 1 g C m^{-2} d^{-1}. As the vegetation developed, photosynthetic uptake of CO_2 started, and on 7 July the fen

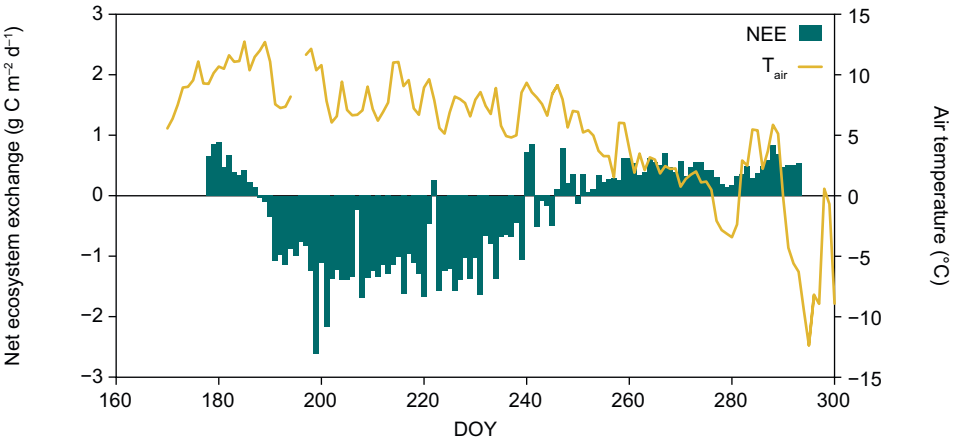

Figure 3.15 Diurnal net ecosystem exchange (NEE) and air temperature (T_{air}) measured in the fen in 2015.

ecosystem switched from being a net source to a net sink of atmospheric CO_2 on a daily basis. The fen acted as a consistent sink for atmospheric CO_2 until 2 September, except for on three days (10, 28-29 August) with overcast conditions and low incoming solar radiation, limiting photosynthesis. During the net uptake period, the fen accumulated 56.3 g C m^{-2}. Post-growing season measurements indicate consistent daily net CO_2 emissions ranging 0.2-0.8 g C m^{-2} d^{-1}, related to variations in temperature.

During the entire measurement period, the fen constituted a sink for atmospheric CO_2, amounting to -31.0 g C m^{-2}. However, it is expected that a significant part of this uptake may be released during the winter period during which measurements are currently not available.

Table 3.8 Summary of the eddy covariance measurement periods and CO_2 exchanges 2008-2015 at the fen site. Please note that the measurement period varies from year to year.

Year	2008	2009	2010	2011	2012	2013	2014	2015
Measurements start	5 Jun	15 May	4 May	15 May	6 Jun	29 May	30 May	24 Jun
Measurements end	29 Oct	31 Oct	9 Oct	14 Oct	31 Oct	22 Oct	28 Jul	21 Oct
Start of net uptake period	–	1 Jul	29 May	28 Jul	16 Jun	23 Jun	18 Jun	7 July
End of net uptake period	16 Aug	27 Aug	18 Aug	7 Sep	31 Aug	24 Aug	–	2 Sep
NEE for measuring period (g C m^{-2})	–45.5	–14.0	–20.9	42.6	–22.3	–24,2	–32.7	–31.0
NEE for net uptake period (g C m^{-2})	–	–42.5	–65.4	–14.3	–61.3	–67.3	–	–56.3
Max. daily accumulation (g C m^{-2} d^{-1})	–2.3	–1.5	–3.1	–1.6	–2.9	–2,7	–2.0	–2.6[a]

4 Nuuk Basic

The BioBasis programme

Maia Olsen, Josephine Nymand, Katrine Raundrup, Peter Aastrup, Paul Henning Krogh, Torben L. Lauridsen and Magnus Lund

This chapter presents the results of the ninth year of the BioBasis monitoring programme at Nuuk. The chapter gives an overview of the activities and presents examples of the results. The programme aims at providing long-term data series on biotic variables from the Kobbefjord area, approximately 20 km south-east of Nuuk. Methods and sampling procedures are described in detail in the manual "Conceptual design and sampling procedures of the biological programme of Nuuk Basic, 2nd edition" (Aastrup et al. 2015).

The programme was initiated in 2007 by the National Environmental Research Institute, now Department of Bioscience, Aarhus University, Denmark, in cooperation with the Greenland Institute of Natural Resources. BioBasis is funded by the Danish Environmental Protection Agency as part of the environmental support programme DANCEA – Danish Cooperation for Environment in the Arctic. The authors are solely responsible for all results and conclusions presented in this chapter, which do not necessarily reflect the position of the Environmental Protection Agency.

4.1 Vegetation

Reproductive phenology

The reproductive phenology has been studied since 2008 in three vascular plant species: The evergreen dwarf shrub *Loiseleuria procumbens*, the herb *Silene acaulis*, and the shrub *Salix glauca*. For each species, four phenology plots cover an ecological amplitude with respect to snow cover, soil moisture, and altitude. In 2015, the recording of phenology started on 17 June (DOY 168) and ended on 29 September (DOY 272). Examples of the results from 2008-2015 are shown and commented on in the following text.

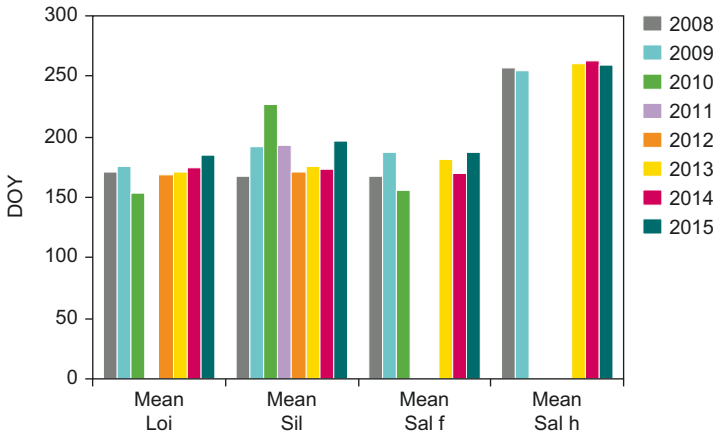

*Figure 4.1 Mean value of day of year (DOY) with 50% flowers/catkins for each of the species (*Loiseleuria procumbens, Silene acaulis*, and* Salix glauca*) in the plant reproductive phenology plots in 2008-2015. Also included are the senescent catkins of* S. glauca *(Sal h). Erratum: Please note that the similar figures in annual reports from 2008-2011 are incorrect.*

Due to late snow melt, flower production occurred later in 2015 than in most other years. In the case of *L. procumbens*, the 2015 season had the latest budding and time of 50% flowering observed so far (figure 4.1, 4.2a and b). At the time of the first visit, 17 June (DOY 168), the snow had melted completely from two plots (Loi1 and Loi4). Due to the location of Loi4 (on top of a hill), this is usually the case, and this plot is usually the first to produce buds and flowers. *L. procumbens* produced more flowers in 2015 than any other year (46% more than in 2009, otherwise the year with the highest number of *L. procumbens* flowers). Most flowers were found in plot Loi2, which accounted for 2/3 of the total flower count in 2015. Senescence was also late, at approximately the same time as in 2009 (figure 4.2c).

The timing of the reproductive phenology events, i.e. budding, flowering and senescence, of *S. acaulis* was comparable to that of 2009 (figure 4.3a-c). The first bud was recorded on 24 June (DOY 175), but most buds appeared around 1 July (DOY 182), whereas in 2014 buds appeared around 10 June (DOY 161). This season, *S. acaulis* had a high level of predation on the flower petals. Identification of the predator was not possible, but predation was observed between 7 July (DOY

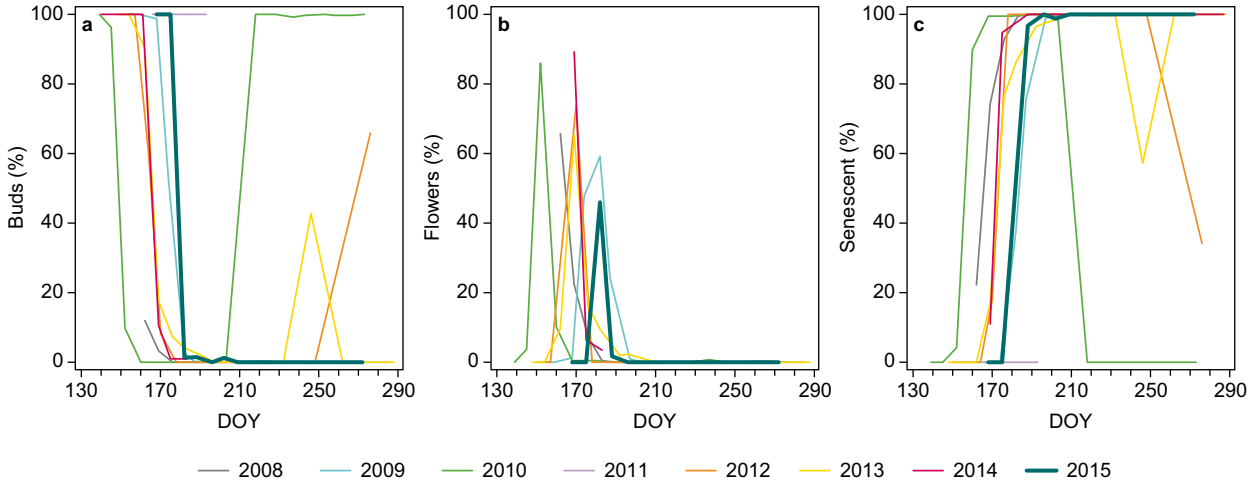

Figure 4.2 Percentage of Loiseleuria procumbens *a) buds, b) flowers, and c) senescent flowers in plot LOI1 during the growing seasons in 2008-2015.*

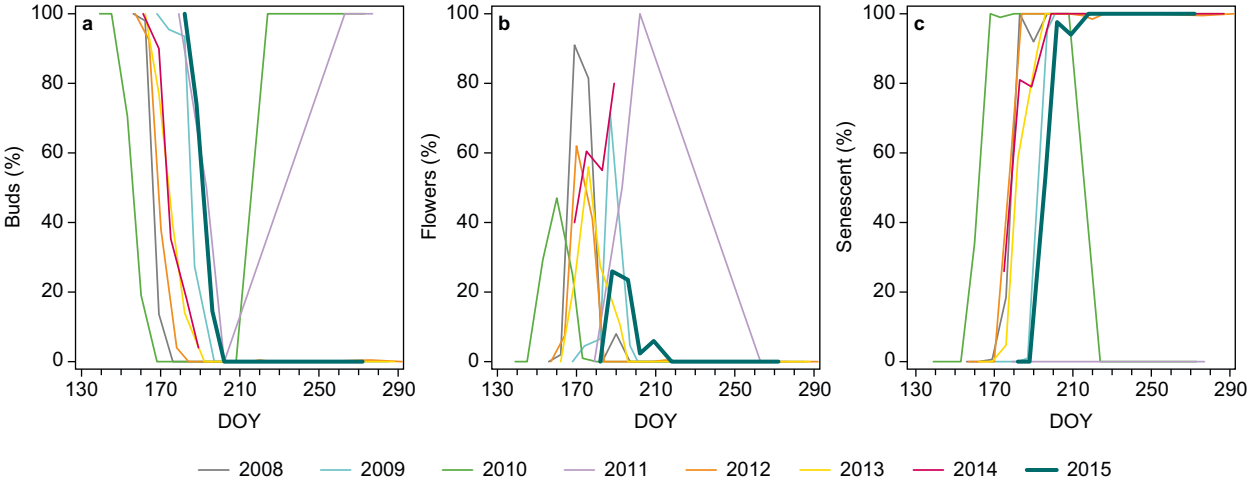

Figure 4.3 Percentage of Silene acaulis *a) buds, b) flowers and c) senescent flowers in plot SIL3 during the growing seasons in 2008-2014.*

188) and 21 July (DOY 202). Thus, total counts were only about 13% of the total count of last season, with plots 2 and 4 being the most heavily predated. Flowering peaked around 9 July (DOY 190) and first senescent flowers were recorded on 15 July (DOY 196).

First male buds of *S. glauca* were observed on 24 June (DOY 175). One week later, on 1 July (DOY 182), both male and female catkins were observed. This is 13 days later than in 2014 and the latest occurrence of both buds and catkins, except for 2011. First appearance of hairs on female catkins was observed on 14 August (DOY 226). The appearance of hairs seems to happen at roughly the same time every year, independent of the timing of i.e. budding and flowering (figure 4.1). There were less catkins produced in 2015 than in 2014. Compared to years not affected by moth larvae, few male catkins and an intermediate amount of female catkins were observed.

In the CO_2 flux plots, *S. glauca* produced less catkins than in 2013 and 2014, but more than the years prior to 2013 (figure 4.4). Control plots (C) and plots with increased temperature (T) produced the largest amount of catkins since 2013, with T plots consistently producing more catkins.

Summing up reproductive plant phenology

The 2015 field season experienced late snow melt and early snow fall. A preliminary review of data related to flowering indicates that 2015 was characterised by:

- Large numbers of flowers in *L. procumbens* plots
- Late timing of budding and flowering, but with senescence similar to 2009
- High predation on *S. acaulis* flowers.

Vegetation greening, NDVI

The seasonal greening of the vegetation was monitored 1) in plots with *Empetrum nigrum ssp. hermaphroditum* and *Eriophorum angustifolium*, 2) in the plant phenology plots, 3) along the NERO line (Bay et al. 2008) and 4) in the CO_2 flux plots. We used a handheld Crop Circle TM ACS-210 Plant Canopy Reflectance Sensor, which calculates the greening index (Normalized Difference Vegetation Index – NDVI). Measurements were made weekly in the *Empetrum nigrum*-plots, *Eriophorum angustifolium*-plots, and the plant phenology plots, and every two weeks along the NERO line. Measurements of NDVI in the CO_2 flux plots were carried out using the SpectroSense 2+ handheld system with two mounted sensors. This is the second season of NDVI measurements in the CO_2 flux plots.

NDVI – Plots

NDVi was measured from 17 June (DOY 168) to 23 September (DOY 266), making it the shortest season (98 days total) since the beginning of the programme in 2008. Season lengths from 2009–2014 ranged between 104 and 142 days.

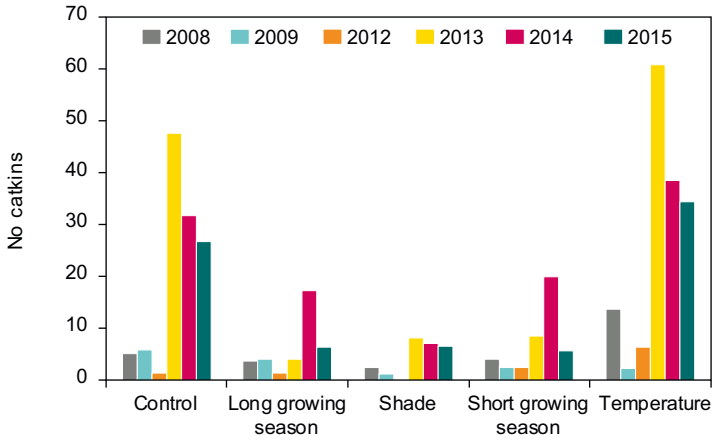

Figure 4.4 Number of catkins counted in CO_2 flux plots in 2008-2015. No catkins were produced in 2010 and 2011 due to heavy predation by moth larvea. Catkins are summed per treatment, Control (C), Long Growing season (LG), Shade (S), Short Growing season (SG) and Temperature (T).

NDVI values in *E. nigrum* plots were low and very close to the values measured in 2009 and 2010 (figure 4.5a). The only year with consistently lower values was 2011. No real peak was apparent, and these plots show little variation throughout the season.

Overall, *E. angustifolium* displayed low NDVI values (figure 4.5b), peaking on 19 August (DOY 231). In previous years, the NDVI values displayed a seasonal bell curve, but in 2015 no drop at the end of the season was observed, possibly due to an early and quick snow fall. Plot Eri1 had the lowest NDVI values, which appears to be a consistent trend.

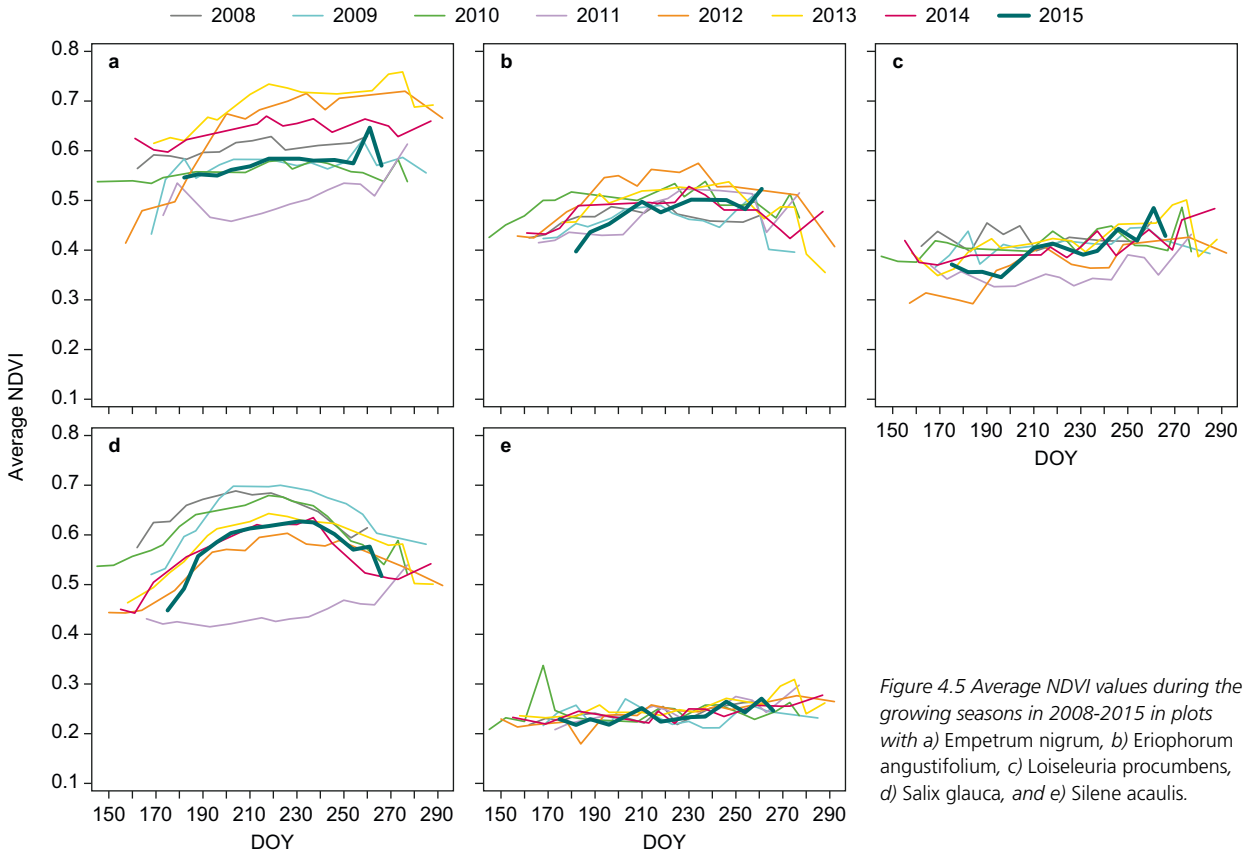

Figure 4.5 Average NDVI values during the growing seasons in 2008-2015 in plots with a) Empetrum nigrum, *b)* Eriophorum angustifolium, *c)* Loiseleuria procumbens, *d)* Salix glauca, *and e)* Silene acaulis.

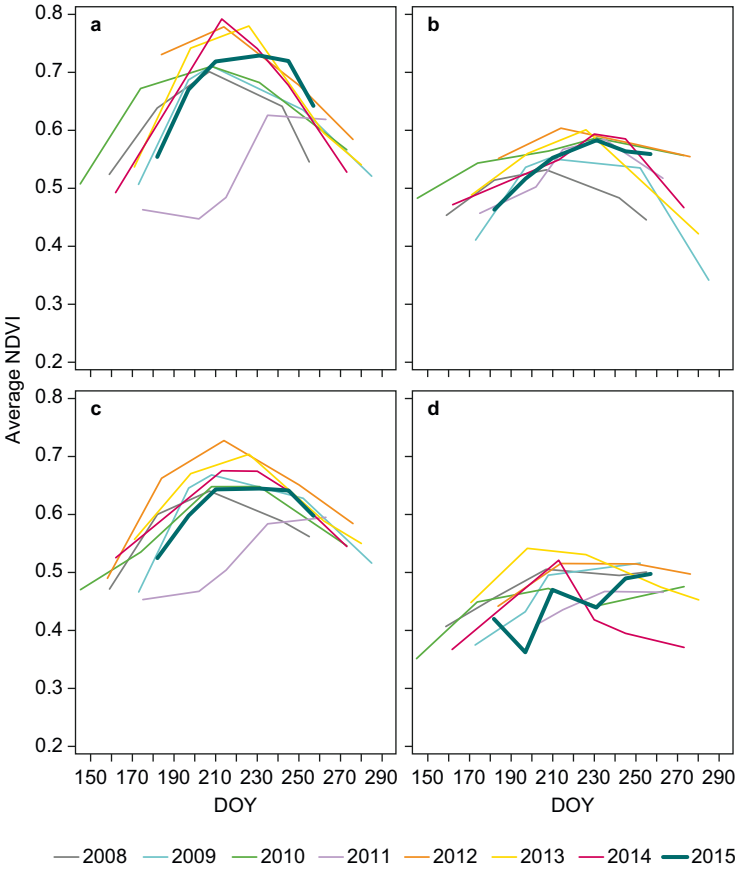

Figure 4.6 Average NDVI values along the NERO line during the growing season from the vegetation types a) dwarf shrub heath, b) copse, c) fen, and d) snow patch.

S. glauca NDVI values were low (figure 4.5d), with a peak on 19 August (DOY 231), approximately 10 days later than previous years. Plot Sal4, with only male plants, peaked on 6 August (DOY 218), which is earlier than previous years. Of the four Salix plots, Sal1 had the lowest vegetation cover and, hence, low average NDVI values due to large areas of the plot being bare soil/gravel.

Low to intermediate NDVI values were recorded in all four *S. acaulis* plots with little variation over time (figure 4.5e). These four plots were very sparsely vegetated and, as such, the measured NDVI values are quite low.

NDVI – NERO line

Measured values in 2015 tended to be intermediate to low, except for the riverbed dominated by *S. glauca*, which reached higher values than average (figure 4.6a-d). Most vegetation types reached maximum NDVI values at around 19 August (DOY 231), 18 days later than in 2014, most likely due to the late snow melt. In 2013, the snow also melted late and NDVI-values exhibited peaks comparable to those measured this season.

NDVI – CO_2 flux plots

NDVI values were measured from 23 June (DOY 174) to 25 September (DOY 268), a total of 94 days, compared to 124 days in 2014. When comparing the average values for the three manipulations C (control), S (shade) and T (temperature), there was little to no difference between either manipulations or values in 2014 (figure 4.7a) and 2015 (figure 4.7b).

NDVI values measured in *L. procumbens* started out low, but with a steady increase all through the season ended up being fairly high (figure 4.5c). The low values measured in June and the beginning of July are not much lower than what was measured in the beginning of the previous years, they just occurred later due to the late snow melt.

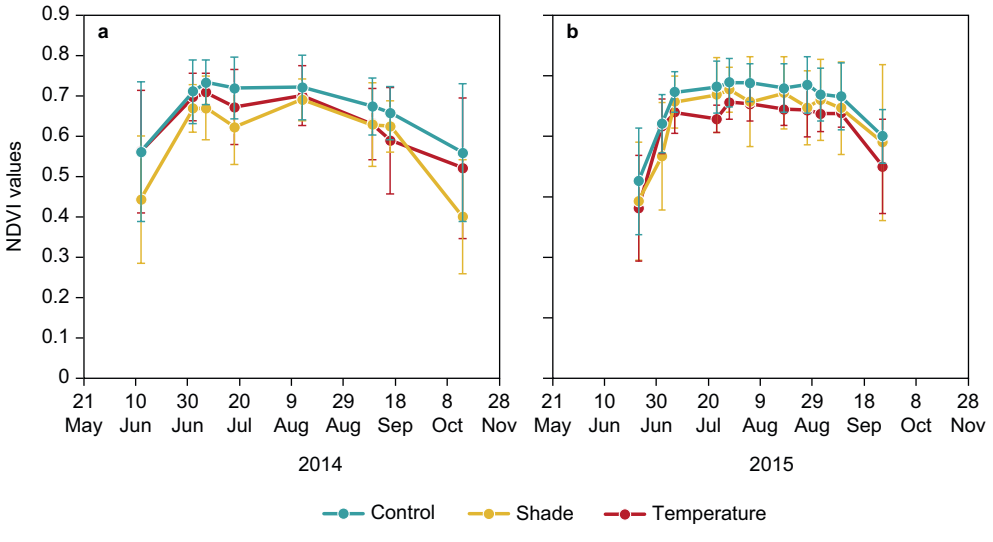

Figure 4.7 Average NDVI values during the growing season in the CO_2 flux plots with three different treatments, Control (C), Shade (S) and Temperature (T), in a) 2014 and b) 2015.

Summing up the vegetation greening

2015 was a very short season, with a late peak in production and generally low NDVI values, in some cases the lowest measured, except for in 2011.

Carbon dioxide exchange

In 2008, a manipulation experiment was initiated with five treatments, each with six replicates. The experiment is located in a mesic dwarf shrub heath dominated by *Empetrum nigrum* with *Salix glauca* as a subdominant species. Treatments include control (C), shortened growing season (SG: addition of snow in spring), prolonged growing season (LG: removal of snow in spring), shading (S: hessian tents) and increased temperature (T: ITEX plexiglas hexagons). We have conducted measurements of land-atmosphere exchange of CO_2 using the closed chamber technique, soil temperature, soil moisture and phenology of *Salix glauca* approximately weekly during June-September in each year. The net ecosystem exchange (NEE) was measured with transparent chambers, while the ecosystem respiration (R_{eco}) was measured with darkened chambers. Gross primary production (GPP) was calculated as the difference between NEE and R_{eco}. The SG and LG treatments were not applied in 2008-2015, therefore, results from these plots can be considered as controls.

The first CO_2 flux measurement day in 2015 was 17 June (DOY 168). Until the last measurement day, 25 September (DOY 268), CO_2 fluxes were measured on 12 occasions (figure 4.8). Generally, all plots functioned as sinks for atmospheric CO_2 at the time of the measurement (midday). Similar to earlier years, NEE was generally more negative (i.e. higher CO_2 uptake) in C plots compared with T and S plots.

In previous years, T plots generally had highest R_{eco} rates, which can be explained by warmer and drier conditions resulting in increased respiration rates. However, in 2014 and again in 2015, R_{eco} rates from T plots were not higher than those from C plots. Highest rates of GPP were generally observed in C plots, while especially S plots had lower GPP rates compared with other treatments. As photosynthesis is driven by solar radiation, shading decreases GPP and build-up of biomass.

Since the extensive outbreak of the larvae *Eurois occulta* in 2011, which defoliated large parts of the heath vegetation in the area, CO_2 flux magnitudes have been high in following years. This trend continued in 2015.

UV-B exclosure plots

Measurements of chlorophyll fluorescence as a measure of plant stress were carried out in the Kobbefjord area in 2015. The impact of ambient UV-B radiation on the vegetation was studied in a mesic dwarf shrub heath dominated by *Empetrum nigrum* and with *Betula nana* and *Vaccinium uliginosum* as subdominant species. The plots were set up between 24 June and 1 July (DOY 175 and DOY 182). Throughout the season, the frames were stable with little maintenance; the set-up was affected by weathering on only

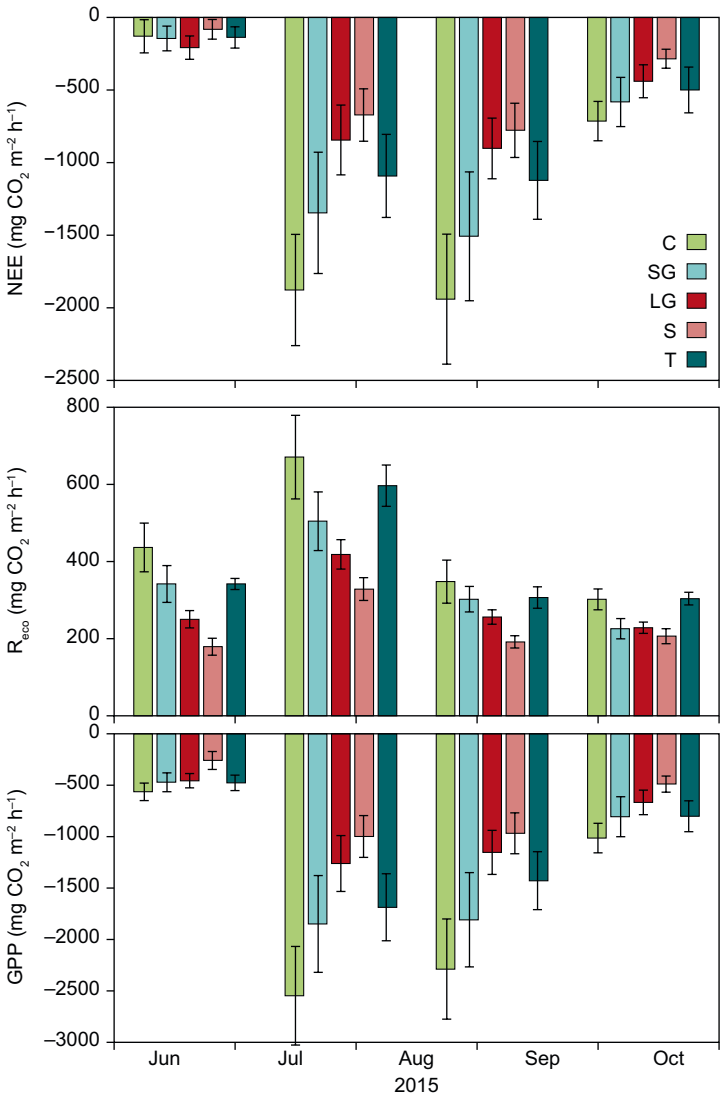

Figure 4.8 Monthly means of net ecosystem exchange (NEE: upper panel), ecosystem respiration (R_{eco}: middle panel) and gross primary production (GPP: lower panel) in 2015 in the CO_2 flux plots. Error bars refer to standard error in spatial variability (six replicates). For explanation of treatment abbreviations, see text.

two occasions, in late August (one Mylar frame) and early September (three Teflon frames), until the frames were removed 1 October (DOY 274).

The ambient UV-B radiation on fluorescence parameters was monitored on *V. uliginosum* and *B. nana*. The total performance index (PI_{total}), integrating responses of antenna, reaction centre, electron transport and end acceptor dependent parameters, is an indicator of the viability of a sample. The exclusion of UV-B is expected to have a positive effect on the total performance index. We measured five times through the season (figure 4.9). The measurements varied considerably at each measurement and through the season, i.e. we found no response of reducing the UV-B radiation. We have no explanation for this. However, previous years have reported a positive effect for the studied species when excluding UV-B radiation.

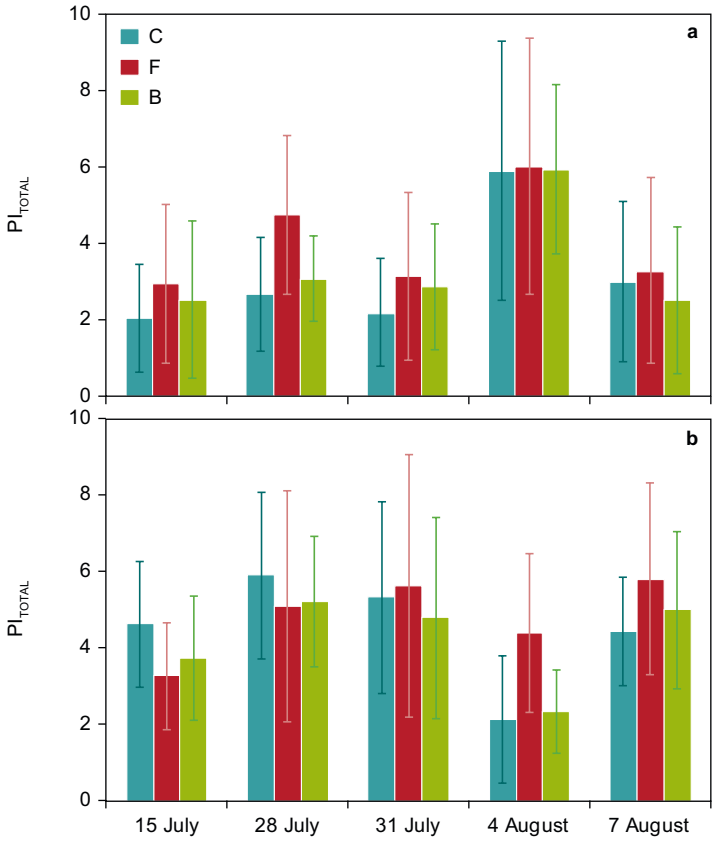

Figure 4.9 Seasonal variations in total performance index for a) Betula nana *and b)* Vaccinium uliginosum. *Treatments are C – Open control (no filter), F – filter control (transparent filter) and B – UV-B reduction (UB-B absorbing filter, Mylar).*

4.2 Arthropods

In Kobbefjord, all four pitfall trap stations (each with eight traps) established in 2007 and the two window trap stations (each with two traps) established in 2010 were open during the 2015 season. The samples are being sorted by the Department of Bioscience, Aarhus University, Denmark.

Pitfall traps were established from 17 June (DOY 168) through 7 July (DOY 183) and they all worked continuously until 29 September (DOY 272) when the liquid began to freeze. In 2015, arthropods were caught during 3420 trap days (including 3040 pitfall-trap days and 380 window-trap days). Former seasons ranged from 3496-5818 trap days (with a mean of 4524 trap days), making 2015 the shortest season since 2010.

Microarthropods

Three sampling sessions for microarthropods in Kobbefjord took place in July, August and September. The sample processing followed the monitoring field manual by Aastrup et al. (2015). The population data structure, as revealed by principal component analysis (PCA) of the correlation matrix of log(x+1) transformed population abundances, is shown in figure 4.10 and 4.11. Species identification was made according to Fjellberg (2015).

The collembolan communities of the four plant communities have retained their characteristic structure during the sampling period covering 2007, 2009, 2010, 2014 and 2015 (Nymand et al. 2008, Raundrup et al. 2010, Nymand et al. 2011). The complete microarthropod dataset revealed changes over the years for a few

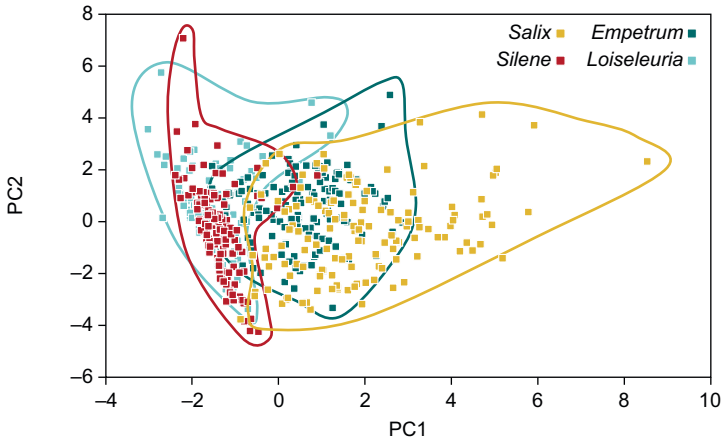

Figure 4.10 PCA plot of the correlation matrix of log-transformed microarthropod community samples showing the complete 5 years of sampling data, n=515, from the years 2007, 2009, 2010, 2014 and 2015. The first and second principal components account for 17% of the sample variation across the four monitoring habitats. Each soil core sample is represented by a square symbol. Lines are drawn around clusters comprising the microarthropod samples belonging to a particular plant community.

of the dominant taxons, but most species were rather stable in their abundance and consistently affiliated with a certain plant community. Thus, the structure of the population abundances was stable as shown by the PCA plot of the first two principal components (figure 4.10) during the period spanning 8 years. The year 2015 conformed to the same pattern (figure 4.11). Table 4.1 ascertains the key species with grey-shading, explaining the PCA clustering of the plant communities in terms of microarthropod species composition. However, the individual plots have unique ecological properties, particularly true for the *Loiseleuria* and *Empetrum* plots (Jensen et al. 2016).

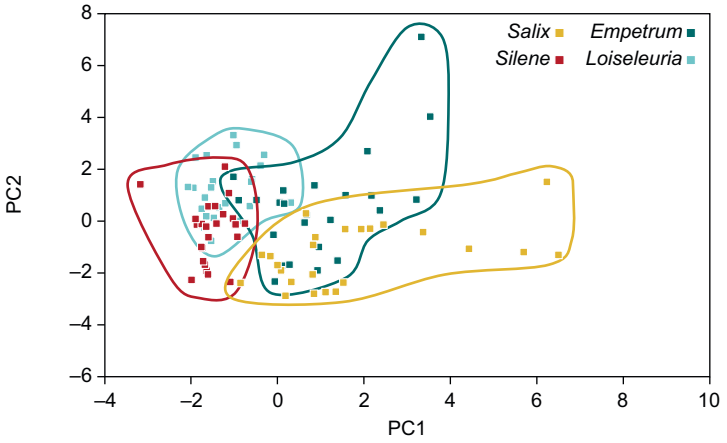

Figure 4.11 PCA plot of the correlation matrix of log-transformed microarthropod population abundances in 2015. The first, PC1, and second, PC2, principal components account for 26% of the sample variation across the four monitoring habitats. Each soil core sample is represented by a square symbol. Lines are drawn around clusters comprising the microarthropod samples belonging to a particular plant community.

Table 4.1 Mean abundances (×1000 individuals m^{-2}) of mites, at order level, and collembolans, at species level, in four vegetation types. Collembolan species are in order of decreasing abundance. Microarthropods are the sum of mites and collembolans. S: Collembolan species richness; mean per sample Shannon diversity: H' = –∑ pi log2 pi, where pi is the proportion of species in a sample to total collembolans; mean equitability: E: H'/log2 n, where n is number of collembolan species. Shaded areas: habitat characterising species.

	Salix glauca	***Empetrum nigrum***	***Silene acaulis***	***Loiseleuria procumbens***
S	16	12	7	12
Mean S per sample	4.8	5.1	1.4	3.2
H'	1.5	1.2	0.51	1
E	0.7	0.52	0.39	0.54
Total microarthropods	75.1	153.9	102.3	192.8
Acari	51.8	78.8	99.1	164.1
Collembola	23.3	75	3.2	28.6
Tetracanthella arctica	3.7	44.4	0.2	23
Folsomia quadrioculata	1.8	11.8		0.3
Tullbergiinae	3.3	4.4	1.4	2.7
Isotomiella minor	5.1	5.3		0.02
Desoria olivacea	7.1	3.2		0.02
Folsomia sensibilis	0.5	3.7	0.02	0.03
Micranurida pygmaea	0.02	1.2	0.7	1.5
Willemia sp.	0.7	0.7	0.6	0.7
Parisotoma notabilis	0.7			0
Lepidocyrtus violaceus	0.2		0.02	0.1
Entomobrya nivalis	0.02			0.2
Heterosminthurus claviger	0.03		0.1	
Desoria tolya		0.1		0
Arrhopalites principalis	0.05	0.03		0
Oligaphorura ursi	0.1			0.02
Isotoma anglicana	0.02	0.05		0.02
Sminthurides schoetti	0.1			
Megalothorax minimus		0.05		
Oribatida	24.1	36.9	41.1	74.1
Actinedida	23.7	38.5	57.6	88.8
Gamasida	3.8	3.5	0.4	1.2
Acaridida	0.1		0.02	

Table 4.2 Total number of passerines counted and the number of censuses per year. Also shown is the number of passerines per census. For explanation of bird abbreviations, see text.

Year/ birds	LB	SB	NW	RP	No of census's	LB/ census	SB/ census	NW/ census	RP/ census
2008	57	61	44	7	9	6.3	6.8	4.9	0.8
2009	39	40	33	37	5	7.8	8.0	6.6	7.4
2010	182	152	110	49	17	10.7	8.9	6.5	2.9
2011	166	131	146	7	14	11.9	9.4	10.4	0.5
2012	102	69	109	37	13	7.8	5.3	8.4	2.8
2013	104	70	156	7	18	5.8	3.9	8.7	0.4
2014	79	86	52	36	15	5.3	5.7	3.5	2.4
2015	70	40	41	31	11	5.4	3.1	3.2	2.4

4.3 Birds

Four passerine species, Lapland bunting *Calcarius lapponicus*, snow bunting *Plectrophenax nivalis*, northern wheatear *Oenanthe oenanthe* and common redpoll *Carduelis flammea*, were counted at 13 census points within the 32 km² Kobbefjord catchment area. A total of 11 censuses were carried out from 23 June (DOY 174) to 23 September (DOY 266) 2015, shorter than previous seasons, which ranged from 118–142 days. All four species of passerines were already present at the time of the first census, and the survey was carried out until no more observations were made at any census point.

The total number of Lapland buntings (LB), snow buntings (SB), northern wheatears (NW), and redpolls (RP) varies between years (table 4.2), yet, since 2011 there has been a downwards trend in observations of LB, SB and NW (figure 4.12). All species but RP had low counts per census in 2015, with SB and NW displaying the lowest counts ever observed during the monitoring in Kobbefjord. Hence, counts of birds per census of SB and NW were 3.1 and 3.2 birds, respectively, while there were 5.4 LB per census (table 4.2). RP counts were 2.4 birds per census, but this

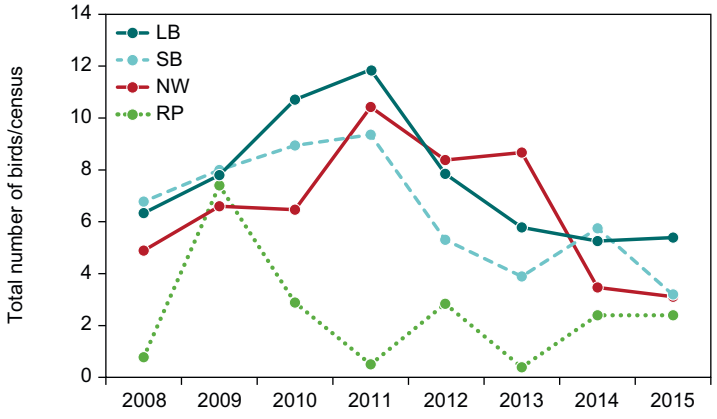

Figure 4.12 Total number of birds counted per census in 2008-2015. For explanation of the bird abbreviations, see text. The lines connecting the dots are for illustrative purposes only.

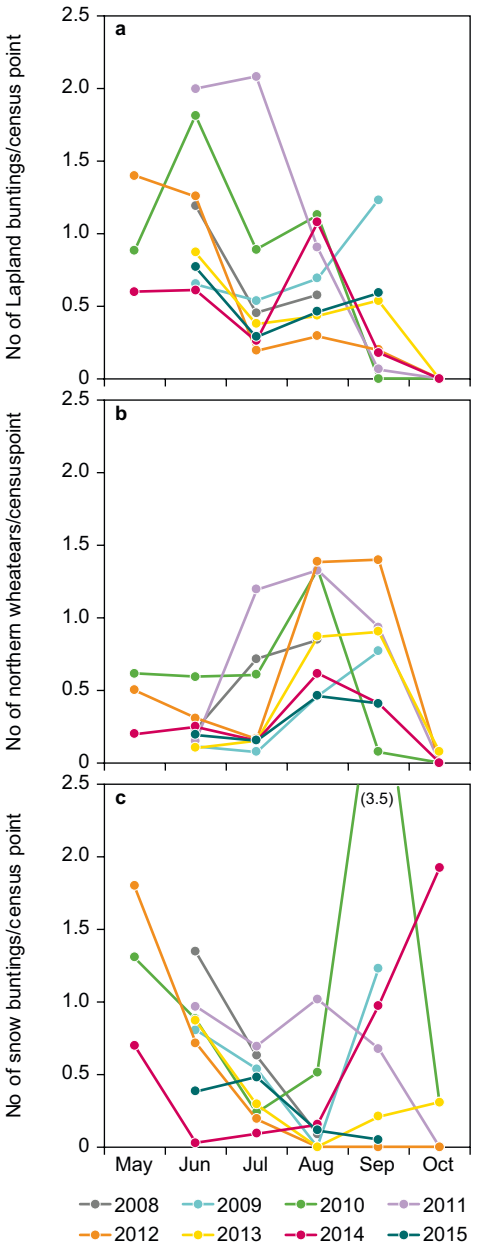

Figure 4.13 Numbers per census during the season in 2008-2015 of a) Lapland bunting, b) northern wheatear and c) snow bunting. The lines connecting the dots are used for illustrative purposes only.

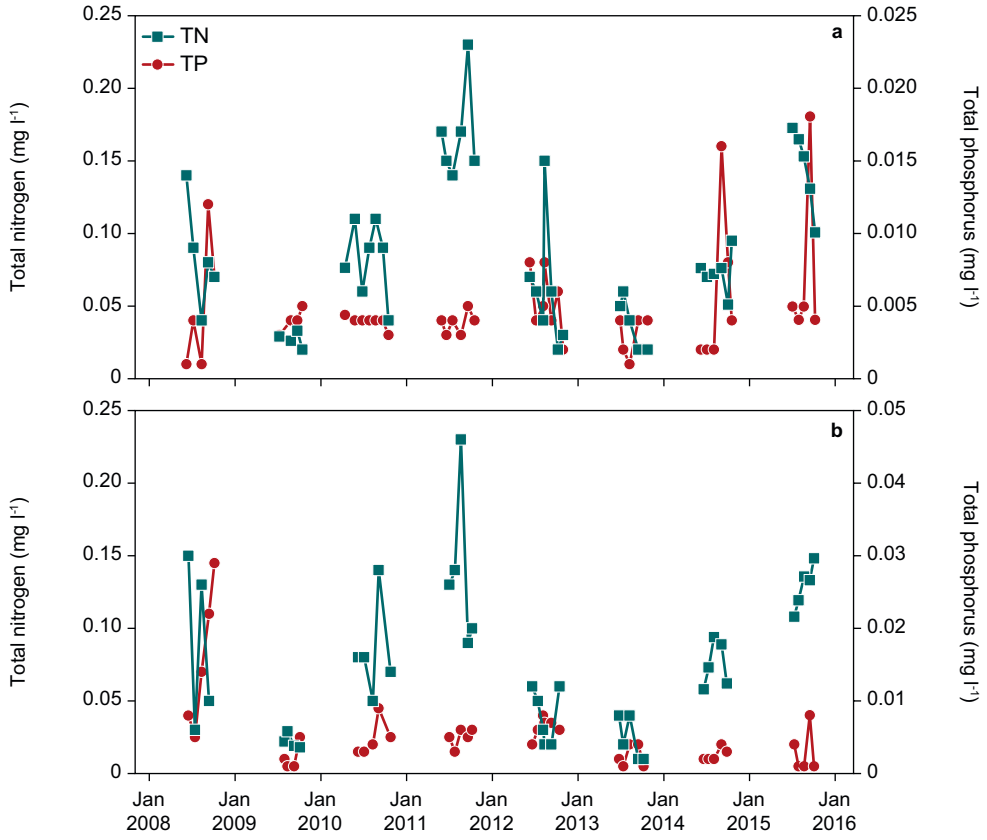

Figure 4.14 Total nitrogen (TN) and total phosphorus (TP) during 2008-2015 in a) Badesø and b) Qassi-sø.

species has fluctuated a great deal over the years, and so a trend is not readily obvious. Observations of SB peaked in July, early in the season, while the remaining passerines peaked in numbers in September (figure 4.13a-c).

4.4 Mammals

The Kobbefjord catchment area is only sparsely populated with mammals. During the field season, no mammals were observed. Faeces of fox and hare were found from time to time.

4.5 Lakes

The Kobbefjord catchment includes three lakes, of which two have been monitored since 2008. They are both deeper lakes with maximum depths of 35 and 27 metres, respectively. Badesø, which is the deepest lake, is situated downstream at 50 m a.s.l., and Qassi-sø upstream at 235 m a.s.l. Qassi-sø is the most wind exposed of the two lakes, and a small glacier drains into the lake resulting in silt input to the system. Due to the higher altitude, Qassi-sø generally has a longer ice covered period than Badesø. In Badesø, Secchi depth and concentrations of suspended solids were back to normal following the flushing event (see Chlorophyll and Secci depth) in August 2014.

Water chemistry and ice cover

In 2015, the ice out date was 1 July (DOY 175) in Badesø and 11 days later, 12 July (DOY 186), in Qassi-sø which was, thus, the latest ice out date in the monitored period (2008-2015) (table 4.3). With ice formation occurring in mid-October, the ice free period was very short in 2015. Both lakes are nutrient poor with relatively large inter-annual and within lake variation. In 2015, the average total nitrogen (TN) concentration in both lakes was higher than the average for the monitored period, 0.146 and 0.128 mg TN l^{-1}, in Badesø and Qassi-sø, respectively (table 4.3; figure 4.14). Average total phosphorus (TP) was 0.007 and 0.003 mg l^{-1} in Badesø and Qassi-sø, respectively; despite being higher in Badesø than the average for the monitored period, concentrations are still low.

Chlorophyll and Secchi depth

Chlorophyll *a* (Chl *a*) is a measure of primary productivity and is correlated to nutrient levels. Since TN and TP is low in both lakes, the Chl *a* levels of the two lakes are low too with most measurements below 1 µg l^{-1} (figure 4.15a). Chl *a* varied notably

Table 4.3 Morphometric data, time weighted average of water chemistry (min-max values) and physical data measured in Badesø and Qassi-sø during the ice free periods from 2008-2015.

Badesø								
Area (ha)	80							
Maximum depth (m)	35							
Mean depth (m)	9.2							
	2008	**2009**	**2010**	**2011**	**2012**	**2013**	**2014**	**2015**
Total phosphorus (mg/l)	0.005 (0.001-0.012)	0.004 (0.003-0.005)	0.004 (0.003-0.004)	0.004 (0.003-0.005)	0.006 (0.002-0.008)	0.003 (0.001-0.004)	0.005 (0.002-0.016)	0.007 (0.004-0.018)
Total nitrogen (mg/l)	0.084 (0.040-0.140)	0.027 (0.020-0.033)	0.08 (0.04-0.11)	0.17 (0.14-0.23)	0.06 (0.03-0.15)	0.037 (0.02-0.06)	0.073 (0.05-0.1)	0.146 (0.100-0.173)
pH	6.92 (6.59-7.13)	6.85 (6.46-7.14)	6.62 (6.09-7.3)	7.1 (6.51-7.85)	n.a.	n.a.	7.27 (6.83-7.6)	6.9 (6.05-7.17)
Conductivity (µS/cm)	20 (19-22)	22 (21-23)	21 (18-26)	21 (15-27)	18 (14-19)	25 (20-42)	21 (17-24)	17 (16-21)
Ice-free (date)	3 Jun	15 Jun	20 May	23 Jun	9 Jun	14 June	10 June	1 Jul
Ice-covered (date)	24 Oct	30 Oct	13 Dec	25 Oct	14 Nov	24 Oct	29 Oct	22 Oct
Ice-free period (days)	143	137	207	124	158	132	141	113
Qassi-sø								
Area (ha)	52							
Maximum depth (m)	27							
Mean depth (m)	7.8							
	2008	**2009**	**2010**	**2011**	**2012**	**2013**	**2014**	**2015**
Total phosphorus (mg/l)	0.015 (0.005-0.029)	0.002 (0.001-0.005)	0.005 (0.003-0.009)	0.005 (0.003-0.006)	0.006 (0.004-0.008)	0.003 (0.001-0.004)	0.003 (0.002-0.004)	0.003 (0.001-0.008)
Total nitrogen (mg/l)	0.09 (0.30-0.150)	0.022 (0.019-0.029)	0.084 (0.050-0.14)	0.138 (0.09-0.23)	0.03 (0.02-0.06)	0.026 (0.01-0.04)	0.077 (0.06-0.09)	0.128 (0.108-0.148)
pH	6.72 (6.44-6.96)	6.87 (6.79-6.93)	6.84 (6.37-7.31)	7.59 (6.79-7.97)	n.a.	n.a.	7.51 (6.95-8.38)	6.8 (6.4-7.2)
Conductivity (µS/cm)	20 (15-24)	16 (16-17)	17 (15-18)	18 (15-20)	15 (10-20)	20 (17-26)	18 (16-19)	15 (12-18)
Ice-free (date)	12 Jun	28 Jun	31 May	1 Jul	18 Jun	22 Jun	20 Jun	12 Jul
Ice-covered (date)	18 Oct	17 Oct	10 Nov	20 Oct	1 Nov	24 Oct	24 Oct	19 Oct
Ice-free period (days)	128	111	163	112	136	124	126	99

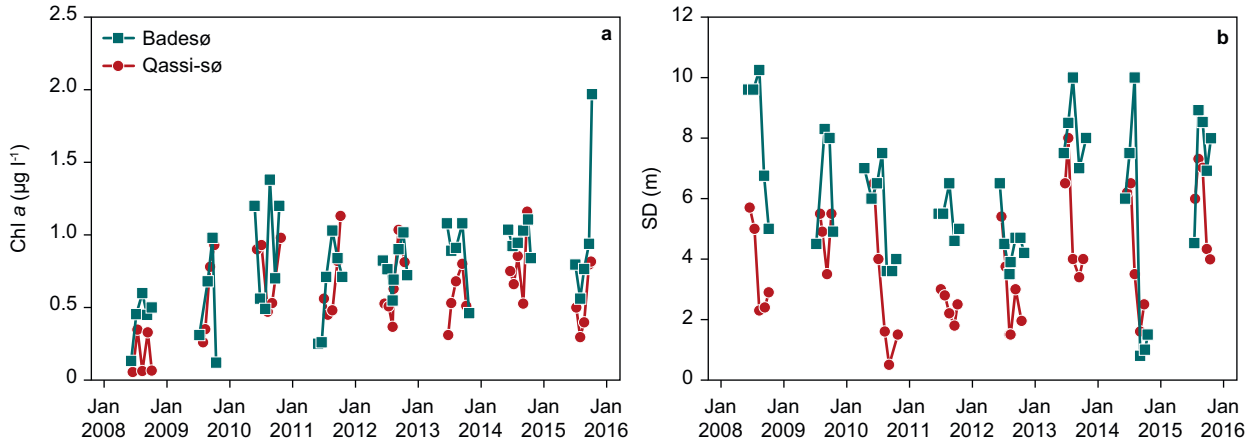

Figure 4.15 Chlorophyll a levels (a) and Secchi depth (b) in Badesø and Qassi-sø during 2008-2015.

between the years, but due to low nutrient levels the variation remains within a very narrow range compared to more nutrient rich lakes. During the first three years of the monitored period, Chl *a* exhibited an increasing trend in both Badesø and Qassi-sø (figure 4.15a), but during the past 5 years average Chl *a* levels have stabilized just below 1 µg l^{-1}; however, in 2015 it was slightly lower, except for one high October value in Badesø. The lower values in 2015 may be due to the generally lower summer temperature. In general, there is a slightly higher Chl *a* level in Badesø compared to Qassi-sø throughout the monitored period, which can be explained by the lower altitude and, consequently, higher temperature in combination with less silt in Badesø and, consequently, better transparency (secchi depth) (figure 4.15b).

Following a year with relatively low Secchi depth, the Secchi depth improved a lot in both lakes in 2015. In Badesø, the Secchi depth was 7.3 m on average and very close to "normal" compared to 2014, where a flushing event of soil and silt via Langesø into Badesø caused a dramatic Secchi depth reduction during September and October 2014 (figure 4.15b). However, the increase in Secchi depth cannot only be explained by the lack of flushing soil/silt in 2015, as Secchi depth also improved by 2.1 m to 5.9 m in Qassi-sø during 2015. The general increase in Secchi depth during 2015 can therefore be explained by a combination of less Chl a and suspended solids in both lakes in 2015 (figures 4.15 and 4.16).

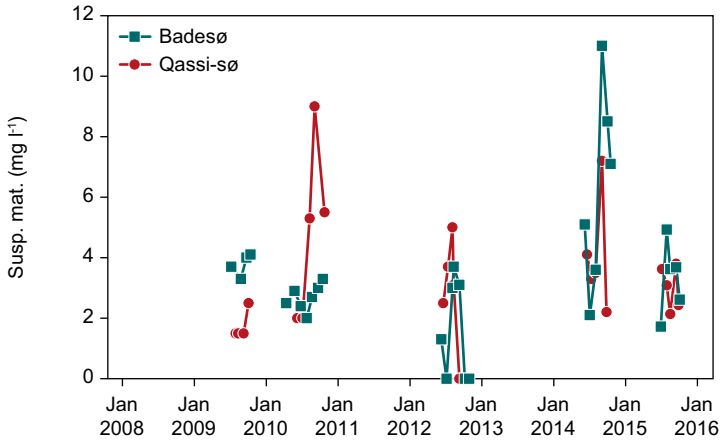

Figure 4.16 Suspended matter (solids) in Badesø and Qassi-sø during 2009-2015.

Zoo plankton

Due to low nutrient levels and low primary production, zooplankton biomasses are generally low in the two lakes. Nevertheless, we found inter-annual variation in total biomass.

In Badesø, zooplankton biomass in 2015 returned to the same level as in 2011-2013, following a biomass reduction in 2014 (figure 4.17a). As in the majority of the previous years, Badesø was dominated by calanoid

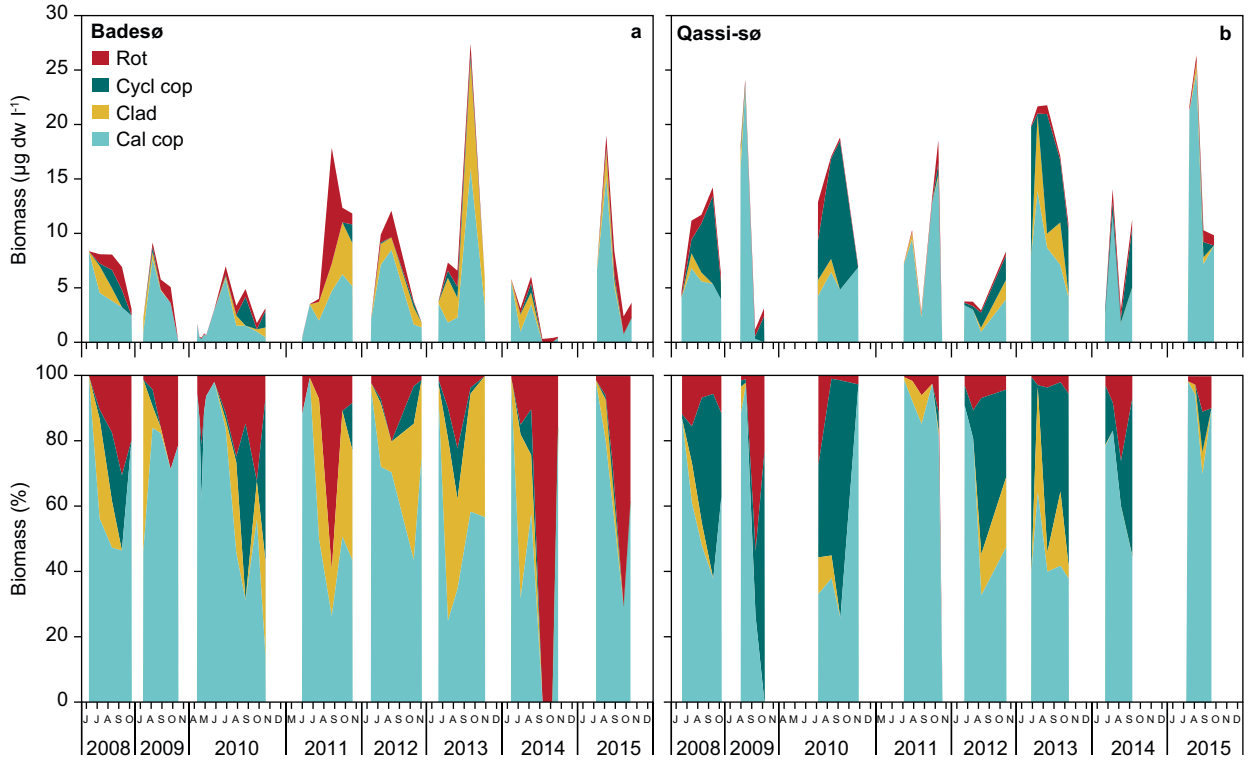

Figure 4.17 Zooplankton biomass (top) and biomass, % (bottom) in Badesø during 2008-2015. Zooplankton is divided into four groups: Cladocerans (Clad), cyclopoid copepods (Cycl cop), calanoid copepods (Cal cop) and rotifers (Rot).

copepods *Leptodiaptomus minutus* during the first half of the ice free period. Following this first period, rotifers gradually took over the dominance and contributed with up to 70% of the total biomass; although the absolute biomass was much lower at the end of the ice free season compared to the beginning of the season (figure 4.17a). When rotifers occur in high biomasses in Badesø, they consist mainly of the large *Asplanchna* together with *Collotheca* spp., but other smaller rotifers (like *Filinia terminalis*, *Keratella* spp. and *Polyarthra* spp. and *Kellicottia longispina*) were also found. In Badesø, the cladocerans *Bosmina* sp. together with *Holopedium* sp. contributed with a relatively large percentage of the zooplankton community during certain periods of the ice free periods from 2011 to 2014.

In August 2014, a large input of soil/silt into Badesø caused dramatic effects to the zooplankton community, as all the large calanoid copepods and the cladocerans disappeared from the system, leaving the rotifers contributing with 100% of the zooplankton biomass (figure 4.17a). However, the calanoid copepods reappeared in the lake in late October 2014 and, as mentioned previously, dominated during early summer 2015. Cladocerans did not recolonize to previous levels in 2015.

The overall inter-annual changes in zooplankton biomass may indicate changes in the predation pressure from fish to the zooplankton. In Badesø, the cladocerans occasionally consist of the small Bosmina together with relatively few *Holopedium sp*. and smaller cyclopoid copepods plus a relatively large contribution of rotifers, reflecting the presence of zooplankton-eating fish.

In Qassi-sø, the zooplankton community is different from Badesø, being dominated by calanoid *Leptodiaptomus minutus* and cyclopoid copepods and, to a minor extent, by cladocerans and rotifers (figure 4.17b). When cladocerans are present in reasonable amounts, the large *Holopedium* sp. is the dominating taxa. In 2015, the calanoid copepods dominated with >80% of the biomass throughout the ice free season. Rotifers and cyclopoid copepods each contributed with up to 10% of the total zooplankton biomass (figure 4.17b). The latter pattern is in contrast to Badesø, where rotifers during 2015 contributed with up to 70% of the total zooplankton biomass. The small contribution from rotifer biomass in Qassi-sø to the total zooplankton biomass, compared to the situation in Badesø (figures 4.17b and 4.17a), reflects the presence and absence of fish in Badesø and Qassi-

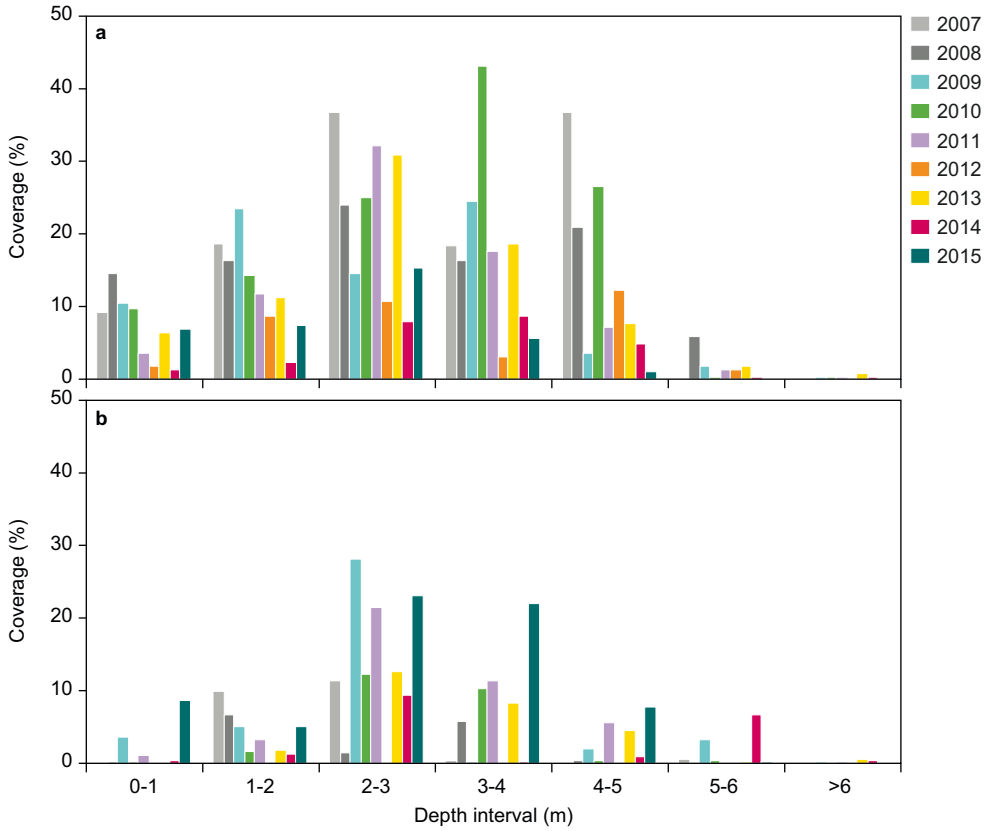

Figure 4.18 Coverage (%) of total submerged vegetation (Callitriche hamulata) in a) Badesø and b) Qassi-sø. No data is available for 2012 in Qassi-sø.

sø, respectively. Despite lower biomass of rotifers in Qassi-sø, similar taxa (*Asplanchna spp.* and *Conochilus unicornis*) dominated in Qassi-sø as in Badesø; however, more rotifer taxa were present in Qassi-sø compared to Badesø.

Another interesting phenomenon in Qassi-sø is the absence or almost lack of cladocerans in certain years (2009, 2011, 2014 and 2015). Preliminary results up to 2014 indicate that short ice free periods (short summers) may reduce the success of the cladocerans (*Daphnia*). This seems still valid after 2015.

Phytoplankton

Due to budget reductions, phytoplankton was not analysed.

Vegetation

Callitriche hamulata dominated the submerged vegetation in both lakes throughout the monitoring period. Coverage varied in the different depth intervals, but overall the maximum coverage was at intermediate depths; 2-4 m (figure 4.18a-b). The lower coverage at the shallowest water is due to wind and wave induced physical stress. At deeper water, the low coverage is due to reduced light availability in combination with a short growing season. At the given nutrient levels, the macrophyte growth in Arctic lakes responds stronger to temperature and the length of the growing season than to chlorophyll level (Mønster, 2013). As a consequence, we also found large inter-annual variability in the coverage. In both lakes, the 2014-coverage was among the lowest measured during 2008-2014, which may reflect the relative cold and short ice free period in 2013. In 2015, there was a general increase in coverage at the shallow and intermediate depths, indicating improved growth conditions at 0-3 m and 0-5 m depth in Badesø and Qassi Sø, respectively (figure 4.18a-b). In contrast, there was a reduction in coverage at the deeper water; 3-6 m and 5-6 m in Badesø and Qassi Sø, respectively. The reduced expansion at larger depths may be explained by a shorter growing season in 2013, 2014 and 2015.

5 NUUK BASIC

The MarineBasic programme

Thomas Juul-Pedersen, Kristine E. Arendt, John Mortensen, Diana Krawczyk, Anja Retzel, Rasmus Nygaard, AnnDorte Burmeister, Dorte Krause-Jensen, Carlos M. Duarte, Martin E. Blicher, Maia Olsen, Ole Geertz-Hansen, Tenna Boye and Malene Simon

This report chapter describes the tenth full year of marine monitoring since the programme was initiated in late-2015. The main objective of the MarineBasic programme is to collect and study long-term trends in key physical, chemical and biological oceanographic parameters of the Godthåbsfjord region. This sub-Arctic programme operates in parallel with the MarineBasis-Zackenberg programme in NE Greenland. The collected data comprise a consistent time series of key marine parameters. Findings from the MarineBasic-Nuuk programme contribute to improving the understanding of this sub-Arctic marine ecosystem as well as enabling the identification, description and quantification of climate change related effects. The sampling frequency and consistent collection of data also facilitate the study of seasonal, annual and inter-annual patterns and variation in key elements of the marine ecosystem.

The sampling programme is comprised of monthly pelagic samplings, annual pelagic length and cross section studies of Godthåbsfjord and the adjacent coastal area, annual studies of macroalgae and macrobenthos, annual counting of seabirds, photo identification of marine mammals and collection of daily satellite and camera images of sea ice conditions in the Godthåbsfjord and Baffin Bay.

The monthly pelagic sampling is conducted at a permanent sampling station ('Main Station' (GF3); 64°07'N, 51°53'W; bottom depth ca. 350 m) located close to the fjord entrance, while the other parameters are sampled in and around the Godthåbsfjord system (figure 5.1). The methods used are described below, but more details can be obtained from the MarineBasis-Nuuk manual (www.nuuk-basic.dk).

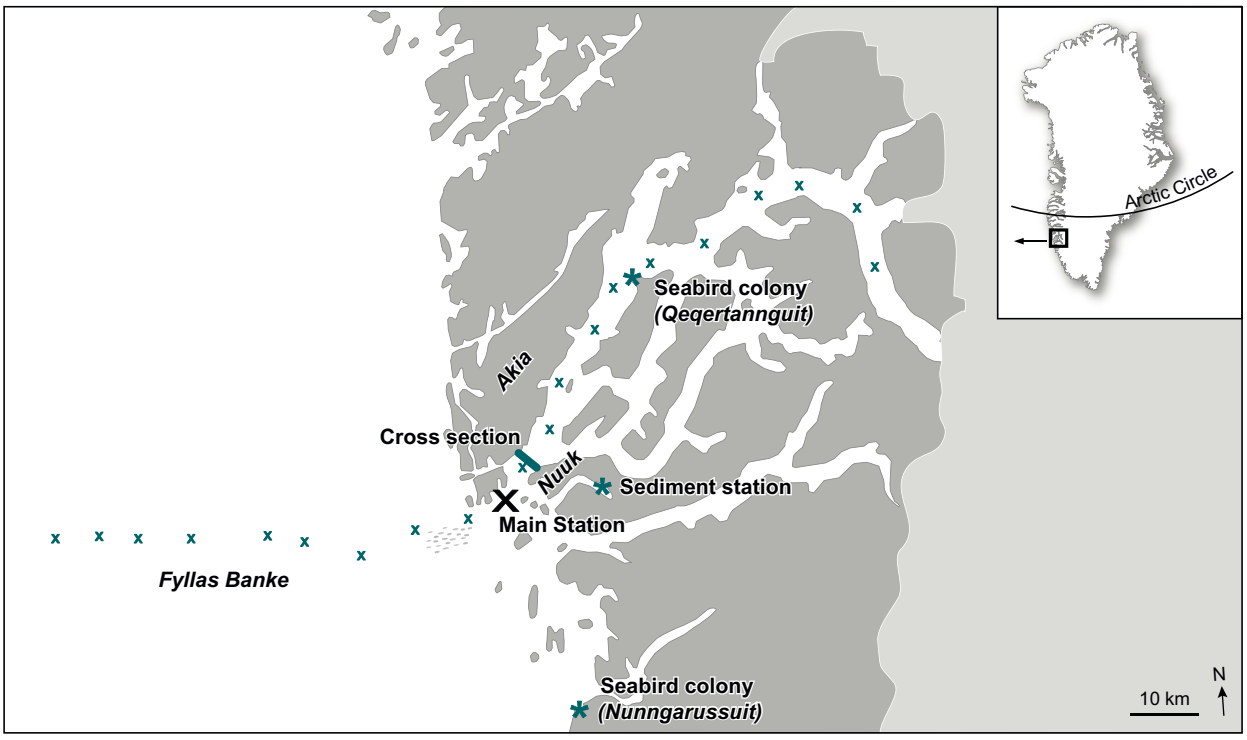

Figure 5.1 Map of sampling stations in and around the Godthåbsfjord system. X represent sampling stations along the hydrographical length section.

5.1 Sea ice

Sea ice conditions Godthåbsfjord monitored using satellite images. MODIS (250m resolution) satellite images were collected for Godthåbsfjord. Microwave-radiometer (AMSR, 3-6 km resolution) satellite images for Baffin Bay, which have been collected previously, are no longer available. Camera images of sea ice discharge covering a cross section of the fjord around Nuuk were collected every 3 hours, but due to establishing a new camera system photos from January to end-March are missing.

MODIS images of the Godthåbsfjord system and adjacent shelf area show that the offshore sea ice only retreated from the region by late April, which is later than in most years, where the ice edge in Baffin Bay often can be found further north than Godthåbsfjord as early as in February/March (figure 5.2). The sea ice cover in Baffin Bay usually disappears completely during summer and starts to form again from the north in October.

Only limited sea ice can be found throughout the year in the sub-Arctic Godthåbsfjord system (figure 5.2). Local land-fast ice during winter is observed mainly at the inner parts of the fjord and in smaller sheltered fjord branches. Sea ice and glacial ice is usually exported out of the fjord in seasonal burst events (e.g. figure 5.3 March, April and October) with longer periods of little or no ice export in between (e.g. figure 5.3 July).

Camera images from previous years covering a cross section of the fjord have shown that sea ice and glacial ice is being exported out of the fjord in seasonal burst events. Much of the sea ice and glacial ice has, however, been shown to melt within the fjord. Collection of camera images covering a cross section of near the fjord entrance (Nuuk) was re-established in 2015.

Collection and analyses of satellite data on sea ice coverage are currently conducted in collaboration with the Greenland Institute of Natural Resources, the Danish Meteorological Institute and Greenland Climate Research Centre (www.natur.gl). Daily satellite images covering Greenland are available at http://www.dmi.dk/groenland/maalinger/satellit/.

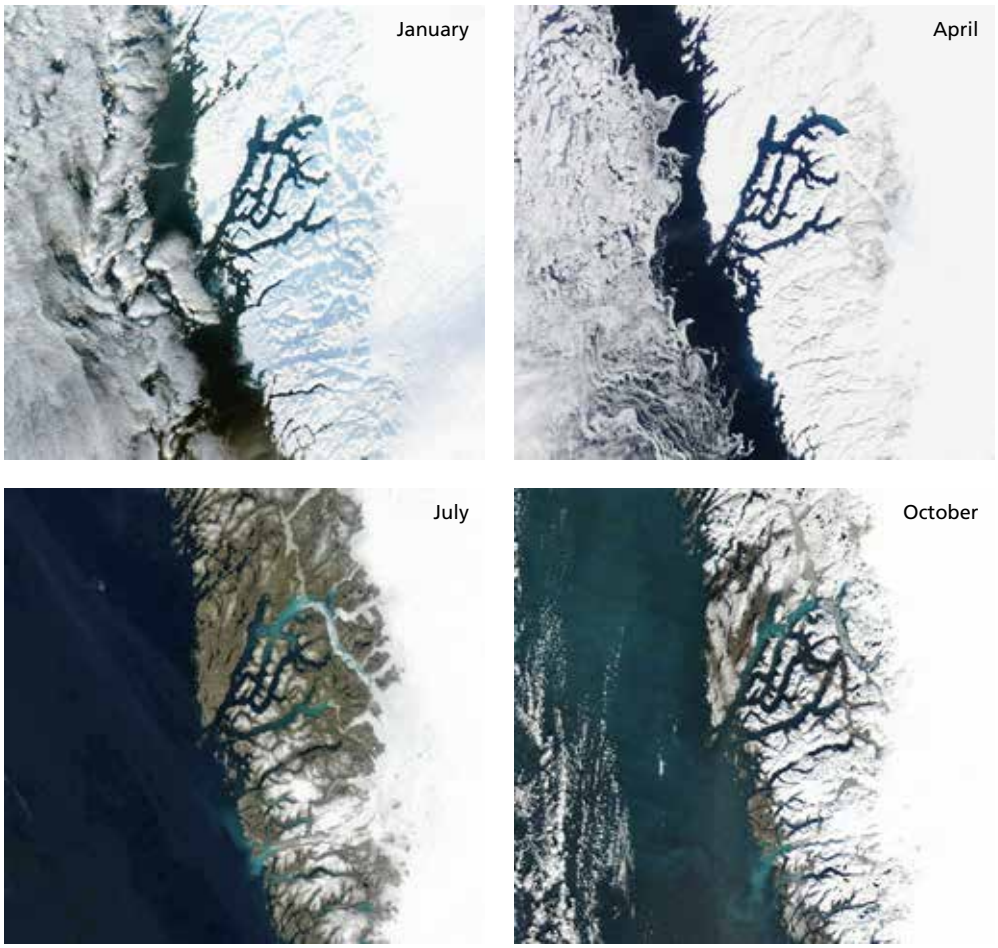

Figure 5.2 Satellite images (AQUA-MODIS) showing sea ice conditions in Godthåbsfjord during January, April, July and October 2015.

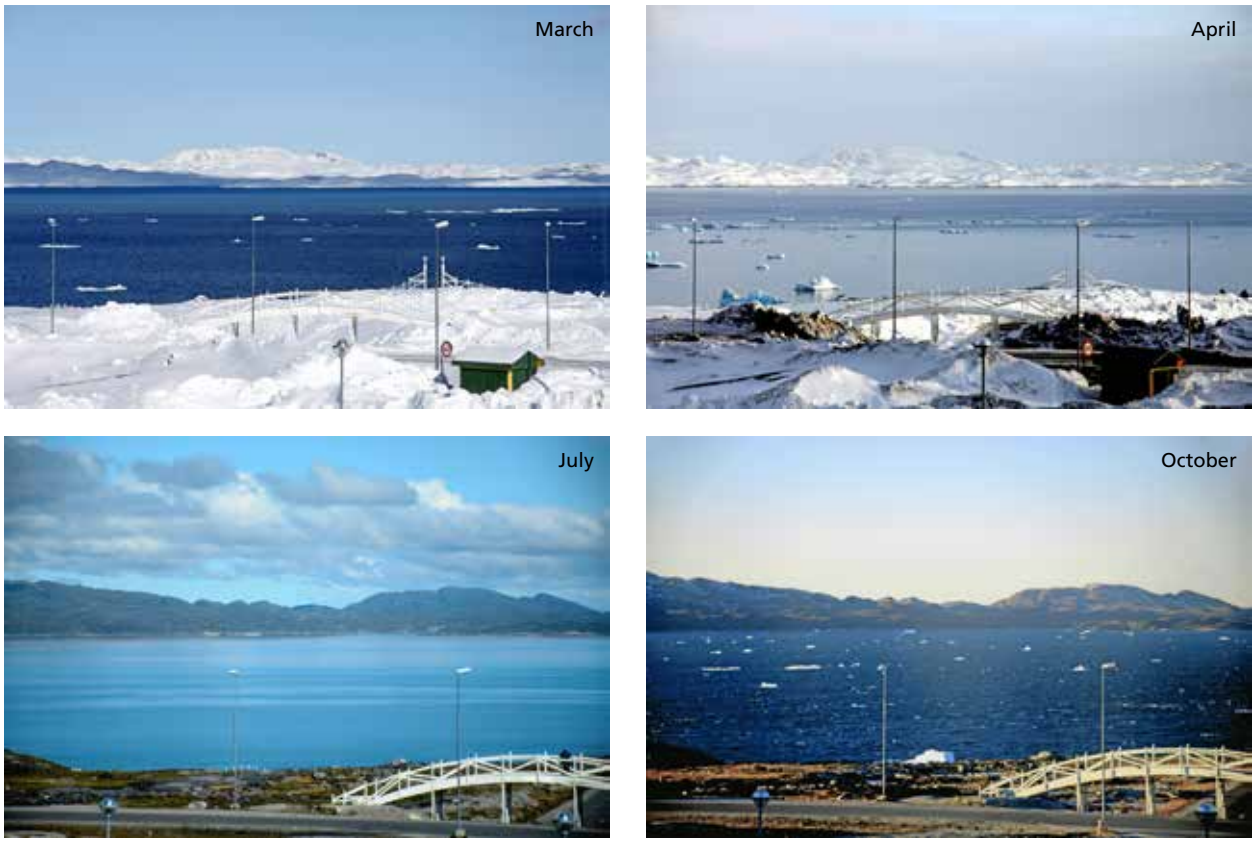

Figure 5.3 Digital images from Godthåbsfjord in March, April, July and October 2015.

5.2 Length and cross sections

The marine monitoring programme includes an annual length section from Fyllas Banke to the ice edge at the innermost part of the fjord (approximately 200 km long, figure 5.1). The length section was conducted on board the research vessel 'R/V Sanna' from 10-18 May 2015. A weak stratification of the surface layer due to early snow and ice melt was observed inside the fjord (figure 5.4). Phytoplankton (i.e. fluorescence; figure 5.4) thrive within the surface layer, where nutrients are still available this early in the productive season, i.e. surface nutrients become limiting later in the season, and satisfactory light conditions are found. The observed weak pycnocline is not strong enough in spring to withstand tidal mixing at the outer sill region, and the phytoplankton biomass is vertically mixed throughout the water column. Conditions on Fyllas Banke with the West Greenland Current on the outside flowing northward, cold water on top and frontal mixing along the edge sustain a high phytoplankton biomass on the bank. These patterns along the length section have also been identified in previous years.

Hydrographical profiles collected in late-May along a narrow cross section of Godthåbsfjord show a pycnocline in the upper 50-100 m (figure 5.5). The highest phytoplankton biomass (i.e. fluorescence) was observed within this surface layer. The surface layer was marginally thicker towards the Nuuk side. This is in contrast to most years, where a stronger surface often is found towards the Akia side due to the prevailing export of fresher surface water out of the fjord along this side.

5.3 Pelagic sampling

Monthly sampling was conducted at the 'Main Station' (GF3, ca. 360m; figure 5.1) including vertical profiles of salinity, temperature, density, turbidity, irradiance (PAR), and fluorescence was measured using a SBE19+ CTD profiler. The monthly sampling programme also included water samples collected for chemical analyses of concentrations of nutrients (NO_x, PO_4^{3-}, SiO_4 and NH_4^+) at standard depths 1, 5, 10, 15, 20, 30, 40, 50, 100, 150, 250 and 300 m. Additional samples were taken for measurements of dissolved inorganic carbon (DIC) and

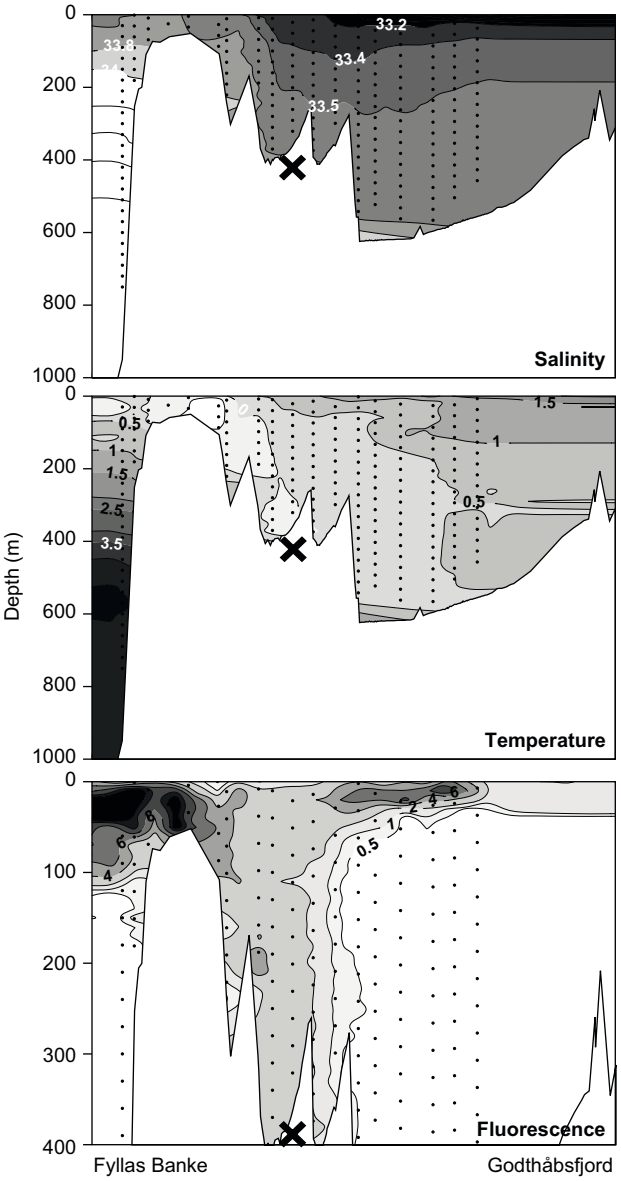

Figure 5.4 Salinity, temperature (°C) and fluorescence along the length section from Fyllas Banke to the inner part of Godthåbsfjord in May 2015. Vertical dotted lines represent sampling stations and depths in increments. X marks the location of the 'Main Station'.

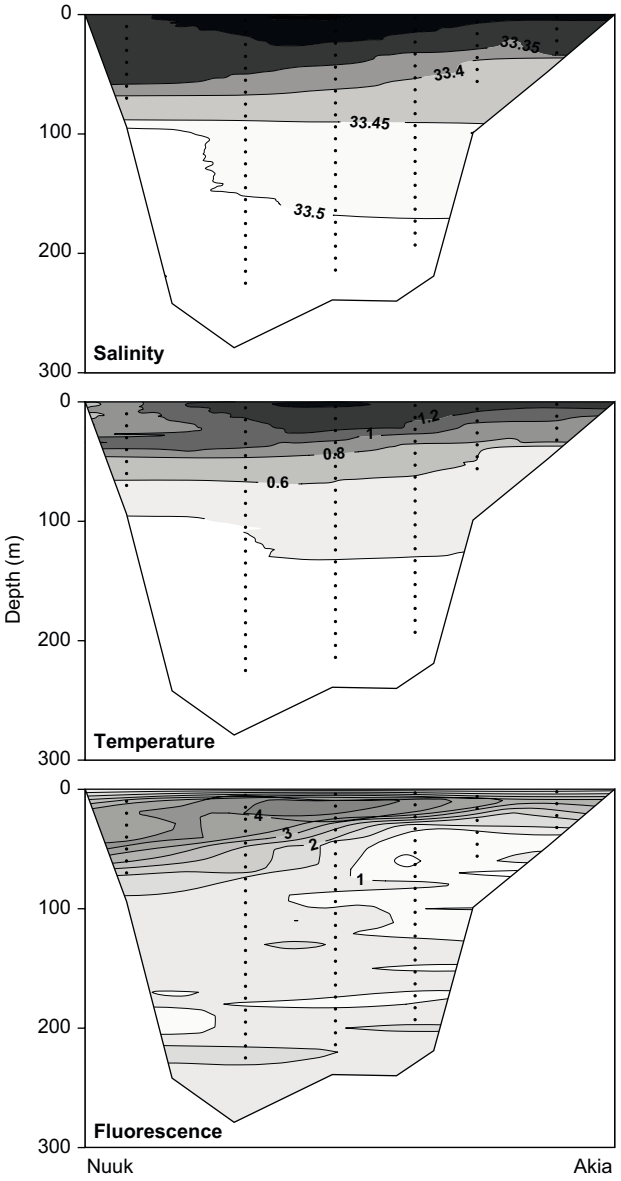

Figure 5.5 Salinity, temperature (°C) and fluorescence along the cross section from Nuuk to Akia in May 2015. Vertical dotted lines represent sampling stations and depths in increments.

total alkalinity (TA) at 1, 5, 10, 20, 30 and 40 m, representing the euphotic zone. Analyses of TA and DIC samples and the calculation of pCO_2 have been delayed and could not be completed in time for this report. In addition to these abiotic (i.e. physical and chemical) parameters, measured key biotic parameters included chlorophyll *a* and phaeopigments concentrations at 1, 5, 10, 15, 20, 30, 40, 50, 100, 150, 250 and 300 m, which is a measure of the phytoplankton biomass. Phytoplankton primary production was also measured monthly using the *in situ* C^{14} incubation method, corrected for *in situ* light conditions, at 5, 10, 20, 30 and 40 m during a ca. 2 hour deployments of a free-drifting mooring array. Unfortunately, the environmental data necessary for calculating the primary production was not obtained in time for this report, but data will be made available subsequently. Triplicate plankton net tows were also taken for zooplankton (45 µm WP2 net from 0-100 m) and phytoplankton (20 µm net from 0-60 m). Unfortunately, the zooplankton data was not processed in time for this report, but they will become available subsequently. To assess shellfish as well as fish larvae at the main station (GF3), single oblique sampling with a bongo net (335 µm) was used each month during 2008–2014. However, sampling was omitted in April and December 2014. Additional samplings

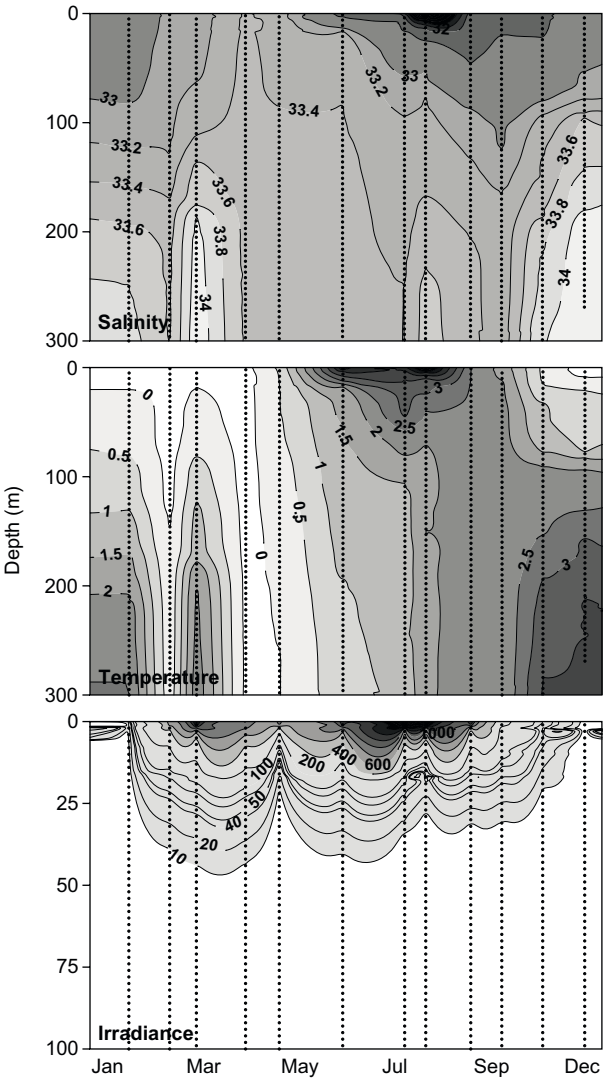

Figure 5.6 Annual variation in salinity, temperature (°C) and irradiance (PAR) at the 'Main Station' in 2015. Vertical dotted lines represent sampling days and depths in increments.

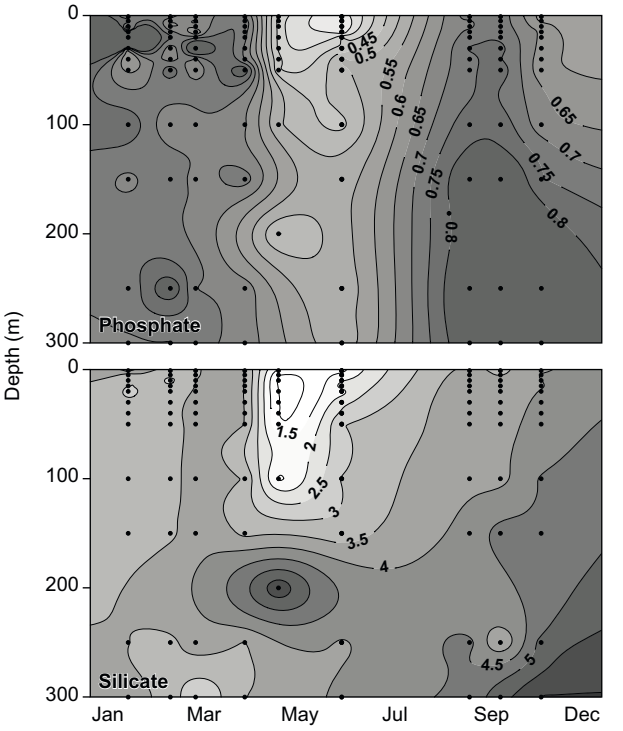

Figure 5.7 Annual variation in phosphate (µM) and silicate (µM) concentrations at the 'Main Station' in 2015. Vertical dotted lines represent sampling days and depths.

with a double oblique bongo net (335 and 500 µm) were carried out along a length section from offshore Fyllas Banke to the inner part of the fjord from 2006 to 2014. The number of collected stations along the length section varies among years, but typically stations FB3,5, FB2,5, GF3, GF7, GF7 and GF10 are attempted to be sampled each year. In 2013, collections also included FB2.5, FB1.5 and a new station "ice edge" close to the ice edge in the inner part of the fjord.

Vertical sinking flux of particulate material was measured using 4 particle interceptor traps also deployed on a free-drifting mooring array at 60 and 65 m (considered the same depth) for ca. 2 hours. The collected material was analysed for chlorophyll *a*, phaeopigments, total particulate carbon and nitrogen, while a sample was saved for identification. Unfortunately, the vertical sinking flux data was not analysed in time for this report due to technical problems, but they will be analysed and made available subsequently.

Abiotic parameters

Winter and early-spring conditions from January to March were characterised by no significant surface stratification, but deep warm and more saline costal inflow in January and March (figure 5.6). A deep coastal inflow was recorded again towards the end of the year in November and December. During spring, i.e. April and May, the weak surface stratification is mixed vertically by tidal forces, forming a largely homogenous water column. The onset of glacial melt combined with air-sea heat exchange and surface runoff in summer strengthen the surface pycnocline withstanding the tidal mixing at the outer sill region. This stratification starts to weaken in autumn, mainly due to a reduction in freshwater runoff, resulting in a largely homogenous water column in September and October. Seasonal light conditions in the water column, i.e. irradiance, generally follow the level of incoming solar radiation during the year (figure 5.6). However, particles in the water column, e.g. phytoplankton cells and silt

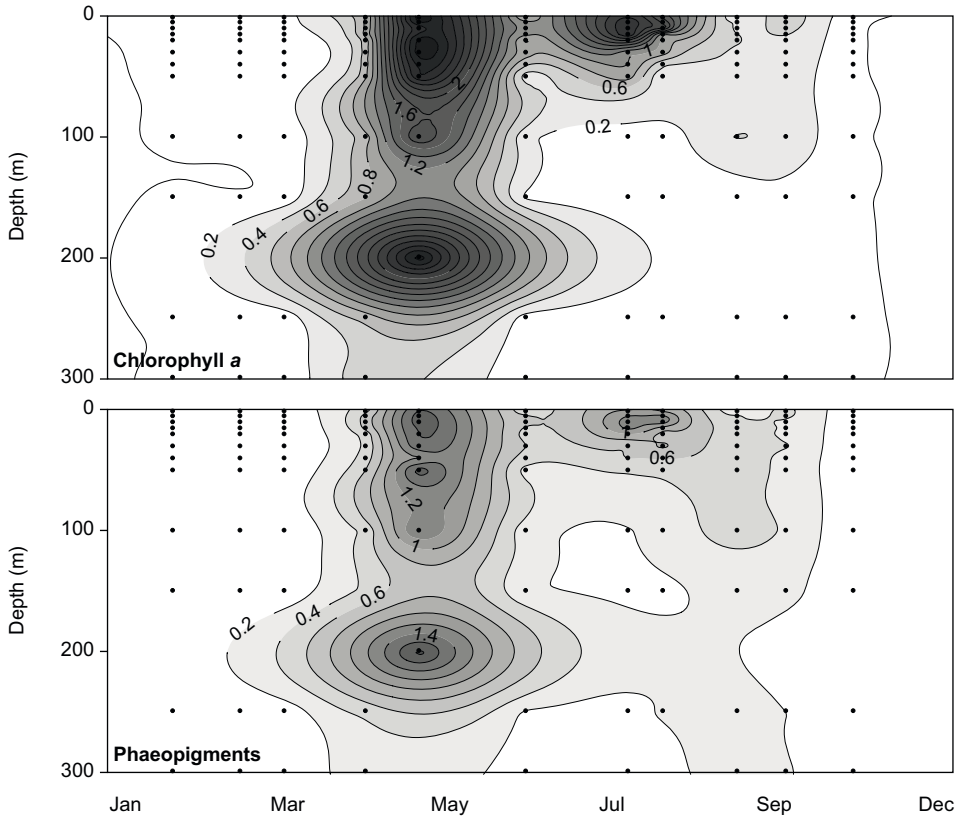

Figure 5.8 Annual variation in chlorophyll a concentration (µg l^{-1}) and phaeopigments concentration (µgl^{-1}) at the 'Main Station' in 2015. Vertical dotted lines on chlorophyll a and phaeopigments plots represent sampling days and depths.

particles, also reduce the irradiance distribution in spring and summer.

Phosphate and silicate showed high concentrations during winter and spring, while production in spring and summer reduced nutrients levels, particularly in the surface layer (figure 5.7). The decreases in primary production in autumn combined with weakening of the surface stratification promote the replenishing of nutrients from below. Nitrate (NO_3) data was not analysed in in time for this report, but will be made available subsequently.

Biotic parameters

Phytoplankton biomass and primary production was also measured as part of the monthly sampling programme (figure 5.8). During winter months, the phytoplankton biomass was negligible on an annual perspective, though very low values were measured during the period with low light levels. Increasing light conditions in spring along with ample nutrient concentrations lead to an immense increase in phytoplankton biomass. Primary production raw data seem to support this trend, however, it was not possible to calculate the final production values due to a delay in obtaining necessary environmental data in time for this report. Lower phytoplankton biomass in June signify post-bloom conditions. The onset of glacial melt and runoff, particularly as sub-glacial discharge, introduces nutrients to the surface waters from deeper fjord waters, which induces a summer phytoplankton bloom. The strong pycnocline in summer withstanding the tidal mixing maintains phytoplankton in suspension, but the pycnocline also reduces the supply of nutrients to the algae in the photic zone. A long lasting summer bloom was observed with significant phytoplankton biomass values lasting into October.

The plankton community

Phytoplankton samples were collected at the 'Main Station' using 20 µm vertical net hauls from 0-60 m water depth (approximate photic zone). Phytoplankton analysis included autotrophic algae, i.e. diatoms, haptophytes, chrysophytes and silicoflagellates and mixotrophic/heterotrophic dinoflagellates with ciliates. Similarly to previous years, diatoms dominated the phytoplankton assemblage throughout the year. The total average proportion of this group was 82% (figure 5.9). The second dominant phytoplankton group was haptophytes, represented by *Phaeocystis pouchetti* - formerly described as *Phaeocystis* sp. and now identified to a species level. Haptophytes showed highest relative abundances in May (45.2%) and June

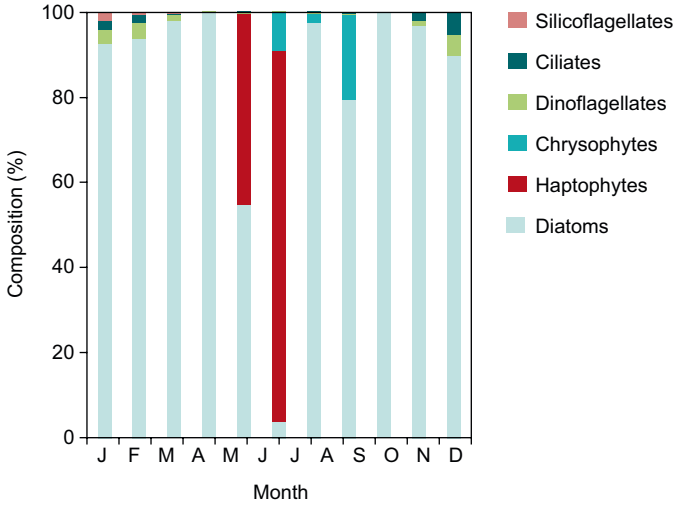

Figure 5.9 Seasonal variations in phytoplankton assemblage (%) at the 'Main Station' during 2015.

Table 5.1 Ten most dominant phytoplankton species presented as their relative accumulated proportion of total cell counts (%) at the 'Main Station' in 2015.

	2015
Chaetoceros sp.	46.5
Phaeocystis pouchetti	58.5
Thalassiosira sp.	65.6
Thalassionema nitzschioides	69.9
Chaetoceros convolutus	73.5
Fragilariopsis oceanica	76.5
Dinobryon balticum	79.3
Thalassiosira ant. var. *borealis*	81.5
Fragilaria cf *sopotensis*	82.9
Fossula cf *arctica*	84.2

(87.2%) (figure 5.9). Diatoms and haptophytes usually constitute the major part of phytoplankton spring blooms in the Godthåbsfjord as well as generally in the sub-Arctic and Arctic regions. During summer, the phytoplankton assemblage was mostly represented by diatoms, similarly to previous years. However, in summer 2015 chrysophytes showed unusually high relative abundances with a maximum of 19.8% in August (figure 5.9). This phytoplankton group has been described in affinity to low-salinity summer waters of high-Arctic fjords. Silicoflagellates showed low relative abundances between January and March (average of 1%). Dinoflagellates and ciliates are typically observed in winter in the Godthåbsfjord prior to the spring bloom. Both groups showed maxima in November, contributing 4.7% and 5.3% of the phytoplankton assemblage, respectively.

Throughout the year, diatom species *Chaetoceros* sp. together with the haptophyte species *Phaeocystis pouchetti* exceeded 50% of the total phytoplankton counts (table 5.1). Interestingly, diatoms were almost entirely composed of *Chaetoceros* sp. (99%) in September - when diatoms recorded a maximum relative abundance of 100% (figure 5.9). In April 2015, large colonies of species belonging to genus *Fragilariopsis* were observed in Godthåbsfjord. These species are generally known as sea ice-associated species and are possibly linked to the extensive and long lasting sea ice cover observed in Baffin Bay in winter 2015. Unlike the previous years, species belonging to a minor phytoplankton group chrysophytes, i.e. *Dinobryon balticum*, were among the dominant this year.

Vertical zooplankton net hauls (45 µm WP2 net) were conducted from 0-100 m. However, the results were not processed in time for this report, but they will be made available subsequently.

Since the beginning of the annual sampling at the 'Main Station' (GF3) in 2008, the abundance of fish larvae has varied over the years, with a temporal shift in species composition during summer (figure 5.10 and 5.11b). In general, sandeel *Ammodytes* sp. larvae dominates the abundance in late winter/early spring (February/March), arctic shanny *Stichaeus punctatus* larvae dominate the abundance in spring (April/May) followed by capelin *Mallotus villosus* larvae dominating the abundance in summer/autumn (July-September). In general, the abundance of sandeel larvae varies greatly between years. In 2013, the abundance of sandeel larvae in February was record high with 50 individuals pr. 100 m^3. However, in 2014 abundance was very low with only 0.58 individuals pr. 100 m^3, which was the lowest observed since 2011. In 2015, sandeel larvae peaked in February with 3.28 individuals pr. 100 m^3, which is the 4th highest value since 2008. Sandeel larvae have a second peak in abundance in summer (June), but in lower numbers than in early spring, except in 2012, where abundance was highest in June. The second peak in June 2015 was correspondingly lower than in February with 0.78 individuals pr. 100 m^3. The abundance of arctic shanny larvae in May 2015 was the 4th highest in the time series since 2008 with 0.74 individuals pr. 100 m^3. The abundance of capelin larvae was lower with 5.42 individuals pr. 100 m^3 in 2015 compared to 20 individuals pr. 100 m^3 in 2012, 2013 and 2014.

American plaice *Hippoglossoides platessoides* larvae peak in abundance in June, and highest numbers were observed in 2011 (10

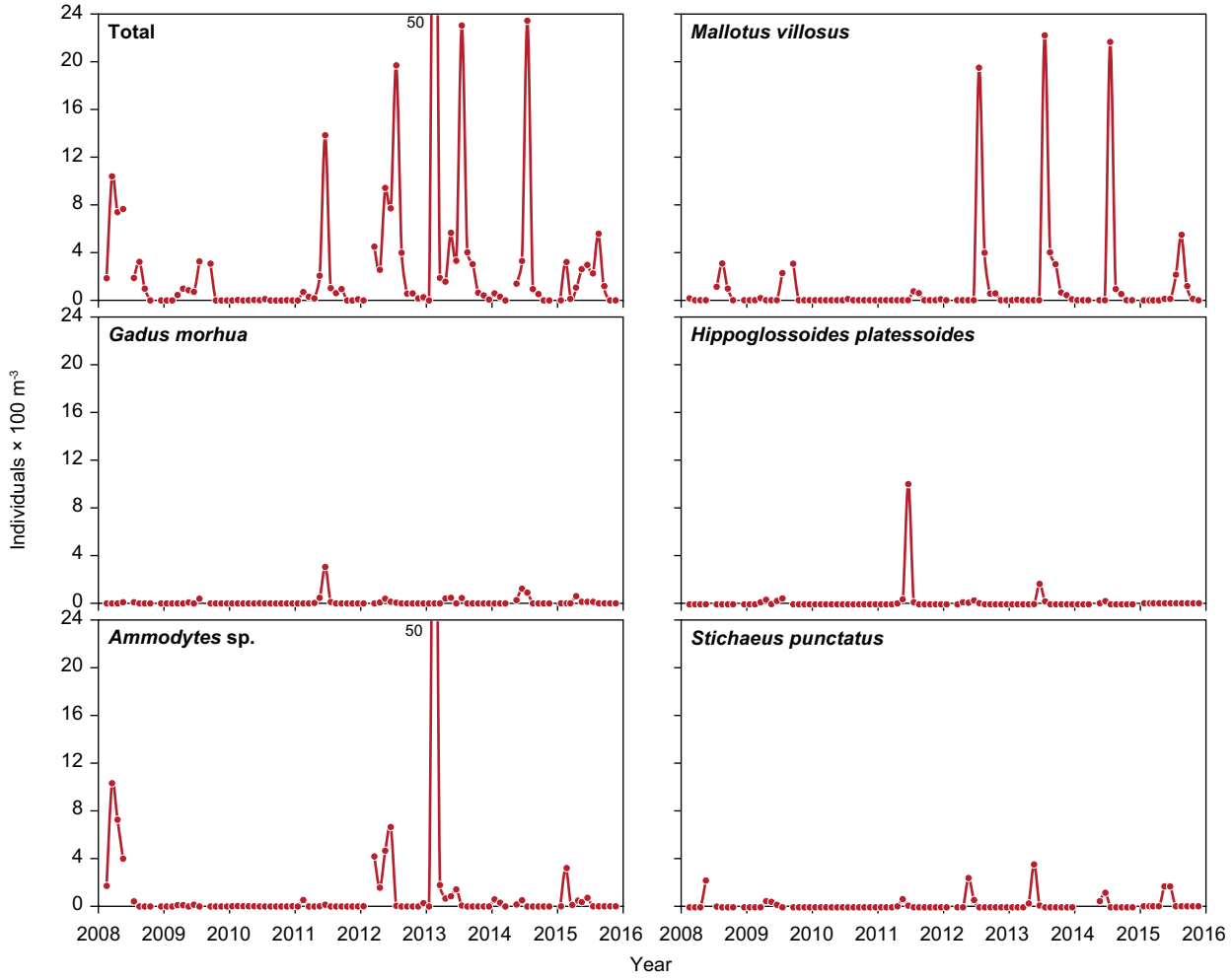

*Figure 5.10 Annual variation in abundance of fish larvae in total, capelin (*Mallotus villosus*), Atlantic cod (*Gadus morhua*), American plaice (*Hippoglossoides platessoides*), sandell (*Ammodytes *sp.*) and arctic shanny (*Stichaeus punctatus*) from 2008 to 2015 at the main station (GF3). Samples were collected each month, except January, June and November 2008, August 2009, February 2012, April and December 2014, December 2015.*

individuals pr. 100 m^3). Since then, no larvae have been found in significant numbers, and the abundance in 2015 was the lowest recorded since 2011. Atlantic cod *Gadus morhua* larvae seem to peak in different months between years from May to June, and the highest numbers were observed in June 2011 (3 individuals pr. 100 m^3). However, in 2015 the highest numbers were observed in April, although in low numbers (0.52 individuals pr. m^3) compared to June 2011. Overall, the abundance of fish larvae varies greatly between years, and especially 2010 was a year with very low abundance of fish larvae in all months. Since 2010, the abundance of fish larvae has increased, and 2013 was the year, with the highest abundance of fish larvae in the time series caused mainly by an increase in sandeel, capelin and arctic shanny larvae in the samples. In 2015, the total abundance of fish larvae was among the lowest recorded in the time series, caused by the numbers of capelin larvae being 75% lower than previous years.

In 2015, at the 'Main Station' no samples were taken in December and no fish larvae were found in the samples from January and November. The highest concentration of fish larvae was found in August (figure 5.11a), where capelin larvae accounted for 97% of the total abundance (figure 5.11b). Sandeel larvae were caught from February to June and dominated the abundance in February and March, however, in low numbers in March. Arctic shanny larvae were caught in May and June and dominated the abundance. Atlantic cod larvae were caught from April to July and had the highest abundance in April, accounting for 47% of the total abundance in that month. Capelin larvae were caught from May to October and dominated the abundance from July. The majority of species were caught in May, as seen in previous years.

On the length section in May 2015, no samples were taken on top of Fyllas Banke (station FB2.5), but the stations on the inner (FB1.5) and outer slope (FB3.5) were cov-

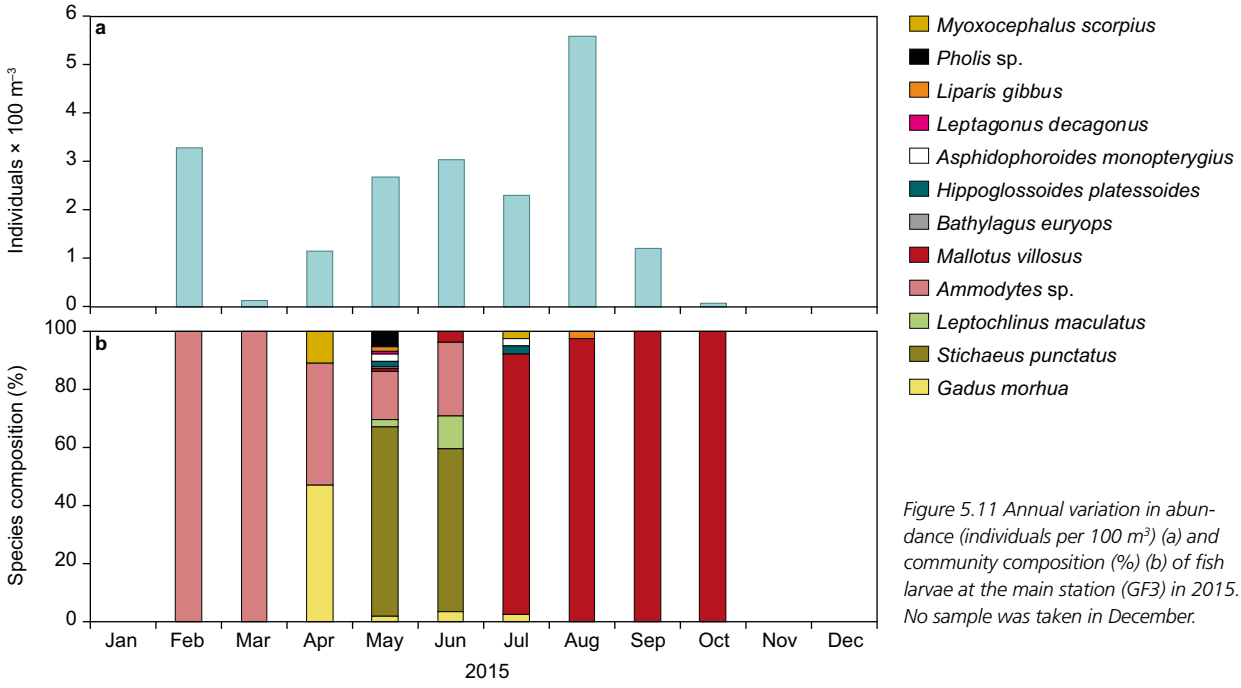

Figure 5.11 Annual variation in abundance (individuals per 100 m³) (a) and community composition (%) (b) of fish larvae at the main station (GF3) in 2015. No sample was taken in December.

ered. The results of the total transect show a similar pattern in fish larvae abundance and species composition as in the years 2006, 2007, 2011 and 2014, with highest abundances found on Fyllas Banke (FB2.5, FB1.5 in 2015) due to high numbers of sandeel larvae (figure 5.12a). Especially in 2006, the abundance was record high with 112 individuals pr. 100m³ (FB2.5). In 2015, the abundance of sandeel larvae on station FB1.5 was the same as in 2006 with 55 individuals pr. 100 m³, which is the highest number recorded in the time series (FB1.5 covered in 2006, 2013, 2014 and 2015).

In 2008, 2009, 2010, 2012 and 2013 highest abundances were found closer to the inlet of the fjord at the 'Main Station', mainly due to the absence of sandeel larvae in the samples from Fyllas Banke (Fyllas Banke was not covered in 2009). In 2015, redfish larvae *Sebastes mentella* were only found on the outer slope of the bank (FB3.5)

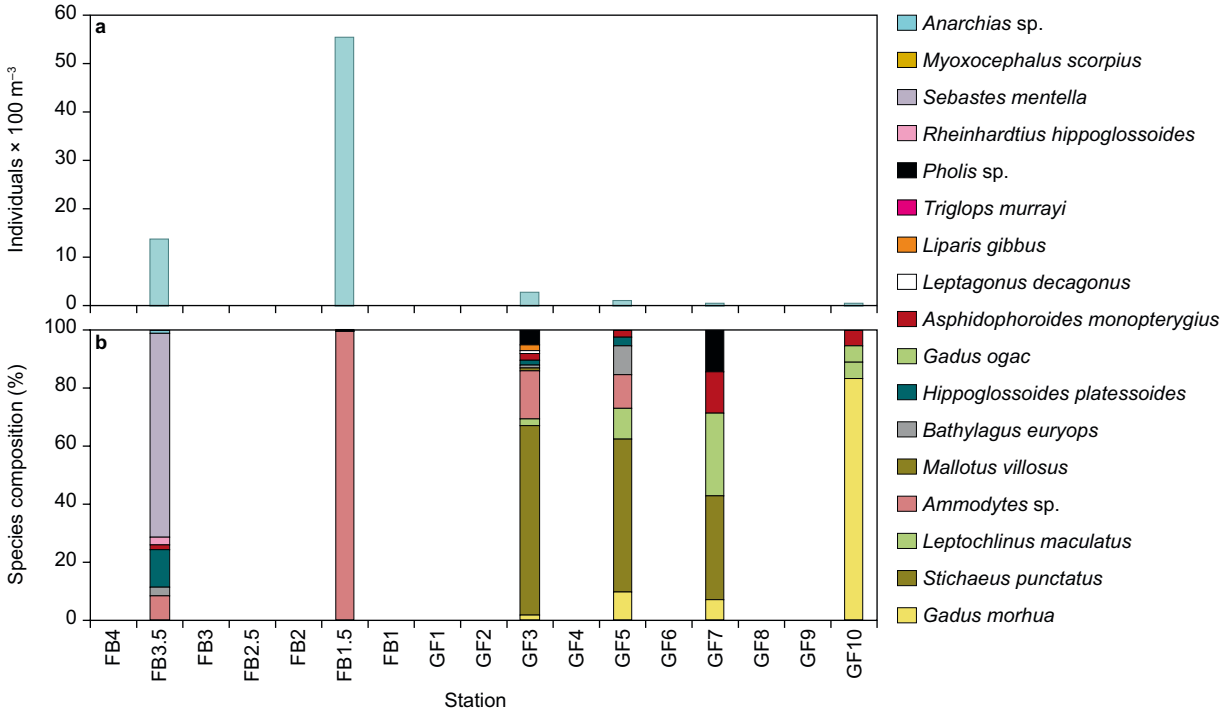

Figure 5.12 Variation in abundance (individuals per 100 m³) (a), and community composition (%) (b) of fish larvae on the length section in May 2015.

at record high numbers (9.6 individuals pr. 100 m^3) and dominated the sample with 70%. More species were found on the outer slope, including a single Greenlandic halibut *Rheinhardtius hippoglossoides* larvae, than on the inner slope towards the fjord (FB1.5), where sandeel larvae dominated the samples with 99.6%.

For the first time in the time series, Atlantic cod was found on all stations on Fyllas Banke in 2014, but not in 2015. Inside the fjord, Atlantic cod was found on all stations with highest concentration at the station deepest within the fjord (GF10), where Atlantic cod dominated the sample with 83%. This is the first time in the time series that Atlantic cod has been found with highest abundance deep inside the fjord, and the abundance is the highest recorded in the time series at this station. Arctic shanny dominated the abundance on all stations inside the fjord, except the station deepest inside the fjord (GF10), where total abundance was lowest. Overall, species composition varied on the length section with fewer species in the samples from the inner slope of Fyllas Banke (FB1.5) and from deeper inside the fjord (GF7 and GF10).

Fish larvae species composition seems to vary between years with most species found in 2014 (table 5.2). More species were found from 2008 due to the implementation of monthly samples from the main station (GF3). In 2006 and 2007, only the length section in May was conducted.

The shellfish larvae community at the 'Main Station' (GF3) showed the characteristic pattern with peak abundance of *Pandalus* sp. in April, one month earlier in than observations from previous years, whereas *Chionoecetes opilio* and *Hyas spp.* peaked in June. Peak density of *Pandalus* sp. was considerably lower in 2015 com-

Table 5.2 Species list of fish larvae 2006-2015.

Species list	2006	2007	2008	2009	2010	2011	2012	2013	2014	2015
Gadus morhua	×	×	×	×	×	×	×	×	×	×
Stichaeus punctatus	×	×	×	×	×	×	×	×	×	×
Leptochlinus maculatus	×	×	×	×	×	×	×	×	×	×
Ammodytes sp.	×	×	×	×	×	×	×	×	×	×
Mallotus villosus		×	×	×	×	×	×	×	×	×
Aspidophoroides monopterygius	×	×	×			×			×	
Bathylagus euryops		×	×	×	×	×	×	×	×	×
Cyclothone sp.		×								
Liparis sp.		×				×		×	×	
Liparis gibbus					×		×			×
Pholis sp.	×	×	×					×	×	×
Pholis fasciatus					×	×	×	×		
Pholis gunellus							×			
Reinhardtius hippoglossoides	×		×			×	×	×	×	×
Myoxocephalus scorpius			×		×		×	×	×	×
Hippoglossoides platessoides			×	×	×	×	×	×	×	×
Sebastes sp.			×			×	×	×	×	
Sebastes mentella										×
Gadus ogac			×	×	×					×
Leptagonus decagonus				×	×	×	×	×		×
Agonidae				×						
Lumpenus lampretaeformis				×	×		×	×	×	
Triglops murrayi						×	×		×	×
Cottidae						×			×	
Anarchias minor									×	
Anarchias sp.						×				×
Total	**7**	**10**	**13**	**11**	**13**	**16**	**16**	**15**	**17**	**16**

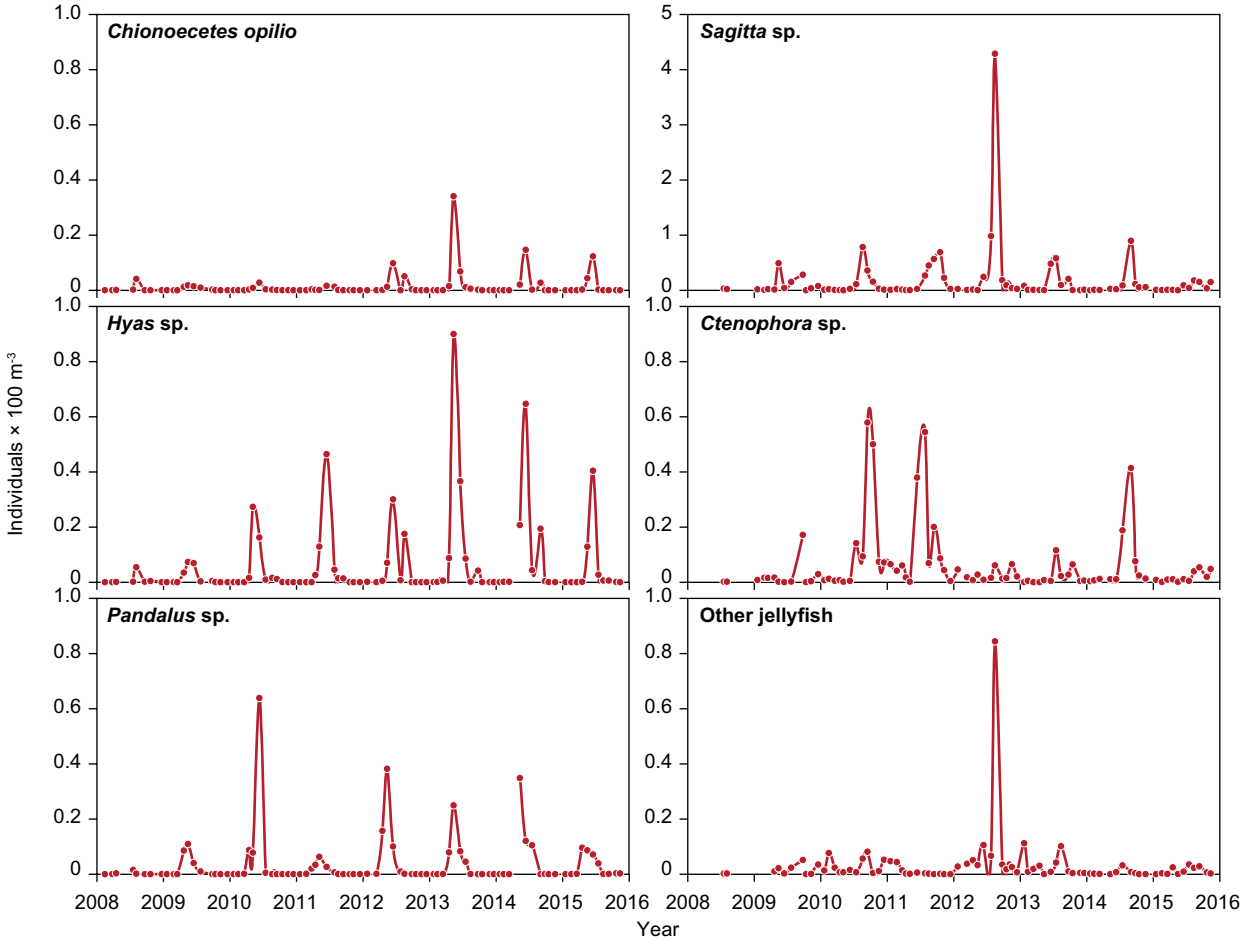

Figure 5.13 Annual variation in abundance (individuals m^{-3}) of Chionoecetes opilio, Hyas *sp.,* Pandalus *sp.* Sagitta *sp.,* Ctenophora *sp. and other jellyfish at the Main Station (GF3) from 2008 to 2015. Samples were collected each month, except November 2008, August 2009, April and December 2014 and December 2015.*

pared to the past three years, but almost at the same low level as observed in 2009 and 2011. Density of *Chionoecetes opilio* declined over 2013 and remained unchanged in 2015, nevertheless, the number of individuals' m^{-3} in June for the past two years has still been higher compared to estimates from 2009 to 2012. The continued increasing trend from 0.05 individuals (m^{-3}) in 2008 to 0.9 individuals (m^{-3}) in 2013 of *Hyas* spp. turned into a 29% drop from 2013 to 2014 and the declining trend continued in 2015 (figure 5.13). Larvae stage zoae I of *C. opilio* and *Hyas* spp. dominated samples in April to June, whereas larvae stage zoae II were more prevalent in July. Low concentrations of megalope stage of *C. opilio* and moderate concentrations of *Hyas* spp megalop stages were observed in October. Throughout the entire years of sampling, abundance of *C. opilio* was low compared to the other crab species *Hyas* spp.

At the 'Main Station' (GF3), the community was mainly dominated by *Ctenophora* and *Sagitta* spp. in all months of sampling, except in the period from April to June, where *Pandalus* spp., *Chionoecetes opilio* and *Hyas* spp. became more abundant. Except for 2010 and 2013, *Sagitta* spp. was the most dominating species from August to December (figure 5.14), whereas *Ctenophora* and other jellyfish dominated the species composition in Jan to March. The number of individuals (m^{-3}) of *Sagitta* spp. was recorded in considerably high numbers and peaked at 4 individuals (m^{-3}) in August 2012, followed by a significant decline in 2013, remained low in 2014, and was observed at record low numbers in 2015 (figure 5.13). In addition, densities of *Ctenophora* and Jellyfish were also at very low levels in 2015 (figure 5.13 and 5.14).

Along the length section at the fixed stations (FB3.5, FB1.5, GF3, GF5 and GF10) from Fyllas Banke (offshore) to the inner part of the fjord (GF10), densities of crab larvae *Chionoecetes opilio* were significantly higher in 2015 compared to the previous year (figure 5.15). In contrast, densities of *Hyas* spp. were lower at the offshore sta-

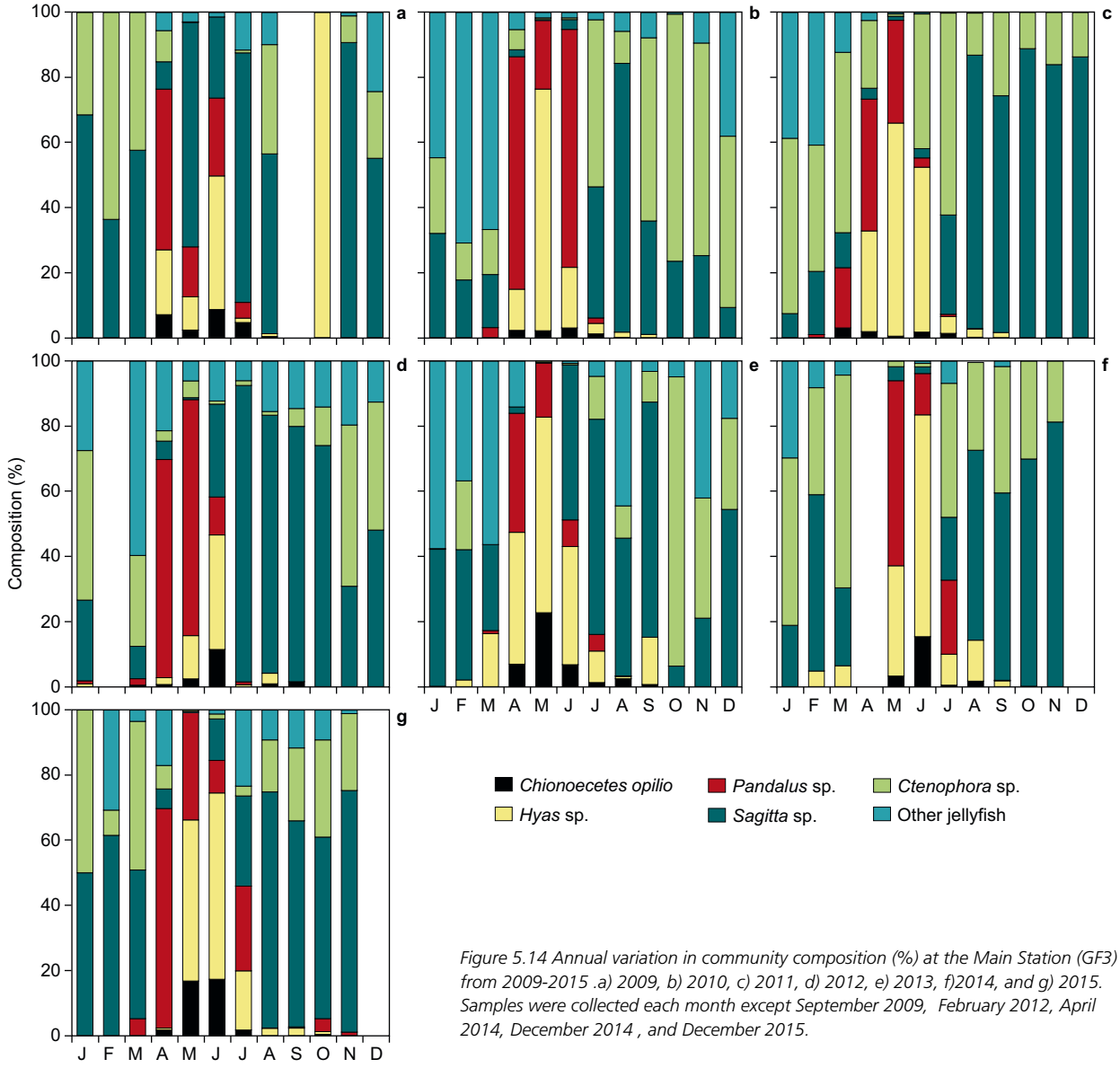

Figure 5.14 Annual variation in community composition (%) at the Main Station (GF3) from 2009-2015 .a) 2009, b) 2010, c) 2011, d) 2012, e) 2013, f)2014, and g) 2015. Samples were collected each month except September 2009, February 2012, April 2014, December 2014 , and December 2015.

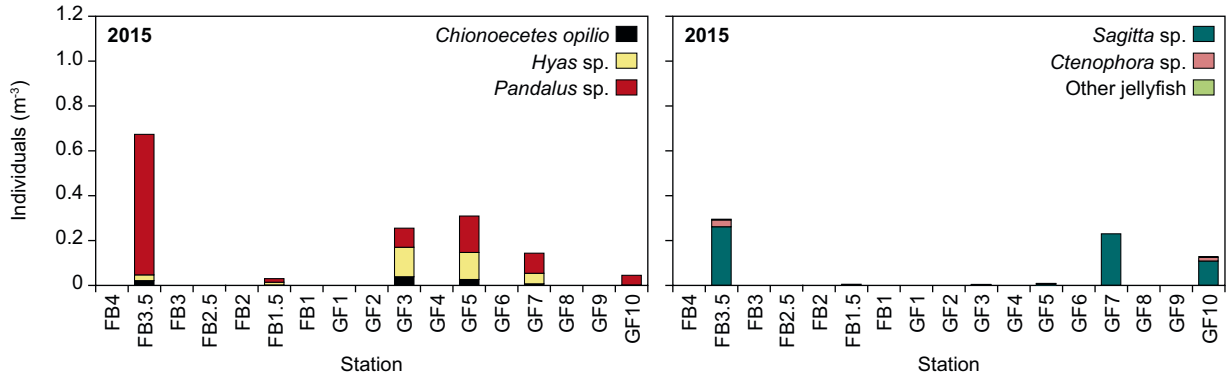

Figure 5.15 Annual variation in abundance (individuals m-3) of Chionoecetes opilio, Hyas *sp.,* Pandalus *sp.* Sagitta *sp.,* Ctenophora *sp. and other jellyfish along the length section from Fyllas Banke (offshore) to the inner part of Godthåbsfjord conducted in May 2015.*

tions, higher at the 'Main Station' (GF3) and GF7 and comparably low abundance of *Hyas* spp. at the most inner station GF10. The commercial species *Chionoecetes opilio* were mainly observed at the offshore stations FB3.5, GF3 and GF5, but were absent at the more inner stations along the fjord transect. *Pandalus* spp. were found at almost all stations along the fjord transect, with variations in density between stations.

Record high density was found at the offshore station FB3.5 and lowest density at the offshore station FB1.5 situated at the shallow water of the Fyllas Banke (figure 5.15). The community composition differed not only between stations, but also between years (figure 5.16). For the past two years, larvae of *Chionoecetes opilio* has been less abundant at all stations compared to previous years. *Sagitta* spp. conquered the community at the inner station GF7 and GF10, except with the occurrence of a few individuals of *Hyas* spp., *Pandalus* spp. and *Ctenophora*. The latter species was most abundant at the most inner station GF10, whereas it was almost insignificant at the offshore stations FB2.5 and FB1.5 (figure 5.16).

Vertical sinking flux

A part of the particulate material produced in the photic zone sinks through the water column towards the ocean sediment. This vertical transport of organic material provides the main source of energy for the benthic communities. Sediment traps moored on free-drift trap arrays for ca. 2 hours are used to measure the sinking flux of particulate material. The collected particulate material is analysed for chlorophyll *a*, particulate organic carbon and nitrogen, and isotopic composition. Unfortunately, the samples were not analysed in time for this report, but the data will be made available subsequently.

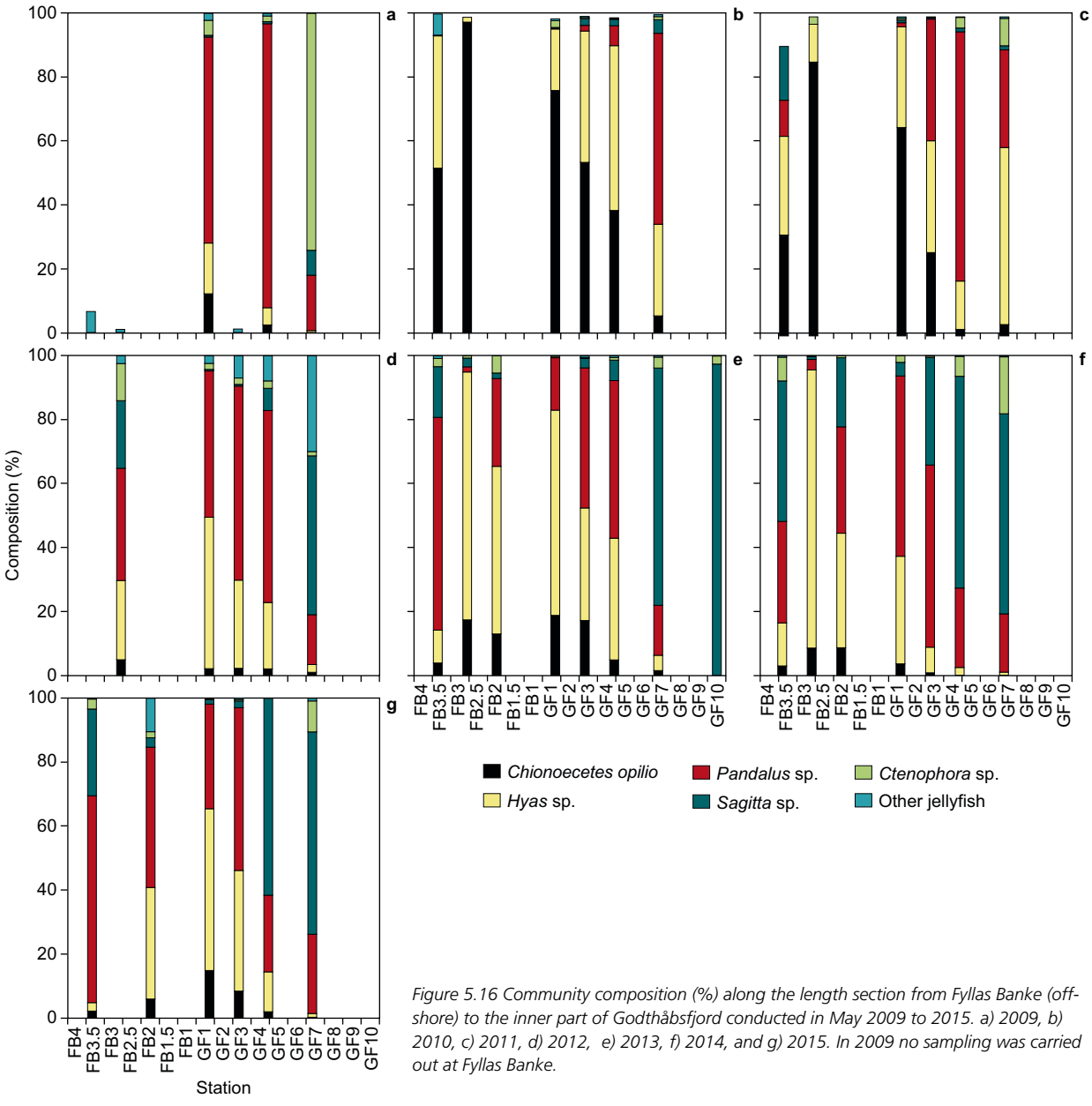

Figure 5.16 Community composition (%) along the length section from Fyllas Banke (offshore) to the inner part of Godthåbsfjord conducted in May 2009 to 2015. a) 2009, b) 2010, c) 2011, d) 2012, e) 2013, f) 2014, and g) 2015. In 2009 no sampling was carried out at Fyllas Banke.

5.4 Sediments

The benthic communities are largely fuelled by organic material sinking from the photic zone. The organic material reaching the benthos is mineralized by benthic organisms or buried in the sediment. Oxygen is the primary oxygen receptor in the upper oxic zone of the sediment, while it is the main receptor in the anoxic zone below. Both processes use oxygen either directly or indirectly, and oxygen uptake into the sediment is, therefore, used to measure the rate of remineralization.

Data from laboratory experiments conducted four times a year on sediment cores collected at a permanent sediment sampling station in Kobbefjord ('Sediment Station', depth ca. 120 m; figure 5.1) were included in the publication Sørensen et al. 2015. The experiments were stopped in 2015, and the existing time series is considered a baseline study. This baseline can be re-examined in the future for significant changes on a longer time scale.

5.5 Benthic flora and fauna

Since 2012, the monitoring of benthic flora and fauna has focused on growth and population dynamics of key species of the tidal zone - the brown macroalgae 'knotted wrack' *Ascophyllum nodosum* and 'blue mussel' *Mytilus edulis* - in relation to temperature, ice cover/light availability and tidal level. Knotted wrack and blue mussel are expected to respond positively to increases in water temperature, as both species are north-temperate with temperature optima (15-20 ºC for *A. nodosum*, Fortes and Lüning 1980) considerably higher than current temperatures in the Godthåbsfjord system. These species have the additional advantages as indicator organisms that 1) their growth is reflected in their morphology (see details below), 2) their presence in the tidal zone facilitates monitoring, and 3) they are important habitat forming species. The blue mussel data from 2015 was not processed in time for the report, but will be made available subsequently.

The coastal waters around Nuuk have a tidal range of 3-5 m, offering a large potential habitat for tidal communities (figure 5.17). The composition of this community varies with exposure to ice and waves (Høgslund et al. 2014), with *Ascophyllum* being a dominant keystone species of protected areas as represented by the monitoring sites in Kobbefjord.

Permanent monitoring plots were established in late August/early September 2012 in inner Kobbefjord in the mid intertidal zone as well as in the upper (MWL +0.5m) and lower intertidal (MWL -0.5m) zones and are revisited annually at the same time of year. Two additional sites were initiated in 2015 in the mid intertidal zone of the central and outer coast of Kobbefjord.

*Figure 5.17 a: Sampling in the tidal zone in Kobbefjord, Nuuk, where knotted wrack (*Ascophyllum nodosum*) dominates the algal community and bladder wrack (*Fucus vesiculosus*) and Fucus evanescence also are abundant (Photo: Peter Bondo Christensen). b: Tips of* A. nodosum *with knots/bladders (Photo: Núria Marbà). c: Blue mussel (*Mytilus edulis*) (Photo: Peter Bondo Christensen).*

Tip growth of Ascophyllum

Knotted wrack grows from the tip and forms an annual knot/bladder, giving rise to its name. The knots allow assessment of annual growth by simply measuring the distance and weighing the tissue between consecutive knots. Actively growing tips were sampled randomly in inner Kobbefjord (upper, mid and lower tidal zones) as well as at the central and outer site of Kobbefjord (mid tidal zone). At each location, the length of the three youngest segments was measured and weighed (i.e. segment 0=tip to base of 1st knot, segment 1=base of 1st to base of 2nd knot and segment 2=base of 2nd to base of 3rd knot).

The size of tip segments increased markedly from segment 0 (initiated the year of sampling) to segment 1 (initiated the previous year) and leveled off towards segment 2 (initiated two years before) (figure 5.18). Hence, the most sensitive tip growth indicator was the annual growth rate of segment 1, as quantified by the increase in size since the previous year (when it was segment 0). Over the period 2012-2015, this tip growth rate was largest in 2012-2013 (table 5.3), likely reflecting the mild winter of the year with very limited sea ice-cover, leaving the inner part of Kobbefjord nearly ice free and the algae exposed to full incident irradiance. Temperature loggings in the lower tidal zone confirmed that the winter 2012/13 was characterised by much higher temperature variability, resulting in lack of ice cover, than the other winters of the period, when an insulating layer of ice covered the shore (figure 5.19).

The size of tip segments also increased from the upper tidal level towards the mid and lower tidal levels, where exposure to wind, desiccation and ice was reduced (figure 5.18). By contrast, the size of the tip segments did not differ markedly between

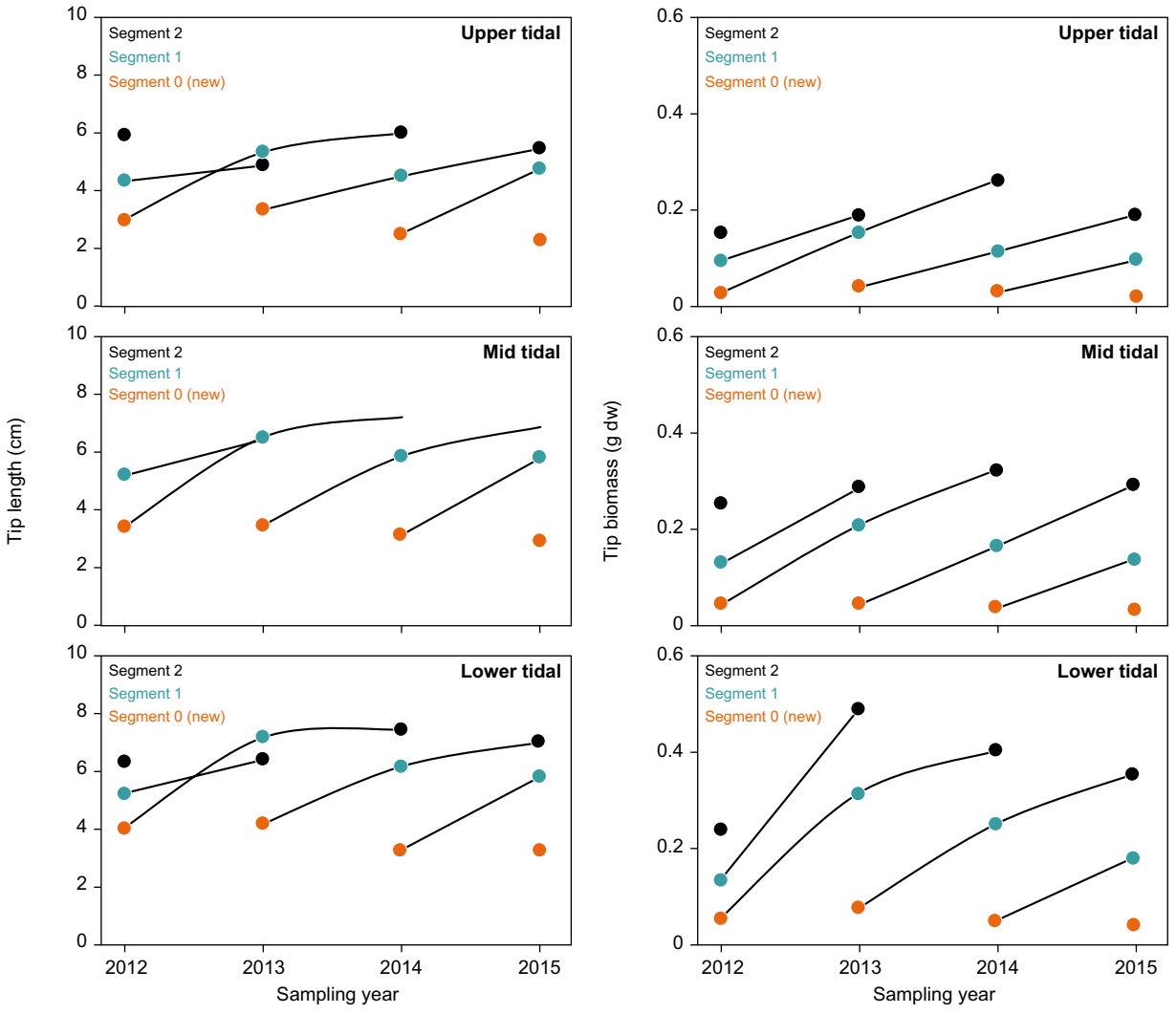

*Figure 5.18 Growth of knotted wrack (*Ascophyllum nodosum*) in inner Kobbefjord (upper, mid and lower tidal zone) in 2012-2015. The three youngest tip segments are shown: Segment 0 (newest, initiated the year of sampling), segment 1 (initiated one year previous to sampling) and segment 2 (initiated 2 years previous to sampling). Data represent averages of about 20 tips in each tidal zone each year.*

the inner, the central and the outer part of the fjord (figure 5.20).

Population dynamics of Ascophyllum

Population structure of knotted wrack was quantified non-destructively in 10 permanent plots (0.25 m × 0.25 m) in the mid-tidal zone in inner Kobbefjord. Each individual (representing 1-several 'shoots' arising from a common basal disk) with bladders and exceeding a minimum length of 5-10 cm was tagged and numbered in 2012, and length (L), minimum age (=number of knots of the longest shoot) and circumference (C) at the base were quantified each year. New individuals arising over the monitoring period were similarly tagged and measured. Based on this information, population density, biomass ($B=0.1057*LC^2$, Merzouk *et al.* unpublished) and age structure of individuals were estimated.

The habitat-forming role of *Ascophyllum* was illustrated by the huge population biomass (range 2012-2015: 13.9±2.2 to 26.5±3.5 kg fw m^{-2}) and density (range 2012-2015: 126±14 to 235±45 individuals m^{-2}, the range due to variable new settling between years, peaking in 2015) completely covering the rocky shore. The bulk of the biomass was composed of 4-10 year old shoots extending 30-80 cm above the surface of the rocks when lifted by the tide, while the longest shoots exceeded 1 m, highlighting the three-dimensionality of the habitat (figure 5.21).

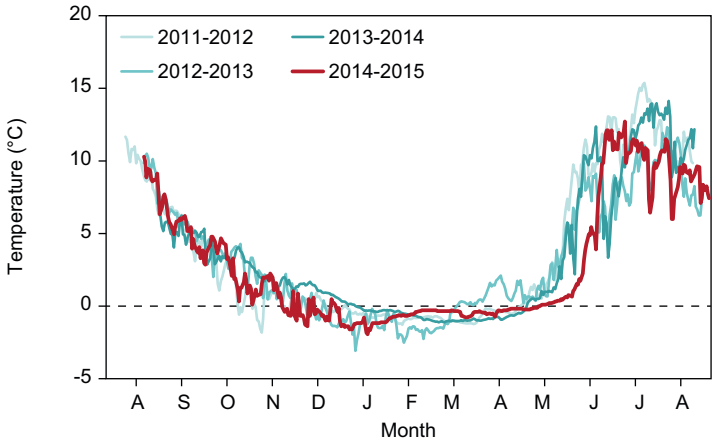

Figure 5.19 Temperature loggings in the lower intertidal zone of the monitoring site in inner Kobbefjord from August 2011 to August 2015.

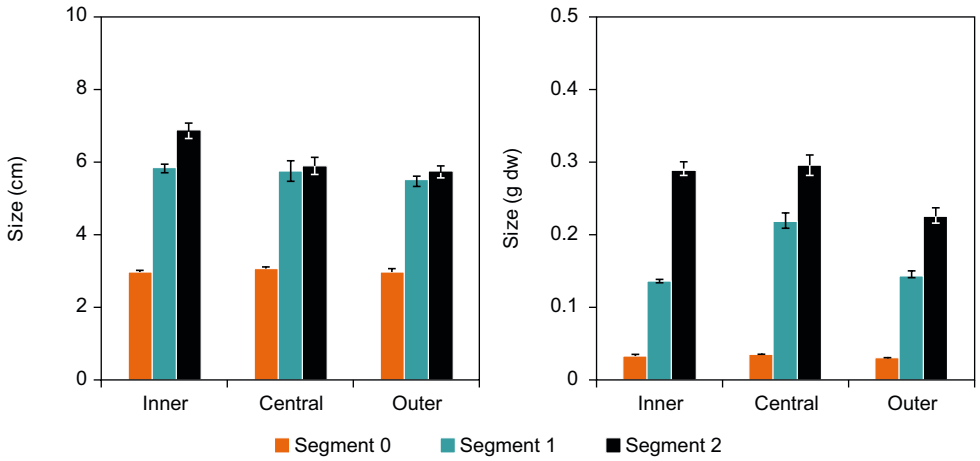

*Figure 5.20 Growth of knotted wrack (*Ascophyllum nodosum*) reflected by size of tip segments from the mid tidal zone at three sites in Kobbefjord: Inner fjord, central fjord and outer fjord. Segment 0 (newest, initiated the year of sampling,), segment 1 (initiated one year previous to sampling) and segment 2 (initiated 2 years previous to sampling). Data are average±s.e of about 20 tips from each site.*

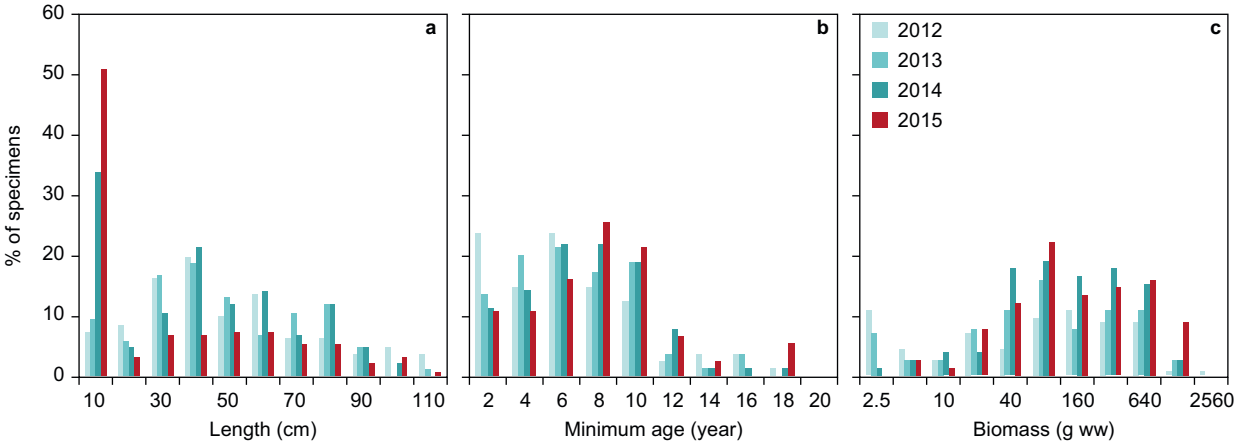

*Figure 5.21 Population structure of knotted wrack (*Ascophyllum nodosum*) in 10 permanent plots located in the mid tidal zone in inner Kobbefjord. Length distribution (upper panel), age distribution (central panel) and biomass distribution (lower panel) of individuals are shown. Recruits <2 cm length are included in the upper panel, but not in the lower panels are included in a but not in b and c.*

Table 5.3 Tip growth rate of Ascophyllum nodosum *expressed as the increase in size of segment 1 over one year (i.e. relative to the previous years' segment 0). Rates are provided in length and biomass units expressed as average±s.e. across the three tidal zones.*

Period	Growth rate (length unit)	Growth rate (biomass unit)
2012-2013	58±2% yr^{-1}	161± 5% yr^{-1}
2013-2014	41±7% yr^{-1}	120±10% yr^{-1}
2014-2015	59±2% yr^{-1}	122±7% yr^{-1}

Population dynamics in terms of net population growth, mortality and recruitment were assessed on the basis of changes in size of marked individuals in combination with observations of appearance and disappearance of individuals between years. The established individuals representing the vast majority of the biomass were quite persistent with loss rates of individuals of only 1.6-6.2% per year (table 5.4). The winter ice foot likely protects *Ascophyllum* against biomass losses during winter storms and helps stabilize the population. However, small new shoots add to the population dynamics, resulting in an overall recruitment rate of 6-111% and a high associated mortality rate (1.6-60%, table 5.2). This mortality rate matches that recorded in other *Ascophyllum* populations (8- 77% yr^{-1}, Åberg 1992ab). The growth of established shoots ensured a biomass increase of the population of 1-50% yr^{-1} during the assessment period 2012-15, which by far outweighed the biomass of lost individuals (table 5.4). The biomass increase was lowest from 2012-2013, probably because of the lack of ice cover during the winter 2013/2014.

5.6 Seabirds

Two key seabird colonies in the vicinity of Nuuk are included in the MarineBasic-Nuuk programme. Additional seabird colonies in the Nuuk area have been visited since 2007. The seabird counts from MarineBasic-Nuuk are reported annually to the Greenland Seabird Colony Database maintained by the Department of Bioscience, Aarhus University.

Qeqertannguit (colony code: 64035)

Qeqertannguit in the interior parts of Godthåbsfjord (figure 5.1) is a low-lying island and holds the largest diversity of breeding seabirds in the Nuuk District. Especially surface feeders, such as gulls *Laridae*, black-legged kittiwake *Rissa tridactyla* and black guillemot *Cepphus grille*, are usually well represented at the site (table 5.5). The steep cliff in the middle of the southeast facing side of the island (kittiwake and Iceland gull *Larus glaucoides*) and a smaller cliff on the northwest facing side (Iceland gull) were counted from the sea using a boat as platform and recounted later using pictures. Black guillemots present on the water around the island were also counted, using the boat as a platform. Counts of the remainder of the island were conducted by foot using direct counts of Apparently Occupied Nests (AON) or territorial behaviour as a criterion of breeding pairs. This year, the island as well as the SE and the NW colony were observed and photographed from boat on June 12.

Other birds observed during the walk, but not considered breeding or not systematically censured, included snow bunting *Plectrophenax nivialis*, Lapland bunting *Calcarius lapponicus* and rock ptarmigan *Lagopus muta*. The number of black guillemot around the island was estimated to 313 individuals. For the first time since the programme started, a pair of nesting white-tailed eagles *Haliaeetus albicilla* was observed with two chicks in the nest.

Arctic tern *Sterna paradisaea* was not observed at the island on June 12 and no nests were found (table 5.5). Complete absence of Arctic tern on Qeqertannguit was also recorded in 2008, 2013 and 2014. Small and mid-sized colonies of Arctic tern in Greenland are known to fluctuate considerably in population size and years of complete failure seem to occur regularly, but the reason is poorly understood.

On the southeast side, kittiwakes were present in larger numbers than in recent years. 80 individuals and 40 apparent nests were counted, the highest number since 2011. The number of Iceland gull has also increased, with 38 AON on the southeast side and 12 AON on the northwest side.

Also observed from the boat were one female common eider *Somateria mollissima*, one pair of red-breasted merganser *Mergus serrator*, and five long-tailed ducks *Clangula hyemalis*.

Qeqertannguit is influenced by legal egg harvesting (great black-backed gull *Larus marinus* and glaucous gull *L. hyperboreus* prior to May 31). Illegal egg harvesting (illegal species such as kittiwake, Iceland gull,

Table 5.4 Population dynamics of Ascophyllum nodosum *populations in the mid intertidal zone in inner Kobbefjord. Data are shown for the established population dominated by large old individuals as well as for the entire population incl. the dynamic population of small recruits. For the latter, we assumed that recruits <5-10 cm length represent the given years colonization and do not persist from year to year. Means±s.e of 10 permanent 25 × 25 cm plots are shown as absolute values (relative values in parenthesis).*

Period	Net. pop. growth Ind. (m^{-2} yr^{-1}) (% yr^{-1})	Recruitment Ind. (m^{-2} yr^{-1}) (% yr^{-1})	Mortality Ind. (m^{-2} yr^{-1}) (% yr^{-1})	Net biomass incr. (% yr^{-1})
The established population excl. small recruits				
2012-2013	-1.6±1.6 (-1.5±1.6)	0	1.6±1.6 (1.5±1.6)	1±13
2013-2014	-1.6±3.1 (-2.6±3.0)	1.6±1.7 (1.1±1.1)	3.3±2.3 (3.7±2.6)	50±18
2014-2015	-6.2±2.7 (-5.6±2.7)	0	6.2±2.7 (-5.6±2.7)	18±8
The entire population incl. small recruits				
2012-2013	4.7±5.5 (3.5±4.6)	6.2±5.0 (5.0±4.2)	1.6±1.6 (1.5±1.6)	
2013-2014	48±18 (29±10)	58±23 (32±12)	9.9±7.0 (9.0±6.2)	As above
2014-2015	53±40 (17±15)	111±42 (39±13)	60±22 (41±14)	

Table 5.5 Breeding seabirds (pairs (P), individuals (I) or Apparently Occupied Nests (AON)) at Qeqertannguit since 2006.

Year	2006		2007		2008		2009		2010	
Species	**No.**	**Unit**	**No.**	**Unit**	**No.**	**Unit**	**No.**	**Unit**	**No.**	**Unit**
Black-legged Kittiwake	45	AON	45	AON	20	AON	55	AON	42	AON
Iceland gull SE side	118	AON	82	AON	33	AON	40	AON	31	AON
Iceland gull NV side	-	AON	**	AON	12	AON	19	AON	13	AON
Great black-backed gull	46	P	38	P	44	P	24	P	40	P
Lesser black-backed gull	10	P	11	P	25	I	21	I	27	I
Glaucous gull	10	P	14	P	13	P	5	P	4	P
Herring gull	-	P	1	I	2	P	1	P	0	P
Arctic tern	150-220	I	150	I	0	I	150	I	54	I
Arctic skua	2	P	2	P	2	P	2	P	2	P
Black guillemot	615	I	562	I	689	I	637	I	790	I
Red-throated diver (*Gavia stellata*)	1	P	1***	I	1	P	1	P	0	P
Red-breasted merganser (*Mergus serrator*)	*		4	P	3	P	0	P	1	P
Year	**2011**		**2012**		**2013**		**2014**		**2015**	
Species	**No.**	**Unit**	**No.**	**Unit**	**No.**	**Unit**	**No.**	**Unit**	**No.**	**Unit**
Black-legged Kittiwake	80	AON	0	AON	1	AON	8	AON	40	AON
Iceland gull SE side	31	AON	11	AON	17	AON	17	AON	38	AON
Iceland gull NV side	20	AON	9	AON	16	AON	0	AON	12	AON
Great black-backed gull	17	P	16	P	18	P	9	P	6	P
Lesser black-backed gull	18	I	1	I	7	I	4	I	3	I
Glaucous gull	2	P	6	P	16	P	5	P	16	I
Herring gull	0	P	1	P	0	P	0	P	0	P
Arctic tern	50	I	50-100	I	0	I	0	I	0	I
Arctic skua	0	P	2	P	2	P	0	P	0	P
Black guillemot	1047	I	708	I	388	I	313	I	614	I
Red-throated diver (*Gavia stellata*)	0	P	0	P	0	P	0	P	0	P
Red-breasted merganser (*Mergus serrator*)	0	P	0	P	0	P	0	P	1	P

*Observed
**These birds are included in number for SE birds
***Seen at coast, but lake was dry and no nest visible

Table 5.6 Counts of breeding seabird at Nunngarussuit since 2006. Counts in Pairs are marked (P), and the remaining counts are of Individuals.

Year	2006	2007	2008	2009	2010	2011	2012	2013	2014	2015
Species	No.	No.	No.	No.	No.	No.	No.	No.	No.	No.
Guillemot unspecified	694	-			-	514	375	654	437	384
Brünnich's guillemot	-	705	388	475	-	-	-	-	-	-
Common guillemot	-	87	36	47	-	-	-	-	-	-
Guillemots on the water	2-300	450	450	-	-	500	2-400	-	300	200
Glaucous gull	20	14	14	12	-	11	4 (P)	-	18 (P)	12
Great black-backed gull	5	5	2	5	-	4	2 (P)	-	-	2
Northern fulmar	23	13	17	11	-	21	10 (P)	20 (I)	4 (I)	0

lesser black-backed gull *L. fuscus*, herring gull *L. argentatus* and egg harvesting after May 31) has been reported several times since the start of the monitoring programme.

Nunngarussuit (colony code: 63010)

Nunngarussuit is located app. 40 km south of Nuuk (figure 5.1). The north facing cliff wall of the small island holds the only colony of guillemots *Uria* sp. in Nuuk District. The colony includes both Brünnich's *Uria lomvia* and common guillemot *U. aalge*. These alcids are deep divers preying on fish and large zooplankton. Photo counts of birds present on the cliff were conducted from the sea (boat) on July 7 (table 5.6). The number of guillemots (both species) on the cliff was 384 individuals, less than observed the previous years. The number of guillemots on the water was estimated to be around 200. The birds were very nervous and took flight when the boat was within 3-400 meters of the colony. Due to the distance and, consequently, the quality of the photos, the two species could not be distinguished. Also observed at the colony were 15 razorbills (*Alca torda*), 12 glaucous gulls with six chicks and two great black-backed gulls.

Other seabird observations south of Nuuk

Simiutat islands

Simiutat consist of three small islands. The following was observed:

Simiutat (63011) July 24: 41 puffins *Fratercula arctica*, 11 black guillemots, three razor-billed auks, one great cormorant *Phalacrocorax carbo* and four female common eiders, one of which had eight ducklings.

Simiutat (63012) July 24: Six puffins, 47 razorbills, 12 black guillemots, one great black-backed gull on the island and 11 flying above it, six common eiders and eight harlequin ducks *Histrionicus histrionicus*. Approx. 30 gulls of unknown species were seen above the island.

Simiutat (63013) July 24: 11 puffins, 16 glaucous gulls, six razorbills, nine great black-backed gulls, 19 great cormorants, five northern fulmar *Fulmarus glacialis*, 12 black guillemots, 10 common eiders and one harlequin duck.

***"The Puffin Island"* at Ravneøerne (63020) July 24:**

190 puffins on the water and in the air, 33 razor-billed auks, 33 black guillemots and one great black-backed gull. On "Puffin Island", there were no obvious nests, however, some were found on the small island just south of it, where 45 puffins were observed outside their burrows. Other species observed during the trip around the area were: 120 black guillemots, 17 great black-backed gulls, nine harlequin ducks, 22 great cormorants, five common eiders and two king eiders *Somateria spectabilis*. Furthermore, 55 puffins were observed.

Qarajat Qeqertaat (63019) July 6:

This site consists of two islands with breeding common eiders:

West island: 49 nests of common eider. Average of 3.7 eggs/chicks per non-empty nest. Otherwise, 455 black guillemots, two purple sandpipers *Calidris maritima*, four pairs of great black-backed gull, 52 mixed gulls flying above the island and one pair of Arctic skua *Stercorarius parasiticus* – light morph. One peregrine falcon *Falco peregrinus* was observed flying through a group of gulls resting on the island. Nine nests of gulls with various numbers of eggs and chicks were found.

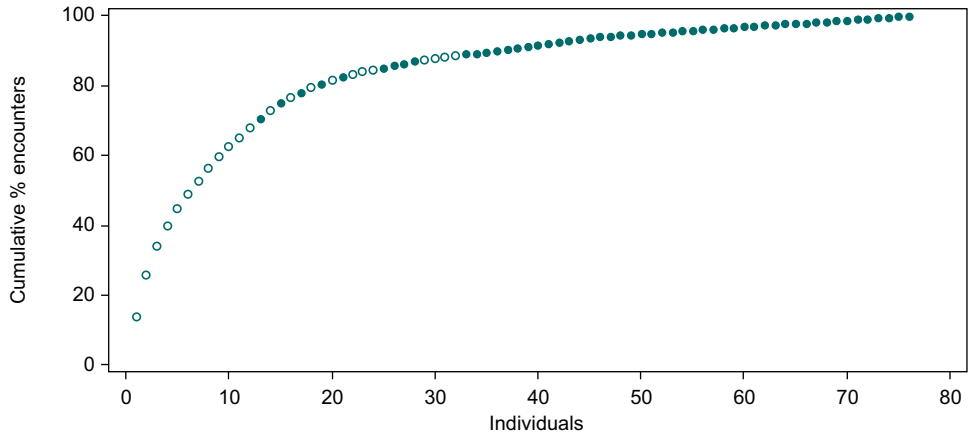

Figure 5.22 The sighting rate of each humpback whale individual. During 2007-2012, more than 30% of the encounters have been based on the same 3 individuals. Open circles are individuals resighted in 2 or more years. Closed circles are individuals sighted for only one year. (From Boye et al. 2014).

East island: 35 nests of common eider. Average of 3.4 eggs per nest with eggs. Additionally, one nest with one egg was found abandoned. Otherwise, 550 black guillemots, 20 mixed gulls flying around above island and approx. 60 mixed gulls resting on the water close to the island. 10 nests of gulls were found with a variety of eggs and chicks.

5.7 Marine Mammals

In the Marine Basis monitoring programme, we use photo-identification to later estimate the number of humpback whales *Megaptera novaeangliae* feeding in Godthåbsfjord each summer and the turnover of whales during a season to understand how much these top-predators eat and, thus, affect the Godthåbsfjord ecosystem.

Photo-identification is a technique used to identify individual animals from photographs showing natural markings such as scars, nicks and coloration patterns (Katona *et al.* 1979). The technique can, in combination with mark-recapture analysis, be used for estimating abundance of marine mammals in specific areas (Smith *et al.* 1999). Photo-identification is also used to investigate residence time (i.e. how long the animals stay in a given area) and site fidelity (i.e. individuals returning to an area in different years) (e.g. Boye *et al.* 2010). In humpback whales, the ventral side of the fluke is used for identification, as the tail contains individual colour patterns, which are individually unique like a human fingerprint. Photo-identification pictures were taken using a digital camera with a 400 mm lens, and in addition the public kindly contributed with identification-photos. In previous years, depending on weather from May to October, dedicated surveys were carried out twice a week from small research boats. Few surveys were conducted in 2015 due to limited personnel. The majority of the photos from this given period were therefore retrieved from locals and tourist.

A total of 18 ID pictures were collected in Godthåbsfjord in 2015, and from these 13 different individuals were identified. As in previous years, the resight rates during the period from 2007-2015 have been listed in table 5.7, but due to the low sample size (as in 2014) this is not necessarily a fair way to present the data, as a potentially large amount of the individuals present in the fjord were not registered. Yet, the individuals with the highest degree of site fidelity are also the individuals that stay within the fjord for the longest periods during the feeding season and are therefore likely to be encountered and photographed more often (Boye *et al.* 2014). Therefore, they are also most likely to be caught as part of the annual quota of humpback whales. During 2013 and 2014, the 3 most site faithful individuals were caught. Together, these 3 individuals accounted for more than 30% of the photos collected in the period 2007-2012 (figure 5.22) and these individuals have been present in the fjord every year (except for one individual that was not registered in the fjord in 2010). Due to their large degree of site fidelity, it is likely that they would have been present during 2015 if they had not been hunted and, consequently, this would have altered the resight rate seen in table 5.7 for 2015.

In the period 2007-2015, a total of 637 ID photos were collected (table 5.7), and from these a total of 109 individual whales have been identified in Godthåbsfjord so far. Between 10 and 33 individuals have been photographed each year.

*Table 5.7 Humpback whale (*Megaptera novaeangliae*) site fidelity to Godthåbsfjord in 2007-2015. Percentage of whales (within 2007-2015) identified in a given year and re-identified the following year in brackets.*

				No. of whales seen in each subsequent year							
Year	**No. of photos**	**ID**	**N**	**2008**	**2009**	**2010**	**2011**	**2012**	**2013**	**2014**	**2015**
2007	49	20	20	8 (40)	6 (40)	7 (27)	5 (24)	5 (19)	5 (15)	2 (20)	0 (0)
2008	143	20	12		6 (40)	10 (38)	7 (33)	9 (33)	8 (24)	4 (40)	1 (8)
2009	38	15	8			7 (27)	6 (29)	8 (30)	4 (12)	2 (20)	1 (8)
2010	68	26	13*				9 (43)	9 (33)	9 (27)	3 (30)	1 (8)
2011	130	21	10*					10 (37)	8 (24)	3 (30)	2 (15)
2012	85	27	13*						9 (27)	5 (50)	0 (0)
2013	88	33	21							6 (60)	1 (8)
2014	18	10	4*								1 (8)
2015	18	13	8								
Total	637	184	68								

*Contains individuals photographed in the fjord prior to 2007
ID number of whales identified the given year
N the number of new individuals the given year

6 Research projects

6.1 Exchange of CO_2 in Arctic tundra: impacts of meteorological variations and biological disturbance

Efrén López-Blanco, Magnus Lund, Mathew Williams, Mikkel P. Tamstorf, Andreas Westergaard-Nielsen, Jean-François Exbrayat, Birger U. Hansen and Torben R. Christensen

The main objectives of this project are (1) to explore the uncertainties in Net Ecosystem Exchange (NEE) gap-filling and partitioning into its two main modulating components, gross primary production (GPP) and ecosystem respiration (R_{eco}), (2) to determine how carbon (C) uptake and C storage respond to the meteorological variability and assess the resiliency of the studied ecosystem to meteorological variability, and (3) to identify how the environmental forcing affects not only the inter-annual variability, but also the hourly, daily, weekly and monthly variability. The intention is to elaborate on the information gathered in an existing catchment area under an extensive cross-disciplinary ecological monitoring programme in low Arctic West Greenland established under the auspices of the Greenland Ecosystem Monitoring (GEM) (http://www.g-e-m.dk). Using a long-term (8 years) dataset to explore uncertainties in NEE gap-filling and partitioning methods and to characterise the inter-annual variability of C exchange in relation to driving factors can provide a novel input into our understanding of land-atmosphere CO_2 exchange in Arctic regions. The time series is focused on the snow-free period. Our measurements typically start around the end of the snow melt (ca. May-June) and extend until the freeze-in period (between September-October). Once the snow melts, the growing season (i.e. the part of the year when the weather conditions allow plant growth) has been reported as the most relevant period defining both spatial (Lund et al. 2010; Mbufong et al. 2014) and temporal (Groendahl et al. 2007, Lund et al. 2012, Aurela et al. 2004) CO_2 variability.

Overall, the ecosystem acted as a consistent sink of CO_2, accumulating -30 g C m^{-2} on average (range -17 to -41 g C m^{-2}) during the years 2008-2015, except 2011, which was associated with a major pest outbreak. The results (figure 6.1.1 and 6.1.2) do not reveal a marked meteorological effect on the net CO_2 uptake despite the high inter-annual variability in the timing of snow melt, start and duration of the growing season. The ranges in annual GPP

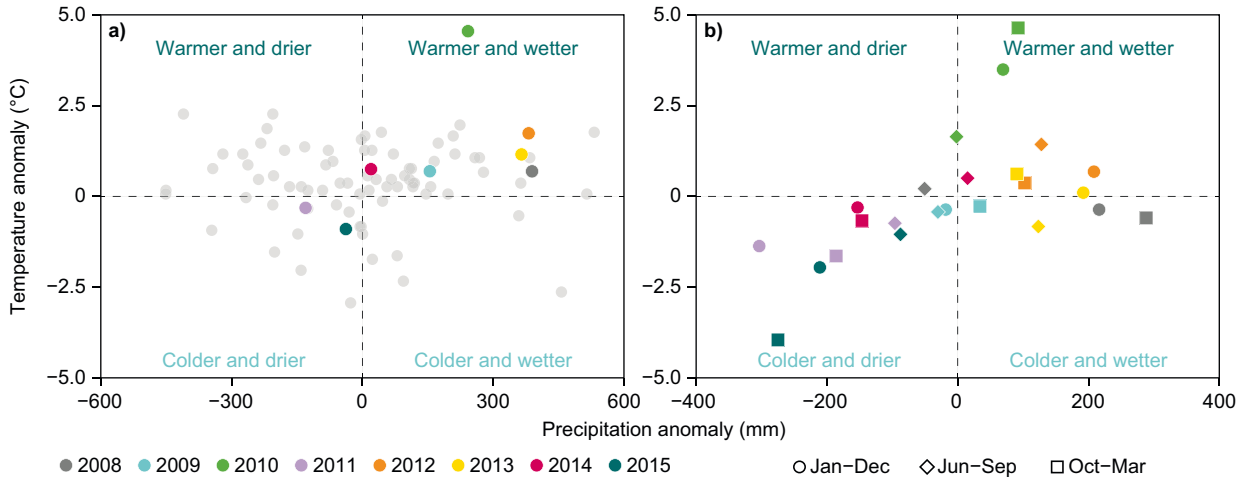

Figure 6.1.1 Annual Temperature (°C) and precipitation (mm) anomalies of the analysed years (2008-2015) compared to the 1866-2007 time series shown as empty circles (Cappelen, 2016).

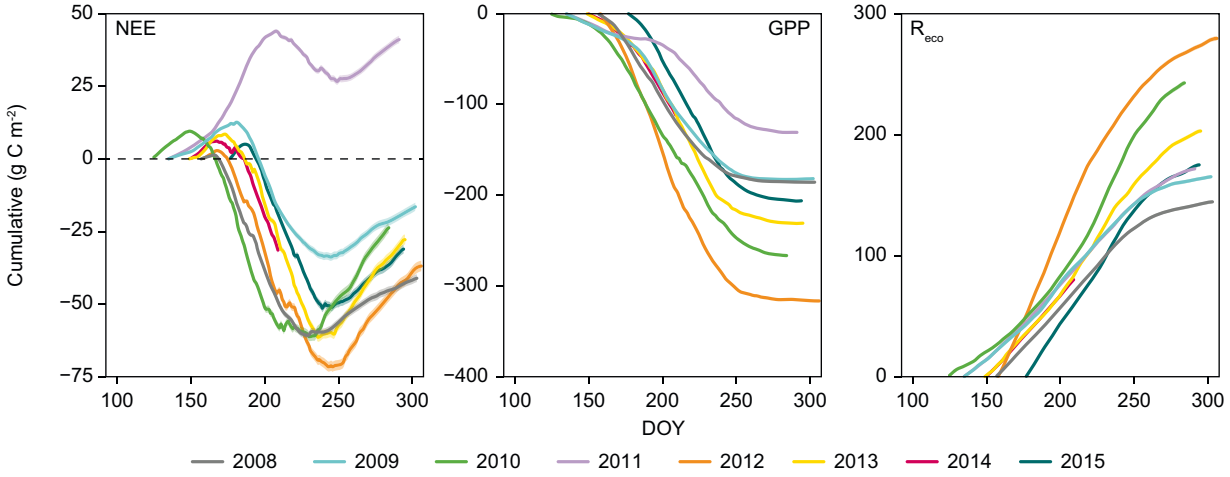

Figure 6.1.2 Cumulative NEE, GPP, and R_{eco} from 2008 through 2015.

(-182 to -316 g C m^{-2}) and R_{eco} (144 to 279 g C m^{-2}) were >5 fold larger and they were also more variable (Coefficients of variation are 3.6 and 4.1%, respectively) than for NEE (0.7%). GPP and R_{eco} were sensitive to insolation and temperatures; and there was a tendency towards larger GPP and R_{eco} during warmer and wetter years. The relative lack of sensitivity of NEE to climate was a result of the correlated meteorological response of GPP and R_{eco}. During the 2011 anomalous year, the studied ecosystem released 41 g C m^{-2}, as biological disturbance reduced GPP more strongly than R_{eco}. With continued warming temperatures and longer growing seasons, tundra systems will increase rates of C cycling although shifts in sink strength will likely be triggered by factors such as biological disturbances, events that will challenge the forecast of upcoming C states.

6.2 Landscape-scale variability and controls on ecosystem CO_2 exchange in southwest Greenland

Ulla Heede

(The following is a reprint of the Undergraduate Dissertation abstract).

The potential for large-scale feedback mechanisms between arctic terrestrial ecosystems and the atmosphere to anthropogenic climate change highlights the necessity to understand controls on carbon cycling in the Arctic. However, the factors driving spatial variability of CO_2 exchange in arctic ecosystems are poorly understood, creating large uncertainties in recent attempts to model the overall arctic carbon balance. This dissertation investigates controls on net CO_2 exchange (NEE) in wet fen and dry heath vegetation in southwest Greenland, using linear multiple regression with the goal of improving understanding of arctic ecosystems' response to environmental and climatic variables across vegetation and hydrological gradients. Species composition and hydrological properties in the two sites are investigated via a vegetation survey and soil moisture measurements, and the difference between the two sites is illustrated using image classification and NDVI mapping. CO_2 flux data is obtained via the eddy covariance technique, and net CO_2 exchange is calculated from post-processing flux measurements. Subsequently, the data is regressed against a range of environmental and climatic variables measured by automatic stations in 30 min. intervals. Throughout the growing season, the heath-site was twice as strong a sink for CO_2 than the fen-site, and flux partitioning indicated that this is caused by higher primary productivity in the heath-site in the beginning of the season and by a higher ratio of respiration to gross primary productivity in the fen-site. The large variation in net carbon uptake between sites highlights the importance of modelling efforts to attend to heterogeneity of species and soil conditions within landscapes. The multiple regression analyses showed that the combination of short- and longwave radiation, surface and depth soil temperatures, and precipitation could explain more than 50% of the variance in net CO_2 exchange in both sites, suggesting the appropriateness of

these variables for predicting NEE across the landscape. Shortwave radiation was the most important variable overall and correlated negatively with CO_2 flux (indicating ecosystems uptake), while rain and surface soil temperature correlated with positive CO_2 flux (indicating ecosystems loss). Contrary to findings in other arctic locations, the analysis suggests that soil respiration in both dry and the wet ecosystems was limited by moisture availability, however, most pronounced in the dry site. Furthermore, by including shortwave radiation in the regression, air and soil temperature variables correlated inversely with CO_2 uptake, hinting that weakening of sink strength might be the dominating short-term response to summer warming in both ecosystems.

6.3 Methane flux measurements with low-cost solid state sensors in Kobbefjord, West Greenland

Hanna Axén

(The following is a reprint of the Master's thesis abstract).

Methane is one of the most important greenhouse gases, and the Arctic region plays an important role in its dynamics. Due to limited observations in this remote and often harsh environment, large uncertainties surround the role of the Arctic region in a warming climate.

In this thesis, I examine the performance of the three low-cost solid state sensors, Figaro sensors TGS2600-B00, TGS2611-C00 and TGS2611-E00. These sensors could present a significant contribution in developing and expanding methane monitoring networks in the Arctic region and furthermore improve the understanding of underlying processes controlling methane emissions. The sensors were added to the existing automatic chamber setup in Kobbefjord, close to Nuuk, West Greenland. Methane fluxes were calculated based on the change in methane concentration when chambers were closed. A reliable fast methane analyser (RMT-200, Los Gatos Research Inc., USA) served as a proxy for methane fluxes, and the sensors' data was compared to this.

The resolution from the three sensors was limited by an analog-to-digital converter, which is expected to contribute to the larger spread in the sensors' data compared to the LGR. Occasional changes of relative humidity inside the chambers resulted in overestimated fluxes. The experimental setup caused low relative humidity inside the syringe containing the sensors. Low relative humidity is known to be problematic, which could be why no clear relationships between the sensors' signal and relative humidity and temperature were found. By filtering data with a relative humidity change 27%, most of the overestimated fluxes are most likely removed. The sensors were able to capture the seasonal trend in the methane fluxes and the magnitude of the seasonal mean fluxes from different chambers. The results could not be statistically supported due to seasonal trends in the data and the lack of replicas.

The sensors differ in sensitivity to other deoxidizing gases. At this site, no indications of such gases were found, but this could be a problem at other sites, meaning that one of the more methane specific sensors may be suitable. Although the TGS2600-B00 sensor showed better results in this study, further tests are required to determine which of the sensors are the best. In conclusion, the results indicate that these sensors with further refinements may well be used for expanding monitoring networks of methane fluxes in the Arctic.

6.4 Arthropod communities

Ejgil Gravesen and Jamin Dreyer

During the summer season 2014, we undertook a pilot study to explore the arthropod communities of a 259 m long transect at a glacier foreland area on a northern slope of the Qassi mountain in the Kobbefjord research area (64°07'N / 51°21'W). The transect began closest to the glacier – 52 m from a snow covered area in front of the glacier running south to north. The transect consisted of 14 "wet" pitfall traps filled with a solution of 25% ethylene glycol to kill and preserve arthropods. Arthropods captured in the wet pitfall traps were identified to order, family (Diptera, Aphidoidae and Acaridae) or to species level (Araneae and Collembola).

The number of arthropod species increased with distance from the glacier. Kobbefjord forelands are home to only a single species of predatory ground beetle *Nebria rufescens* (Ström) and a single spe-

cies of predatory harvestman *Mitopus morio* (Fabricius). The earliest foreland spider colonizers all belong to the Linyphiid subfamily group, Erigoninae, while spiders belonging to the subfamily group, Linyphiinae, were later colonizers to the glacier foreland area (measured in 2014).

To measure arthropod abundance, diversity and trophic linkages, 21 "wet" and 21 "dry" pitfall traps were operated from July-August 2015 in three distinct ground cover types (gravel, bare ground, and vegetated) in a foreland area at the northern face of a mountain peak north of Kobbefjord. Soil, water and organic matter content in the topsoil were measured during periods of dry weather. Soil moisture and organic matter were greatest in vegetated patches and equivalently low in both gravel and bare ground patches. Not surprisingly, total arthropod abundance of all three functional groups, detritivores, predators and herbivores, increased from gravel to bare ground to vegetated patches.

To collect predators for DNA gut content analysis, dry pitfall traps without fluid were used. The live arthropod predators (ground beetle (*N. rufescens*), harvestmen (*M. morio*), and several spider species in the family Linyphiidae) were collected from the dry pitfall traps and individually placed in 1.5 mL tubes filled with 95% ethanol. Total DNA was extracted from the predators, including the contents of their guts, which were screened for prey DNA, using prey specific primers - specific to Collembola, Diptera, and Aphididae.

Both ground beetles (*N. rufescens*) and harvestmen (*M. morio*) were confirmed as multi-channel feeders, consuming both types of detritivores (Collembola and Diptera) and an herbivore (Aphididae). Collembola were a common prey item, and spider consumption of Collembola increased in direct relationship to their abundance in each habitat type. Ground beetles consumed Collembola most often in gravel patches, while detectable Collembola DNA was only detected in harvestmen from vegetated areas. Diptera (flies) were consumed by all three predators, but most often by ground beetles and nearly equally across all patch types. Curiously, aphid DNA was only detected in beetles and harvestmen from bare ground patches, where aphid abundance was very low and there were no vascular plants for them to feed on, perhaps suggesting aphid movement into these areas where they could be easy prey for the predators.

7 Nuuk Basic

Disturbance in the study area

Maia Olsen

The study area at Kangerluarsunnguaq/Kobbefjord is situated approximately 20 km south-east of Nuuk and can be reached by boat within half an hour. It is a public area and admittance is free to anyone.

Public disturbance falls in the following categories:

- Visits by boats in the head of the fjord – no landing
- Visits by boats in the head of the fjord – people take a short walk inland and return within a few hours or less.
- Visits by boats in the head of the fjord – people go on land and spend the night in a tent close to the coast.
- Hiking through the area – there is a hiking route from Nuuk to the inland passing through the area.
- Visits by snow mobile – during winter people visit the area from Nuuk.
- The electrical power transmission line between Nuuk and the hydro power plant in Kangerluarsunnguaq/Buksefjord runs through the area.
- Ordinary flights by fixed winged aircrafts passing over the study area in cruising altitude or in ascent or descent to or from Nuuk.
- Helicopter flights at cruising altitude passing over the study area or following the transmission line at low altitude.
- Helicopter flights visiting the climate stations for maintenance – once or twice during the season.

There have been only few interactions between visitors in the study area and the different setups and the cabin. In July, a large group of people camped in a number of tents in the area between the bridge and the BioBasis gas-flux setup for one night. Foxes have moved and laid droppings in the pitfall traps. The cabin has undergone repair necessitating a number of visits from Biobasis Logistics workers.

The monitoring programmes themselves have brought disturbance to the area, i.e. transportation between Nuuk and the head of the fjord, housing of personnel, walking between study plots and around study plots. Especially the permanent plots in the *Empetrum* heaths and the fens have signs of wear. Furthermore, the wear around and between the BioBasis gas-flux measuring plots has become increasingly noticeable. The area close to the cabin, where most visitors put up their tents, is showing signs of wear as is the trail between the boat landing site and the cabin.

Transportation between Nuuk and the study site in Kangerluarsunnguaq/Kobbefjord has been conducted on an irregular basis, but during most of the season there was transportation two to three days a week (Tuesdays and Thursdays, or Mondays, Wednesdays, and Fridays). During most of the season, the cabin was used temporarily by two to four persons.

Walking around the study plots has had a wearing effect on the vegetation and it should be considered marking permanent trails between study sites and study plots.

Furthermore, in 2015 a drone was flown around the catchment for 10 days to photograph and map the area.

In conclusion, it is estimated that monitoring activities only had minor impact on the vegetation and terrain.

8 Logistics

Henrik Philipsen

In 2015, the Greenland Institute of Natural Resources (GINR) Logistics section took care of the transport and maintenance work related to NuukBasic in Kobbefjord in co-operation with experienced people from the NuukBasic programmes.

In 2015, the field season in Kobbefjord started 13 January and ended 3 December. In this period, 40 scientists and logistics staff had 337 man-days and 33 man-days in the study area, respectively.

The transportation of logistics staff, technicians, scientists, visitors and guests from Nuuk to the research area in Kobbefjord was carried out by GINRs boats "Erisaalik", "Aage V. Jensen II Nuuk" and "Avataq". The boats were donated by Aage V. Jensen's Charity Foundation in 2005, 2007 and 2014. The total number of sailing days to Kobbefjord used by Logistics, BioBasis, GeoBasis and ClimateBasis were 73 in 2015. MarineBasis used 23 sailing days from 15 January to 18 December to sail to study areas in Kobbefjord and Godthåbsfjord.

In 2014/2015, the winter was very hard and long, even though it was possible to sail to the head of Kobbefjord with GINRs boat "Erisaalik" in January. From early February until mid-June, there was 2–5 kilometers ice from the head and out into Kobbefjord. In April and early June, NuukBasic labourers were disembarked at the edge of the ice, from where they walked or used skies to get to the cabin and study area. On 15 June, the Danish Navy vessel "Knud Rasmussen" broke the sea ice in Kobbefjord, so it was possible to sail with GINRs boat "Aage V. Jensen II Nuuk" the following day to the head of the fjord. From 16 June until 3 December there was no sea ice in Kobbefjord.

58 official and other guests made visits to the research area in Kobbefjord in 2015.
16 June: 10 former and coming members of The Sirius Dog Sledge Patrol, Arctic Command and advisor Peter Schmidt Mikkelsen.
25 August: 12 students and 7 teachers from high school Master Classes, Denmark; 2 guides from a cruise ship.
1 September: 26 persons, The Nordic Council of Ministers; Climate and Air Pollution Group (KoL), Denmark.

NuukBasic scientists who do not live in Nuuk were accommodated in GINRs Annex and at Biologstationen, where they spent a total of 446 nights. Accommodation in the cabin and tents in Kobbefjord accounted for 176 nights in total.

The buildings in Kobbefjord were established in 2008 and 2009 and were fully equipped in 2010. The buildings are donated by Aage V. Jensen's Charity Foundation.

The cabin has a ramp for skidoo, a catwalk, a terrace and 11 m² storage room under the living room. The cabin is fitted with an entrance, a laboratory with hot and cold water, a bathroom with earth closet and shower, a living room with kitchen, four berths and a heating oven.

The generator hut is equipped with a ramp, working bench, vice and tools. Electric power was delivered from two portable 4 kW gasoline generators from 2013 and 2014. One 5 kW diesel generator from 2008 is used as backup. In 2015, gasoline consumption for generators was 685 liters. The heating oven inside the cabin used 40 liters of diesel.

Water supply came from the nearby river and was connected from 23 June until 25 September. Freshwater consumption was 8 000 liters in 2015. A drainpipe for grey household water was connected from 23 June until 25 September.

All kinds of daily household and toilet garbage – in total 301 kg - were returned to Nuuk during the season.

Communication to Nuuk was done using Iridium satellite telephones, while local communication to boats and others was done with a stationary VHF-radio in the cabin and portable VHF-radios. Four new portable VHF-radios were bought in 2015.

There were four operational days with the snowmobile in April.

Eight helicopter trips were made by Air Greenland to the area in 2015:
21 April: three scientists from Greenland Survey made a trip to a nearby glacier.
12 to 15 June: three technicians from Greenland Survey perform maintenance work at the climate stations.
24 July: four scientists from Greenland Survey made a trip to the nearby glacier.
8 August: two scientists again made a trip to the nearby glacier.

9 Acknowledgements

MarineBasis wish to acknowledge the crew on board the 'R/V Sanna' for their valuable assistance during this year's May cruise. We also thank Louise Mølgaard, Sigga Joensen, Gabriela Garcia, Lars Heilmann, Flemming Heinrich, Kunuk Lennert, Sofie R. Jerimiassen, Signe Jeremiassen, Jørgen Sethsen, Andrzej Witkowski and Marek Zajaczkowski for field and technical assistance. We would also like to acknowledge Thomas Krogh, Jens Weinell, Rebecca Scheuerlein, Paul Batty, Morten S. Frederiksen, Anna Haxen, Winnie Martinsen, Peter B. Christensen, Carsten Egevang, Bo Bergstrøm and Ditte M. Mikkelsen for their contribution to the programme in previous years.

10 Personnel and visitors

Compiled by Jannik Hansen

Carl Isaksen, Greenland Institute of Natural Resources, Greenland
Carlos Duarte, King Abdullah University of Science and Technology, Saudi Arabia
Daniel Rudd, University of Copenhagen, Denmark
Dorte Krause, Aarhus University, Denmark
Dorthe Petersen, Asiaq - Greenland Survey, Greenland
Efren Blanco, Aarhus University, Denmark
Ejgil Gravesen, Denmark
Erik Lysdal, COWI, Denmark
Flemming Heinrich, Greenland Institute of Natural Resources, Greenland
Frederik Mathiassen, Asiaq - Greenland Survey, Greenland
Hanna Axén, Lunds Universitet, Sweden
Hans Ole Jensen, Greenland Institute of Natural Resources, Greenland
Henrik Philipsen, Greenland Institute of Natural Resources, Greenland
Jakob Lund, Greenland Institute of Natural Resources, Greenland
Jakob Abermann, Asiaq – Greenland Survey, Greenland
Josephine Nymand, Greenland Institute of Natural Resources, Greenland
Katrine Raundrup, Greenland Institute of Natural Resources, Greenland
Klaus Nygaard, Greenland Institute of Natural Resources, Greenland
Kristian Greisen, Greenland Institute of Natural Resources, Greenland
Kristine Arendt, Greenland Institute of Na-tural Resources, Greenland
Lars Heilmann, Greenland Institute of Natural Resources, Greenland
Lise Lotte Sørensen, Aarhus University, Denmark
Louise Holm Christensen, Asiaq - Greenland Survey, Greenland
Lucas Davaze, Asiaq - Greenland Survey, Greenland
Maia Olsen, Greenland Institute of Natural Resources, Greenland
Majbritt Westring Sørensen, Asiaq - Greenland Survey, Greenland
Majken Djurhuus Poulsen, Geological Survey of Denmark and Greenland, Greenland
Malene Olesen, Greenland
Maria L. Burup, University of Copenhagen, Denmark
Marie Rasch, University of Copenhagen, Denmark
Mark Hopwood, University of Southampton, England
Martin Nauta, Asiaq - Greenland Survey, Greenland
Ole Geertz-Hansen, Greenland Institute of Natural Resources, Greenland
Per Hangaard, Asiaq - Greenland Survey, Greenland
Peter Hegelund, Greenland Institute of Natural Resources, Greenland
Peter Schmidt Mikkelsen, Greenland Institute of Natural Resources, Greenland
Rasmus Dyrmose Nørregaard, Aarhus University, Denmark
Salik Enequist, Asiaq - Greenland Survey, Greenland
Stefan Jansen, Asiaq - Greenland Survey, Greenland
Stefan Wacker, Asiaq - Greenland Survey, Greenland
Susse Wegeberg, Aarhus University, Denmark
Søren Hofman Christiansen, University of Copenhagen, Denmark
Torben Røjle Christensen, University of Lund, Sweden & Greenland Climate Research Centre, Greenland
Ulla Heede, University of Cambridge, United Kingdom
Two tourist guides from "The Seabourn Quest"
10 from Arctic Command, Defence Command, Denmark
Magnus Limborg with12 students and 6 teachers, Denmark
The Nordic Council of Ministers, Climate and Air Pollution Group (KoL), 26 people, Denmark
The Nordic Committee of Senior Officials for Education & Research (25 people)
Naalakkersuisoq for Nature, Environment and Energy Mala Høy Kúko, Greenland, and the Minister for Energy, Utilities and Climate Lars Chr. Lilleholt, Denmark with delegations

11 Publications

Compiled by Jannik Hansen

Scientific papers

Bendtsen, J., Mortensen, J. and Rysgaard, S. 2015. Modelling subglacial discharge and its influence on ocean heat transport in Arctic fjords. Ocean Dynamics, 65, 1535-1546, doi:10.1007/s10236-015-0883-1.

Bendtsen, J., Mortensen, J., Lennert, K. and Rysgaard, S. 2015. Heat sources for glacial ice melt in a west Greenland tidewater outlet glacier fjord: the role of subglacial freshwater discharge. Geophysical Research Letters, 42, 4089-4095, doi:10.1002/2015GL063846.

Hancke, K., Dalsgaard, T., Sejr, M.K., Markager, S. and Glud, R.N. 2015. Phytoplankton Productivity in an Arctic Fjord (West Greenland): Estimating Electron Requirements for Carbon Fixation and Oxygen Production. PLoS ONE 10(7): e0133275. doi:10.1371/journal.pone.0133275.

Juul-Pedersen, T., Arendt, K.E., Mortensen, J., Blicher, M., Schrøder, D.S. and Rysgaard, S. 2015. Seasonal and interannual phytoplankton production in a sub-Arctic tidewater outlet glacier fjord, SW Greenland. Marine Ecology Progress Series, Vol. 524: p. 27-38.

Kramshøj M., Vedel-Petersen I., Schollert M., Rinnan Å., Nymand J., Ro-Poulsen H. and Rinnan R. 2016. Large increases in arctic biogenic volatile emissions are a direct effect of warming. Nature Geoscience, doi: 10.1038/ngeo2692

Krause-Jensen, D., Duarte, C.M., Hendriks, I.E., Meire, L., Blicher, M.E., Marbà, N. and Sejr, M.K. 2015. Macroalgae contribute to nested mosaics of pH variability in a sub-Arctic fjord, Biogeosciences 12:4895-4911, DOI: 10.5194/bg-12-4895-2015.

Krawczyk, D.W., Witkowski, A., Juul-Pedersen, T., Arendt, K.E., Mortensen, J. and Rysgaard, S. 2015. Microplankton succession in a SW Greenland tidewater glacial fjord influenced by coastal inflows and runoff from the Greenland Ice Sheet. Polar Biology, 38, 1515-1533, doi:10.1007/s00300-015-1715-y.

Machguth, H., Thomsen, H.H., Weidick, A., Abermann, J. and 24 more. 2016. Greenland surface mass-balance observations from the ice-sheet ablation area and local glaciers. Journal of Glaciology, vol.62, isuue 235, pp. 1–27. doi: 10.1017/jog.2016.75.

Meire, L., Søgaard, D.H., Mortensen, J., Meysman, F.J.R., Soetaert, K., Arendt, K.E., Juul-Pedersen, T., Blicher, M.E. and Rysgaard, S. 2015. Glacial meltwater and primary production as drivers of strong CO_2 uptake in fjord and coastal waters adjacent to the Greenland IceSheet. Biogeosciences, 12, 2347-2363, doi:10.5194/bg-12-2347-2015.

Murray, C., Markager, S., Stedmon, C.A., Juul-Pedersen, T., Sejr, M.K. and Bruhn, A. 2015. The influence of glacial melt water on bio-optical properties in two contrasting Greenland fjords. Estuarine, Coastal and Shelf Science, Vol. 163B, p. 72-83.

Nielsen, S. S., von Arx, G., Damgaard, C. F., Abermann, J., Buchwal, A., Büntgen, U., Treier, U., Barfod, A. and Normand, S. 2017. Xylem anatomical features provide mechanistic explanation for spatio-temporal variability in growth rates of *Betula nana* from western Greenland. Arctic, Antarctic, and Alpine Research, Vol. 49, No. 3, pp. 359–371 DOI: http://dx.doi.org/10.1657/AAAR0016-041

Olesen, B., Krause-Jensen, D., Marbà, N. and Christensen, P.B. 2015. Eelgrass *Zostera marina* in subarctic Greenland: dense meadows with slow biomass turnover in cold waters. Marine Ecology Progress Series, Vol. 518, 107-121.

Sørensen, H.L., Meire, L., Juul-Pedersen, T., Meysmann, F., Rysgaard, S., Thamdrup, B. and Glud, R.N. 2015. Seasonal carbon cycling in a Greenlandic fjord: An integrated pelagic and benthic study. Marine Ecology Progress Series, DOI: 10.3354/meps11503.

Vedel-Petersen I., Schollert M., Nymand J. and Rinnan R. 2015. Volatile organic compound emission profiles of four common arctic plants. Atmospheric Environment 120: 117–126.

Reports

Arctic Marine Biodiversity Monitoring Plan Greenland, 2015 Implementation. National one page update. Conservation of Arctic Flora and Fauna (CAFF).

Circumpolar Biodiversity Monitoring Program Marine Steering Group. 2015. Arctic Marine Biodiversity Monitoring Plan Annual Plan 2014: Annual Report on the Implementation of the Circumpolar Biodiversity Monitoring Program's Arctic Marine Biodiversity Monitoring Plan (CBMP-Marine Plan). CAFF Monitoring Report No.13. CAFF International Secretariat, Akureyri, Iceland.

Juul-Pedersen, T., Arendt, K.E., Mortensen, J., Krawczyk, D., Rysgaard, S., Retzel, A., Nygaard, R., Burmeister, A.D., Krause-Jensen, D., Marbà, N., Olesen, B., Sejr, M.K., Blicher, M.E., Meire, L., Geertz-Hansen, O., Labansen, A.L., Boye, T. and Simon, M. The MarineBasis programme 2014. In Jensen, L.M. and Christensen, T.R. (eds.) *in press*. Nuuk Ecological Research Operations, 8th Annual Report, Aarhus University, DCE – Danish centre for Environment and Energy.

Mortensen, J. 2015. Report on hydrographic conditions off Southwest Greenland June/July 2014, Serial No. N6416, NAFO SCR Doc. 15/001.

Presentation at symposiums, workshops, meetings and conferences

Kramshøj M., Vedel-Petersen I., Schollert M., Rinnan Å., Nyman J., Ro-Poulsen H. and Rinnan R. 2015. Large increases in arctic biogenic volatile organic compound emissions are a direct effect of warming. Integrating arctic plant and microbial ecology (21st ITEX meeting), Uppsala, Sweden, 16-18 September, 2015 (poster).

Mortensen, J., Bendtsen, J. and Rysgaard, S. 2015. A synthesis of the ongoing seasonal work in a west Greenland tidewater outlet glacier fjord, Godthåbsfjord, AGU Fall 2015, San Francisco.

Mortensen, J., Bendtsen, J. and Rysgaard, S. 2015. Ilulissat Climate Days 2015. Circulation and heat sources for glacial melt in a west Greenland fjord, 2-4 juni, Ilulissat.

Rinnan, R. 2016. Drastically Increased Emissions of BVOCs from Arctic Vegetation Communities Under Climate Change. Plant volatiles Gordon Research Conference, Ventura, CA, USA. Jan 31-Feb 5, 2016 (talk).

Rinnan R., Vedel-Petersen I., Priemé A., Haugwitz M.S., Rinnan Å., Dahl M.B, Nymand J. 2015. Does climate change alter chemical composition of arctic tundra plants and soil? 17th International Conference on Near Infrared Spectroscopy, Foz do Iguassu, Brazil, 18-23 October, 2015 (poster).

Popular science and outreach

Juul-Pedersen, T., Søgaard, D.H. and Arendt, K.E. 2015. Coordinating and teaching the university course "Arctic Marine Ecosystems", 27 April–5 June, Nuuk.

Juul-Pedersen, T. 2015. Teaching a high school class "Marine økosystemer, ressourcer og klimaforandringer omkring Grønland", 26 August, Nuuk.

Juul-Pedersen, T. 2015. Interview, Associated Press, 21 July, Nuuk.

Juul-Pedersen, T. 2015. Interview, De Volkskrant, 14 August, Nuuk.

12 References

Compiled by Jannik Hansen

Aastrup, P., Nymand, J., Raundrup, K., Olsen, M., Lauridsen, T.L., Krogh, P.H., Schmidt, N.M., Illeris, L. and Ro-Poulsen, H. 2015. Conceptual design and sampling procedures of the biological programme of NuukBasic. 2 edition. Aarhus University, DCE – Danish Centre for Environment and Energy.

Boye , T.K., Simon, M.J. and Witting, L. 2014. How may an annual removal of humpback whales from Godthaabsfjord, West Greenland, affect the within-fjord sighting rate? Journal of Cetacean Research and Management 14: 51-56.

Boye, T.K., Simon, M.J. and Madsen, P.T. 2010. Habitat use of humpback whales in Godthåbsfjord, West Greenland, with implications for commercial exploitation. Journal of the Marine Biological Association of the United Kingdom 90: 1529-1538.

Cappelen, J. 2016. Greenland – DMI Historical Climate Data Collection 1873-2015 - with Danish Abstracts, DMI, Technical report 16-05.

Fjellberg, A. 2015. Chapter 6 Collembola (springtails, collembolans). Pages 48-82 in J. Böcher, N. P. Kristensen, T. Pape and L. Vilhelmsen, editors. The Greenland Entomofauna: An Identification Manual of Insects, Spiders and their Allies. Brill.

Fortes, M.D. and Lüning, K. 1980. Growth rates of North Sea macroalgae in relation to temperature, irradiance and photoperiod. Helgoländer Meeresunters 34: 15-29.

Hansen B.U., Christensen, L.H.K., Tamstorf, M.P., Lund, M., Højlund, S., Burup, M.L., Raundrup, K., Mastepanov, M., Westergaard-Nielsen, A. and Christensen, T.R. 2013. Nuuk Basic: The GeoBasis Programme. In Jensen, L.M. and Rasch, M. (eds.). Nuuk Ecological Research Operations, 6th Annual Report, 2012. National Environmental Research Institute, Aarhus University, Denmark. 84 pp.

Hansen B.U., Christensen, L.H., K., Tamstorf, M.P., Lund, M., Højlund, S., Burup, M.L., Raundrup, K., Maste-panov, M., Westergaard-Nielsen, A. and Christensen, T.R. 2014. Nuuk Basic: The GeoBasis Programme. In Jensen, L.M. and Rasch, M. (eds.). Nuuk Ecological Research Operations, 7th Annual Report, 2013. National Environmental Research Institute, Aarhus University, Denmark. 84 pp.

Hansen B.U., Hill, K., Pedersen, S.H., Christensen, L.H., K.M., Tamstorf, M.P., Sigsgaard, C., Fruergaard, M., Lund, M., Raundrup, K., Mastepanov, Westergaard-Nielsen, A. and Christensen, T.R. 2012. Nuuk Basic: The GeoBasis Programme. In Jensen, L.M. and Rasch, M. (eds.). Nuuk Ecological Research Operations, 5th Annual Report, 2011. National Environmental Research Institute, Aarhus University, Denmark. 84 pp.

Hansen B.U., Iversen, K.M., Tamstorf, M.P., Sigsgaard, C., Fruergaard, M., Højlund, S., Lund, M., Raundrup, K., Mastepanov, M., Falk, J.M., Ström, L., Westergaard, A., Rasmussen, B.H. and Christensen, T.R. 2010. Nuuk Basic: The GeoBasis Programme. In Jensen, L.M. and Rasch, M. (eds.). Nuuk Ecological Research Operations, 3rd Annual Report, 2009. National Environmental Research Institute, Aarhus University, Denmark. 80 pp.

Hansen B.U., Pedersen, S.H., Iversen, K.M., Tamstorf, M.P., Sigsgaard, C., Fruergaard, M., Højlund, S., Lund, M., Raundrup, K., Mastepanov, M., Ström, L., Westergaard-Nielsen, A., Rasmussen, B.H. and Christensen, T.R. 2011. Nuuk Basic: The GeoBasis Programme. In Jensen, L.M. and Rasch, M. (eds.). Nuuk Ecological Research Operations, 4th Annual Report, 2010. National Environmental Research Institute, Aarhus University, Denmark. 80 pp.

Høgslund, S., Sejr, M.K., Wiktor, Josef Jr., Blicher, M.E. and Wegeberg, S. 2014. Intertidal community composition along rocky shores in South- west Greenland: a quantitative approach. Polar Biology 37: 1549–1561. DOI 10.1007/s00300-014-1541-7.

ISO 1100-2. 1998. Measurement of liquid flow in open channels – Part 2: Determination of stage-discharge relation, ISO 1100-2, International Organization for Standardization, Switzerland.

Iversen, K., Rasmussen, S. and Thorsøe, K. 2008. Nuuk Basic: The ClimateBasic programme. In Jensen, L.M and Rasch, M. (eds.) Nuuk Ecological Research Operations, 1st Annual Report, 2007. Copenhagen, Danish Polar Centre, Danish Agency for Science, Technology and Innovation, Ministry of Science, Technology and Innovation. 111 pp.

Jensen, L.M., Topp-Jørgensen, E., Schmidt, N.M. and Christensen, T. 2016. Nuuk Ecological Research Operations, 8th Annual Report, 2014. Department of Bioscience, Aarhus University, Denmark. 86 pp.

Katona, S.K., Baxter, B., Brazier, O., Kraus, S., Perkins, J. and Whitehead, H. 1979. Identification of humpback whales by fluke photographs. The behavior of marine mammals. Pages 33-44 in Winn, H.E. and Olla, B.L. (eds). Behavior of marine mammal science. Volume 3. Cetaceans. Plenum press, New York, NY. 438 pp.

Mønster, T. 2013. Betydningen af klimaforandringer for vækst og dybdeudbredelse af *Callitriche hamulata* i lavarktiske søer i Grønland. Master's thesis, Institut for Bioscience, Aarhus Universitet.

Nymand, J., Aastrup, P., Lauridsen, T.L., Krogh, P.H., Petersen, M.H., Illeris, L. and Ro-Poulsen, H. 2008. 4 NUUK Basic. The BioBasic Programme. Pages 28-37 in L.M. Jensen and M. Rasch, editors. Nuuk Ecological Research Operations, 1st Annual Report, 2007. Danish Polar Centre, Danish Agency for Science, Technology and Innovation, Ministry of Science, Technology and Innovation, 2008.

Nymand, J., Aastrup, P., Raundrup, K., Lund, M., Albert, K.R., Krogh, P.H., Rasmussen, L.M. and Lauridsen, T.L. 2011. NUUK BASIC: The BioBasis programme. Pages 30-44 in L. M. Jensen and M. Rasch, editors. Nuuk Ecological Research Operations, 4th Annual Report 2010. Aarhus University, DCE – Danish Centre for Environment and Energy.

Pernosky, M., Hangaard, P., Christensen, L., Thorsøe, K. and Knudsen, M. 2013. The ClimateBasic programme. In Jensen, L.M & Rasch, M. (eds.) Nuuk Ecological Research Operations, 6th Annual Report, 2012. Aarhus University, DCE – Danish Centre for Environment and Energy. 95 pp.

Pernosky, M., Hill, K., Hangaard, P., Larsen, M., Thorsøe, K., Knudsen, M. and Petersen, D. 2012. ClimateBasic programme. In Jensen, L.M & Rasch, M. (eds.) Nuuk Ecological Research Operations, 5th Annual Report, 2011. Aarhus University, DCE – Danish Centre for Environment and Energy. 92 pp.

Raundrup, K., Aastrup, P., Nymand, J., Lauridsen, T.L., Johannsson, L.S., Krogh, P.H., Lund, M. and Rasmussen, L.M. 2010. NUUK BASIC: The BioBasis programme. Pages 29-41 in L.M. Jensen and M. Rasch, editors. Nuuk Ecological Research Operations, 3rd Annual Report, 2010. National Environmental Research Institute, Aarhus University.

Smith, T.D., Allen, J., Clapham, P.J., Hammond, P.S., Katona, S., Larsen, F., Lien, J., Mattila, D., Palsbøll, P.J., Sigurjónsson, J., Stevick, P.T. and Øien, N. 1999. An Ocean-basin-wide mark-recapture study of the North Atlantic humpback whale (*Megaptera novaeangliae*). Marine Mammal Science 15: 1-32.

Sørensen, H.L., Meire, L., Juul-Pedersen, T., de Stigter, H.C., Meysman, F.J.R., Rysgaard, S., Thamdrup, B. and Glud, R.N. 2015. Seasonal carbon cycling in a Greenlandic fjord: an integrated pelagic and benthic study. Marine Ecology Progress Series 539: 1-17.

Tamstorf, M.P., Iversen, K.M., Hansen B.U., Sigsgaard, C., Fruergaard, M., Højlund, S., Andreasen, R.H., Mastepanov, M., Falk, J.M., Ström, L. and Christensen, T.R. 2009. Nuuk Basic: The GeoBasis Programme. In Jensen, L.M. and Rasch, M. (eds.). Nuuk Ecological Research Operations, 2nd Annual Report, 2008. National Environmental Research Institute, Aarhus University, Denmark. 80 pp.

Westring Sørensen, M., Wacker, S., Hangaard, P., Christensen, L.H. and Abermann, J. 2016. ClimateBasis Monitoring Program Nuuk Basic 2015 Qualtity Control Report, Asiaq.

Åberg, P.A. 1992a. A Demographic Study of Two Populations of the Seaweed *Ascophyllum nodosum*. Ecology 73: 1473-1487.

Åberg, P.A. 1992b. Size-based demography of the seaweed *Ascophyllum nodosum* in stochastic environments. Ecology 73: 1488-1501.

13 Appendix

Day of Year Calendar

Regular years	Jan	Feb	Mar	Apr	May	Jun	Jul	Aug	Sep	Oct	Nov	Dec
1	1	32	60	91	121	152	182	213	244	274	305	335
2	2	33	61	92	122	153	183	214	245	275	306	336
3	3	34	62	93	123	154	184	215	246	276	307	337
4	4	35	63	94	124	155	185	216	247	277	308	338
5	5	36	64	95	125	156	186	217	248	278	309	339
6	6	37	65	96	126	157	187	218	249	279	310	340
7	7	38	66	97	127	158	188	219	250	280	311	341
8	8	39	67	98	128	159	189	220	251	281	312	342
9	9	40	68	99	129	160	190	221	252	282	313	343
10	10	41	69	100	130	161	191	222	253	283	314	344
11	11	42	70	101	131	162	192	223	254	284	315	345
12	12	43	71	102	132	163	193	224	255	285	316	346
13	13	44	72	103	133	164	194	225	256	286	317	347
14	14	45	73	104	134	165	195	226	257	287	318	348
15	15	46	74	105	135	166	196	227	258	288	319	349
16	16	47	75	106	136	167	197	228	259	289	320	350
17	17	48	76	107	137	168	198	229	260	290	321	351
18	18	49	77	108	138	169	199	230	261	291	322	352
19	19	50	78	109	139	170	200	231	262	292	323	353
20	20	51	79	110	140	171	201	232	263	293	324	354
21	21	52	80	111	141	172	202	233	264	294	325	355
22	22	53	81	112	142	173	203	234	265	295	326	356
23	23	54	82	113	143	174	204	235	266	296	327	357
24	24	55	83	114	144	175	205	236	267	297	328	358
25	25	56	84	115	145	176	206	237	268	298	329	359
26	26	57	85	116	146	177	207	238	269	299	330	360
27	27	58	86	117	147	178	208	239	270	300	331	361
28	28	59	87	118	148	179	209	240	271	301	332	362
29	29		88	119	149	180	210	241	272	302	333	363
30	30		89	120	150	181	211	242	273	303	334	364
31	31		90		151		212	243		304		365

Day of Year

Leap years	Jan	Feb	Mar	Apr	May	Jun	Jul	Aug	Sep	Oct	Nov	Dec
1	1	32	61	92	122	153	183	214	245	275	306	336
2	2	33	62	93	123	154	184	215	246	276	307	337
3	3	34	63	94	124	155	185	216	247	277	308	338
4	4	35	64	95	125	156	186	217	248	278	309	339
5	5	36	65	96	126	157	187	218	249	279	310	340
6	6	37	66	97	127	158	188	219	250	280	311	341
7	7	38	67	98	128	159	189	220	251	281	312	342
8	8	39	68	99	129	160	190	221	252	282	313	343
9	9	40	69	100	130	161	191	222	253	283	314	344
10	10	41	70	101	131	162	192	223	254	284	315	345
11	11	42	71	102	132	163	193	224	255	285	316	346
12	12	43	72	103	133	164	194	225	256	286	317	347
13	13	44	73	104	134	165	195	226	257	287	318	348
14	14	45	74	105	135	166	196	227	258	288	319	349
15	15	46	75	106	136	167	197	228	259	289	320	350
16	16	47	76	107	137	168	198	229	260	290	321	351
17	17	48	77	108	138	169	199	230	261	291	322	352
18	18	49	78	109	139	170	200	231	262	292	323	353
19	19	50	79	110	140	171	201	232	263	293	324	354
20	20	51	80	111	141	172	202	233	264	294	325	355
21	21	52	81	112	142	173	203	234	265	295	326	356
22	22	53	82	113	143	174	204	235	266	296	327	357
23	23	54	83	114	144	175	205	236	267	297	328	358
24	24	55	84	115	145	176	206	237	268	298	329	359
25	25	56	85	116	146	177	207	238	269	299	330	360
26	26	57	86	117	147	178	208	239	270	300	331	361
27	27	58	87	118	148	179	209	240	271	301	332	362
28	28	59	88	119	149	180	210	241	272	302	333	363
29	29	60	89	120	150	181	211	242	273	303	334	364
30	30		90	121	151	182	212	243	274	304	335	365
31	31		91		152		213	244		305		366

Greenland Ecosystem Monitoring

Greenland Ecosystem Monitoring (GEM) is an integrated monitoring and long-term research programme on ecosystem dynamics and climate change effects and feedbacks in Greenland.

ClimateBasis Programme

The GEM ClimateBasis Programme studies climate and hydrology providing fundamental background data for the other GEM programmes.

GeoBasis Programme

The GEM GeoBasis Programme studies abiotic characteristics of the terrestrial environment and their potential feedbacks in a changing climate.

BioBasis Programme

The GEM BioBasis Programme studies key species and processes across plant and animal populations and their interactions within terrestrial and limnic ecosystems.

MarineBasis Programme

The GEM MarineBasis Programme studies key physical, chemical and biological parameters in marine environments.

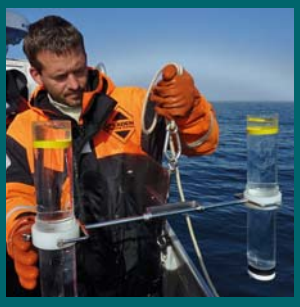

GlacioBasis Programme

The GEM GlacioBasis Programme studies ice dynamics, mass balance and surface energy balance in glaciated environments (only at Zackenberg Research Station).

AARHUS UNIVERSITY

ASIAQ

GEUS

Grønlands Naturinstitut
Pinngortitaleriffik · Greenland Institute of Natural Resources

DTU Technical University of Denmark

UNIVERSITY OF COPENHAGEN